

1 Development of a multi-

2 disciplinary toolkit to study

3 time cells in the

4 hippocampus

5 by

6 Kambadur Gundu Ananthamurthy

7 (NCBS-1524; GS2011; NST119)

8 PI: Prof. Upinder S. Bhalla

9 TCM: Prof. Sumatra Chattarji, Dr. Mukund Thattai

10 **Table of Contents**

11

Chapter 1 – Introduction

12

Control and coordination

13 The vertebrate Central Nervous System (CNS), consisting primarily of
14 the central ganglia (brain) and the spinal cord, samples and receives
15 information from the external world offering top-down control over the
16 activity of all parts of the body. Functions like exploration, food
17 acquisition, and danger aversion, all involve complex coordination
18 between,

19 ● the Sensory Systems (that integrate information from the
20 environment),
21 ● the Memory Systems (that integrate sensory information with
22 prior experience), and
23 ● the Motor Systems (that integrate motor plans and execute
24 movement).

25

Projects and overall goals

26 The overall focus of the work and experiments described in this Thesis
27 was to study Memory Systems, specifically, in terms of,

28 **Project I:** How do sensory representations transform with
29 learning?

30 **Project II:** How does the timing of cellular activity adjust to
31 behavioural task variables?

32 **Project III:** What is the best way to detect and score time-tuned
33 cellular activity?

34 Narrowing down, we as a lab were interested in the mammalian
35 hippocampus, a brain structure which is important for consolidating
36 information (from Sensory and other Memory Systems) to enable
37 certain kinds of short-term memory and the translation of short-term
38 memory to long-term.

39 **Theories on the function of the hippocampus**

40 Three main ideas of hippocampal function studied over the past few
41 decades in increasing order of popularity are,

42 A Response Inhibition - Studied mostly in the 1960's, this
43 perspective described the Hippocampus as important to the
44 ability of animals to inhibit their impulses and natural, habitual,
45 or dominant behavioral responses to stimuli, in order to select
46 more appropriate responses. This perspective was justified by
47 two observations with regard to animals with hippocampal
48 damage - 1) these animals tended to be hyperactive, and 2)
49 were unable to withhold previously learnt responses. British
50 psychologist Jeffrey Alan Gray developed this perspective to
51 link hippocampal activity with anxiety (McNaughton & Gray,
52 2000).

53 B Episodic Memory – This perspective was popularized by the
54 psychological studies on Patient H. M. (Henry Molaison), who
55 had been suffering from epileptic seizures and had to undergo
56 extensive hippocampectomy (surgical destruction of the

57 hippocampi), as treatment. American neurosurgeon William
58 Beecher Scoville and British-Canadian neuropsychologist
59 Brenda Milner were pioneers of this study and were able to
60 describe severe anterograde and partial retrograde amnesia in
61 the patient post surgery (Scoville & Milner, 1957). Since the late
62 2000's, the discovery and description of time cells (B. Kraus et
63 al., 2013; B. J. Kraus et al., 2015; MacDonald et al., 2011, 2013;
64 Modi et al., 2014; Pastalkova et al., 2008), has reinvigorated this
65 perspective.

66 C Spatial Cognition - Originally popularized by the remarkable
67 work of American-British neuroscientist John O'Keefe and his
68 American psychologist Lynn Nadel, the link between
69 Hippocampal function and spatial navigation and coding was
70 solidified with the discovery and subsequent descriptions of
71 Place Cells (Morris et al., 1982; O'Keefe & Dostrovsky, 1971;
72 O'Keefe & Recce, 1993). This perspective is the most popular
73 amongst the known and studied functions of the Hippocampus
74 and has been the subject of a large body of work. Indeed, the
75 Nobel Prize in Physiology or Medicine 2014 was awarded to
76 John O'Keefe, May-Britt Moser, and Edvard I. Moser, for "The
77 Brain's Navigational Place and Grid Cell System".

78 **The hippocampus and time cells**

79 Damage to the hippocampal system has been shown to cause the
80 impairment of long-term memory or amnesia, in human patients,
81 rodents, and non-human primates. Interestingly, such damage to the
82 Hippocampus seems to have no observable effect on the capacity for

83 acquisition and expression of skilled performance. These two results
84 suggest the role of the Hippocampus in certain kinds of memory, but
85 not all.

86 Anatomically, the hippocampal system receives input from, and in turn,
87 projects to the neocortical brain regions that serve as the site to
88 process higher order categories and modalities of information. It is thus
89 suggested that the Hippocampus holds a privileged position in the
90 brain, receiving the outcomes of the computation of the brain's various
91 modules, and relating to them. A large majority of the cortical
92 information is sent to the Hippocampus via the Entorhinal Cortex (EC).
93 This information is processed in roughly three stereotactically and
94 molecularly separable layers of cells in the following order: EC
95 → Dentate Gyrus → CA3 → CA1. This pathway from the EC to the CA1
96 has three separate synaptic connections (across the layers) and is also
97 known as the Trisynaptic Pathway. The output of the CA1 is then sent
98 to other cortical areas.

99 The activity of neurons in the hippocampus of awake, behaving
100 animals is modulated by significant stimuli or objects in the
101 environment as well as relationships between temporally discontiguous
102 but relevant, paired stimuli. With the discovery of Place cells, it was
103 clear that the CA1 of rats navigating a spatial environment,
104 showcased location specific firing fields. With the discovery of Time
105 cells, it was shown that the CA1 of rats could elicit spatiotemporal
106 sequences of activity whenever the animal required to make a link
107 between stimuli or events, even with a stimulus-free period in between.
108 This provided an important physiological parallel to the spatial learning
109 as well as episode learning deficit seen with damage to the
110 Hippocampus.

111 The hippocampus supports a robust form of synaptic plasticity called
112 Long-Term Potentiation (LTP), viz., brief patterned activation of
113 particular pathways produces a stable increase in synaptic efficacy that
114 may last for hours to weeks. This is also an important mechanism often
115 suggested as the answer to how the hippocampus manages short-term
116 declarative memory.

117 In an experiment published in 2008, Eva Pastalkova and colleagues
118 from Gyorgy Buzsaki's lab had rats navigate a figure 8 maze, with the
119 animal being rewarded with water, in between trials, if they managed to
120 alternate between the left and right arms. There was a catch however.
121 Just before launching into the left or right arms, the animal had to
122 spend a fixed amount of time running a treadmill, held in place. This
123 would allow self-motion cues, but with the absence of any other
124 external stimuli. Impressively, single-units recorded from the
125 Hippocampal CA1 cells revealed strong correlation with the time spent
126 on the treadmill, despite the absence of external cues, and that
127 different cells tuned to different time points, forming a spatiotemporal
128 sequence of activation (Pastalkova et al., 2008). In a different
129 experiment published in 2011, Christopher J. MacDonald and
130 colleagues from Howard Eichenbaum's lab had rats had to go around
131 a maze and perform a olfactory task when they were first presented
132 with an odour, then made to wait for a delay period in a cordoned off
133 section of the maze, before being allowed to either dig for a reward or
134 continue on the maze, depending on the odour presented. As trials
135 progressed, Hippocampal CA1 cells were recorded (single-units) and
136 found to not only be modulated by the decision to be taken, but also to
137 the amount of time spent in the delay period. Experimentally, the delay
138 period could be elongated or shortened, each having an effect on

139 remapping of the tuning fields of the various CA1 cells, but to different
140 extents (MacDonald et al., 2011). This study was often scrutinized
141 since there was the confound of the animals moving in space,
142 potentially invoking Place cells.

143 In 2013, the Eichenbaum group published their findings with head-fixed
144 rats (no movement in space) performing a Delayed Match-To Sample
145 (DMS) task with pairs of odours, where again time tuned activity could
146 be observed with a sequence of Hippocampal CA1 cell activations, that
147 depended on the identity of the first odour (MacDonald et al., 2013). In
148 2014, Mehrab Modi, Ashesh Dhawale, and Upinder Bhalla published
149 their results with head-fixed mice learning and performing a Trace Eye-
150 Blink Conditioning (TEC), wherein it was observed that Hippocampal
151 CA1 cell activity sequences emerged in close relation to the acquisition
152 of behavioural performance, thus cementing the idea that sub-
153 populations of Hippocampal CA1 cells could bridge temporal gaps
154 between relevant, paired stimuli, and that they did so with the activity
155 of time-tuned cells (Modi et al., 2014).

156 Finally, it was important to study if these apparently time-tuned cells
157 were tuned to the actual duration of time in a delay period, or whether
158 it was more important for these cells to track the distance run. In an
159 experiment published in 2013, Benjamin Kraus and colleagues from
160 Howard Eichenbaum's lab again had their rats navigate a figure 8
161 maze, but with a motorized treadmill in the central arm, to
162 experimentally regulate the running speed. With this setup, the study
163 was successful at delineating that both time spent running and
164 distance run were important features, and that different cells could tune
165 to either of the features (B. Kraus et al., 2013). Whenever
166 Hippocampal CA1 cells showcased time-tuned activity (as opposed to

167 space/location-tuned activity), such cells were dubbed “Time Cells”
168 (Eichenbaum, 2017; B. Kraus et al., 2013).

169 **“Single-cell, multi-trial” vs. “multi-cell, single-
170 trial” approaches in Neuroscience**

171 A dominant, early perspective in neurophysiology had been to record
172 activity from a single cell, over many trials, under a variety of
173 conditions (bath applications in slice physiology, different physiological
174 conditions like stress and genetic background). For more than one
175 recorded cell, the process would be repeated, till the dataset was
176 complete.

177 An intermediate perspective was to record from multiple cells
178 simultaneously, yet treat each cell independently for analysis towards
179 correlation and mechanism studies, across many repeats of
180 experimental conditions or trials (same as above).

181 An important and more modern perspective is to record from multiple
182 cells simultaneously, and use this network or population activity to
183 decode single-trial characteristics (position, time, stimulus presence,
184 etc.) using very powerful numerical and mathematical algorithms
185 involving (but not limited to) Bayesian Decoding and Information
186 Theory. The essential idea is that the neuronal code of the brain is not
187 defined just by the activity of single neurons since they may only
188 encode very specific fractions of the experience, but rather that the
189 population encodes the full experience, using a number of distributed
190 and redundant strategies.

- 191 • Bayesian Decoding: Using the activity of multiple,
192 simultaneously recorded neurons to develop a likelihood
193 estimate of the evidence (firing rate combinations) to the
194 experimental parameter (spatial position, relative time, etc.)
195 and combine this with the experimentally determined prior
196 (probability), to obtain estimates of the conditional or
197 posterior probability of a parameter value, given evidence.
198 Bayes' Rule describes

$$P(A|B) = P(B|A).P(A)/P(B)$$

200 ... where,

201 A: Parameter value (position, time, etc.)

202 B: Evidence (cellular firing rate)

203 P(A): Prior Probability (experimentally defined)

204 P(B): Probability of evidence (Firing Rate)

205 P(A|B): Posterior probability of parameter value given
206 evidence

207 P(B|A): Likelihood estimate of evidence given parameter
208 value (based on recordings)

209 This methodology has been used to not only successfully
210 predict specific time points in a trial from population activity, but
211 has also been used to observe that the population activity from
212 a session of recording is able to predict time points in trials
213 conducted on subsequent sessions of recording, up unto 3-4
214 sessions (Mau et al., 2018).

- 215 • Information Theory: Using recorded cellular activity to
216 estimate how much information this activity carries about
217 experimental parameters (position, time, stimuli, etc.). Three
218 essential metrics have been used,
- 219 1. Information per activity spike (I_{spike}), in bits/spike
 - 220 2. Information per unit time (I_{sec}), in bits/sec

221 3. Mutual Information (MI) between evidence and
222 parameter value, in bits

223 William Skaggs, Bruce McNaughton and colleagues published a
224 series of experiments working out the value of Information Theory
225 based approaches to Deciphering the Hippocampal code, reviewed
226 previously (Skaggs et al., 1996). This idea was later adapted strongly
227 by the field but focus throughout, remained on Place Cells.

228 An interesting study published in 2018 even used synthetic test
229 datasets to go to the extent of estimating place cell detection algorithm
230 performance on the basis of I_{spike} , I_{sec} and MI (Souza et al., 2018). They
231 found,

232 1. MI could outperform the other two in a variety of scenarios.
233 2. I_{spike} and I_{sec} may still be useful in identifying unique
234 subpopulations of Place Cells.
235 3. Important algorithmic adjustments could be made to the
236 calculations of I_{spike} and I_{sec} , to equalize performance between
237 them and MI.

238 There was clear nuance in the population code that required such a
239 perspective during analysis. Eichenbaum and colleagues popularized
240 the use of such metrics in the context of Time Cells (Mau et al., 2018),
241 yet a systematic approach to identifying the best algorithms for Time
242 Cells was requisite.

243 A major step forward with “multi-cell, single-trial” approaches is the
244 benefit of resolving how each cell and inter-cell interactions contribute
245 to stimulus representation, behavioural task variables, and other brain-
246 intrinsic computation. Technological advances in large-scale
247 neurophysiology recordings such as the increased density of tetrode
248 drives, neuropixels, optical sectioning and microscopy, resonant

249 scanning, etc., have enabled the discovery of well coordinated
250 sequences of cellular activity such as Sharp Wave Ripples (SWRs),
251 Replay, and behavioural timescale spatio-temporal sequences, *in vivo*.
252 This is primarily due to a radical improvement to an experimenter's
253 ability to simultaneously record from multiple cells (Foster, 2017),
254 going from yields of ~10 cells to even ~10⁴ cells, per animal.

255 **Single-Unit Electrophysiology vs 2-Photon 256 Calcium Imaging to study the Hippocampus**

257 The most well characterized and studied function of the Hippocampus
258 and surrounding tissue (Entorhinal Cortex, Parasubiculum, etc.) is the
259 role these tissue systems played in Spatial Navigation and Coding.
260 Single-Unit Electrophysiology was paramount to being able to isolate
261 the activity from individual cells, and eventually was used to discover
262 and describe properties of Place Cells (O'Keefe & Dostrovsky, 1971),
263 Grid Cells (Fyhn et al., 2004; Hafting et al., 2005), Head-Direction Cells
264 (Taube et al., 1990), along with numerous other important
265 physiological discoveries. However, even with advances in the density
266 of tetrode recordings, the yield of recorded cells from any given animal
267 was often limited to <100 cells. It was only with the invention of
268 Neuropixels (Jun et al., 2017) that this yield could be expanded to
269 ~1000 cells. We had opted to utilize calcium imaging by 2-Photon
270 Microscopy (Denk et al., 1990; Stosiek et al., 2003). This methodology
271 allowed us to record ~100 cells per session with our mice. In contrast,
272 we encountered significant cost to the recording frame rate on account
273 of the limitations of the technique.

274 The hippocampi (one in each hemisphere) of the mouse brain lie ~1
275 mm below the most superficial layers of cortex (just inside the cranium),
276 a barrier typically too wide for typical 1-photon fluorescence imaging
277 systems (Confocal, Spinning Disk, etc.). This poses a very difficult
278 challenge for imaging preparations since there are hardware and other
279 technical limits to how long the working distance of microscope
280 objectives can be made. The use of 2-photon microscopy combined
281 with combinations of cortical excavations (to aid physical access),
282 microendoscopes, prisms to guide emitted fluorescence, have all been
283 used to achieve deep brain imaging based recordings at cellular
284 resolution, in rodents (Andermann et al., 2013; Aronov & Tank, 2014;
285 Attardo et al., 2015; Barreto et al., 2009; D. A. Dombeck et al., 2007,
286 2009, 2010; D. Dombeck & Tank, 2014; Harvey et al., 2009; Murray &
287 Levene, 2012; Velasco & Levene, 2014; Ziv et al., 2013).

288 All imaging preparation standardizations described in this thesis invoke
289 2-Photon calcium imaging of Hippocampal CA1 cells at cellular
290 resolution (1 pix = ~1 μ m), following cortical excavations just above the
291 left hippocampus (Dombeck et al., 2010).

292 **Calcium Imaging by 2-Photon Microscopy**

293 Typically, as cells become activated and elicit action potentials, there is
294 often a large concomitant influx of Ca^{2+} ions through voltage gated
295 calcium channels all around the perisomatic membrane, amongst other
296 cellular compartments. Several organic dyes have been developed that
297 reversibly bind Ca^{2+} ions in the cytosol and either become fluorescent
298 or emit greater fluorescence (often with a red shift) when in this Ca^{2+} -
299 bound state (Paredes et al., 2008). Additionally tremendous advances
300 in molecular biology has seen the deployment of Genetically Encoded

301 Calcium Indicators (GECIs) that may be exogenously incorporated into
302 the genome of target cells. These GECIs serve the same function as
303 organic calcium dyes, but may easily be replenished in the cytosol
304 given the cell's natural machinery for transcription and translation, and
305 whose Fluorescence properties can be engineered for brightness,
306 responsivity, Ca^{2+} binding K_d , and fluorescence emission wavelengths.
307 The number of cells that may be recorded by fluorescence is often only
308 limited to either the spread of the organic dye or the imaging
309 magnification settings, allowing for yields of 100-1000.

310 A major advancement in Fluorescence Imaging was the invention of
311 Confocal and Multiphoton (typically 2-Photon) Microscopes, which
312 allowed for unprecedented recording signal-to-noise by optical
313 sectioning. 2-Photon Imaging itself was an important development for
314 the neurophysiology of tissue greater than 300 μm in thickness, typical
315 of rodent brain tissue, because it avoids wasteful excitation of imaging
316 planes that are not in focus. The 2-Photon effect requires two photons
317 of longer wavelength (lower energy per photon), to near
318 instantaneously excite a fluorophore, a phenomenon that is most likely
319 only possible at the focal point of the microscope objective lens.
320 Additionally, longer wavelengths of excitation light can more easily
321 penetrate deeper layers of tissue, due to comparatively lower
322 scattering or Rayleigh effect (Denk et al., 1990; Helmchen & Denk,
323 2005).

324 The Hippocampus (specifically the Hippocampal CA1) was the main
325 brain structure of interest for all our physiology experiments, and lies
326 under about 1 mm of cortical tissue for mice. This is a depth that is
327 difficult to image even with 2-Photon Microscopy. The typical
328 methodology employed in such cases is to perform a cortical

329 excavation just above the Hippocampus filling the crevice with optically
330 clearer agarose or silicone elastomer. Even so, the Hippocampal CA1
331 cell body layer (*Stratum Pyramidale*) still lies about 150-300 µm below
332 the external capsule and corpus callosum fibers (left intact for chronic
333 imaging). Accordingly, we combined cortical excavation with 2-Photon
334 microscopy, using a long working distance objective with a wide field of
335 view, imaging cytosolic Ca²⁺ activity with the help of either an organic
336 dye (OGB-1; acute imaging) or a GECI (GCaMP6f; chronic imaging).

337 An important perspective that has motivated the use of Imaging based
338 physiology recordings (as opposed to Electrophysiological methods)
339 other than potential yield, is that imaging provides anatomical
340 confirmation of any particular recorded cell, and this in turn allows for
341 a Unambiguous isolation of the same cell across multiple imaging
342 sessions (across days and weeks). Single-Units are ultimately
343 only algorithmically resolved and this can be done only for cells
344 that are active and are represented in multiple spatially
345 separated electrodes. However, very recently, Ashesh Dhawale
346 and colleagues from Bence Olveczky's lab have devised a
347 solution to track the movement of electrodes in tissue over time
348 and use this information to ensure chronic recording of the
349 same units (Dhawale et al., 2017). This technique was not
350 available at the time when experiments for this thesis were
351 started.
352 b Unambiguous detection of the lack of activity in an otherwise
353 recorded cell. Since the cell can be anatomically identified
354 independent of activity, it is possible to observe the absence of
355 Ca²⁺ activity. Automated cell ROI detection (Francis et al., 2012;
356 Maruyama et al., 2014; Mukamel et al., 2009; Pachitariu et al.,
357 2017; Pnevmatikakis et al., 2016) (Francis et al., 2012;

358 Maruyama et al., 2014; Mukamel et al., 2009; Pachitariu et al.,
359 2017; Pnevmatikakis et al., 2016) simplifies the pre-processing
360 step of cell isolation even over large batch sizes. These
361 procedures inherently require the use of the calcium activity
362 profiles of recorded cells. This meant that this advantage was
363 lost in over the course of the experiments.

364 **Automated ROI detection for large-scale Calcium** 365 **Imaging datasets**

366 A number of automated ROI detection algorithms have been cited in
367 literature that require minimal user intervention, perform relatively fast
368 identification for a large number of identified sources (putative cells).
369 Some popular algorithms include PCA/ICA (Mukamel et al., 2009),
370 Suite2p (Pachitariu et al., 2017), and Non-Negative Matrix
371 Factorization (NNMF)(Pnevmatikakis et al., 2016), which all have been
372 developed to the extent where comparable or oftentimes much better
373 ROI detection is achieved than as compared to the more tedious hand-
374 drawn ROIs which scales very poorly with orders of cells recorded.
375 We have strictly followed Suite2p (Pachitariu et al., 2017) for all
376 physiological ROI (cell sources) described in this thesis.

377 **A brief introduction to associative learning based** 378 **behaviour**

379 Prior to the early 20th century, Structuralism was a dominant
380 perspective in Psychology, insisting on introspection - the observation
381 and report of one's own mind and thoughts. Experiments and

382 discoveries by Ivan Pavlov at the Military Medical Academy in
383 Petrograd (St. Petersburg), eventually led to a dramatic shift in
384 perspective, with the birth of Classical Conditioning, a type of
385 associative learning. Following the very same methodology advocated
386 by Francis Bacon (early 17th century), quantitative data from carefully
387 conducted animal experiments were recorded, with the idea to narrow
388 down on a small number of hypotheses that could explain experimental
389 observations.

390 Ivan Pavlov provided essential demonstrations of anticipation and
391 made tremendous progress in understanding the circumstances on
392 which anticipation depends, and this is why Classical Conditioning is
393 also often referred to as Pavlovian Conditioning. Following Pavlov's
394 studies (Pavlov, 1927), it was proposed that Classical Conditioning
395 was a prototypical example of Association. While it does have caveats
396 such as covert learning when observable behaviour may be blocked
397 (Dickinson et al., 1983; Krupa & Thompson, 2003), Associative
398 learning is rich with a variety of animals and association tasks that
399 have been crucial to study memory and learning over the past century.

400 Typically, animals require no prior training to elicit a behavioural or
401 motor movement to biologically potent stimulus (appetitive or aversive),
402 called an Unconditioned Stimulus (US). Examples include food, water,
403 electrical shock, temperature shock, etc.. Without pairing with a US, a
404 neutral stimulus elicits no observable response from an animal, and
405 such a stimulus is called a Conditioned Stimulus (CS). Examples
406 include simple auditory tones, flashes of light, among others.

407 Classical Conditioning is both the behavioural procedure as well as the
408 learning process that results from the pairing of a previously neutral

409 stimulus (CS) with a biologically potent stimulus (US). Repeated
410 pairing allows animals to make implicit associations between the CS
411 and US, and essentially anticipate the occurrence of the US, once the
412 CS is observed. Animals report this forecasting feat by producing the
413 same response that they would to a US, albeit often a milder version.
414 Typical protocols for Classical Conditioning, follow the regime of
415 Forward pairing, viz., - the CS is presented before the US, and this
416 temporal structure will be followed unanimously across all behaviour
417 experiments described in this thesis.

418 The standardization of the behavioural task, physiological recording
419 (imaging) preparation, as well as the custom analysis routines to look
420 for various physiological features will be described in this thesis.
421 Combining these multi-disciplinary approaches allowed us to develop a
422 toolkit to study Time Cells in the Hippocampus, under strict behavioural
423 contexts.

424 **Short Summaries of the 3 projects**

425 **Project I - How do sensory representations transform 426 with learning?**

427 Sensory Systems Neuroscience is a very popular field spanning
428 studies looking at numerous brain regions and sub-regions in the
429 cortex and hippocampus, *in vivo* (R. A. Andersen et al., 1993; Fassihi
430 et al., 2017; Khan et al., 2010; Meeks et al., 2010; Petersen, 2019;
431 Poort et al., 2015; Voelcker et al., 2022), among several others. Many
432 if not most of these studies describe neural activity in animals with
433 expert levels of behavioural learning and performance. Lacunae still
434 remain as to mechanisms deployed during active or online learning
435 especially in the early stages of behavioural training.

436 We deployed our experiments with the intention to study how Calcium
437 Imaging by 2-Photon could reveal finer population level details of
438 network activity as the animals were tested on the learning of an
439 operant conditioning or lick behaviour task. We were able to,

- 440 1. Prototype OGB-1 based calcium imaging *in vivo*, from head-
441 fixed mice in a manner suited to combined behaviour and
442 recording experiments, and
- 443 2. Study preliminary data from animals that correlation based
444 functional activity clusters of recorded CA1 cells have spatial
445 organization during bouts of spontaneous activity.

446 However, we were not satisfied with the level and rate of learning in
447 our test animals eventually leading to a search for more stable
448 behaviour paradigms in mice. Additionally, the use of OGB-1 as the
449 Calcium Indicator also had to be abandoned since this fundamentally
450 disallowed multi-day tracking of the same cells. We discuss our
451 prototyping efforts and preliminary data for this project in detail, in the
452 first few sections each of Chapters 2 (“Behaviour”) and 3 (“Imaging”).

453 **Project II - How does the timing of cellular activity adjust
454 to behavioural task variables?**

455 Research on the cerebellum has made substantial progress in the
456 elucidation of network mechanisms correlating well with external
457 stimulus timing based variables, as animals learn Trace Eye-Blink
458 Conditioning and Delay Conditioning (Kalmbach, Davis, et al., 2010;
459 Kalmbach, Ohyama, et al., 2010; Medina et al., 2000; Ohyama et al.,
460 2003; Siegel & Mauk, 2013). The predominant studies on time cells in
461 the hippocampus have focused on the context of appetitive reinforcing

462 stimuli (Eichenbaum, 2004, 2017; B. Kraus et al., 2013; B. J. Kraus et
463 al., 2015; MacDonald et al., 2011, 2013; Mau et al., 2018; Pastalkova
464 et al., 2008). However, hippocampal mechanisms for Trace Eye-Blink
465 conditioning have not been studied in detail, especially given the
466 different behavioural context of aversive unconditioned stimuli.

467 We prototyped a GCaMP6f based *in vivo* Hippocampal preparation
468 that allowed for chronic, longitudinal recordings of hippocampal CA1,
469 by 2-Photon Calcium Imaging (D. A. Dombeck et al., 2010) that could
470 be combined with a stable and adaptable learning protocols of Trace
471 Eye-Blink Conditioning (Siegel et al., 2015).

472 From our preliminary set of recordings we were able to,
473 1. Detect Time Cells in our population recordings,
474 2. Observe signs of expansion of the time cell sub-population over
475 early stages of learning, and
476 3. Observe shifts in the timing of peak for known, chronically
477 tracked time cells, typically moving away from the US and
478 towards the CS.

479 Technical difficulties prevented us from expanding our experimental
480 recording datasets to the point where these results could be looked at
481 more critically and the results may be sufficient for publication. We
482 discuss our prototyping efforts and preliminary data for this project in
483 detail, in the last few sections each of Chapters 2 (“Behaviour”) and 3
484 (“Imaging”).

485 **Project III - What is the best way to detect and score**
486 **time-tuned cellular activity**

487 Given that we had collected a reasonable sample of multi-day tracked
488 cells while head-fixed mice were being trained to a Trace Eye-Blink
489 Conditioning (TEC) task, we wished to move forward to identifying
490 Time Cells in the most reliable way, with the aim to drawing quality
491 conclusions from the physiology recordings.

492 The paper entitled “Synthetic Data Resource and Benchmarks for Time
493 Cell Analysis and Detection Algorithms” (Ananthamurthy & Bhalla,
494 2023) was a consolidation of our progress to analyse physiology data
495 from real and synthetic cells expressed as calcium activity trials and
496 sessions.

497 Here, we used a computational approach and developed categorically
498 labelled, user definable, large scale synthetic datasets, as a test bed to
499 compare and benchmark the predictions made by popular time cell
500 detection algorithms. We were able to test the sensitivity of these
501 computational algorithms across a wide array of experimental
502 recording parameters, and could ultimately conclude the best
503 operational regimes for each of them. All of the code base for this
504 project is freely available online
505 (<https://github.com/bhallalab/TimeCellAnalysis>) and is intended to be a
506 resource to researchers.

507 The paper is attached as Chapter 4 (“Analysis”).

508 **Bibliography**

509 Abe, R., Sakaguchi, T., Matsumoto, N., Matsuki, N., & Ikegaya, Y.
510 (2014). Sound-induced hyperpolarization of hippocampal neurons.

- 511 *Neuroreport*, 25(13), 1013–1017.
512 <https://doi.org/10.1097/WNR.0000000000000206>
- 513 Ananthamurthy, K. G., & Bhalla, U. S. (2023). Synthetic Data Resource
514 and Benchmarks for Time Cell Analysis and Detection Algorithms.
515 *ENeuro*, ENEURO.0007-22.2023.
516 <https://doi.org/10.1523/ENEURO.0007-22.2023>
- 517 Andermann, M. L., Gilfoy, N. B., Goldey, G. J., Sachdev, R. N. S.,
518 Wölfel, M., McCormick, D. A., Reid, R. C., & Levene, M. J. (2013).
519 Chronic Cellular Imaging of Entire Cortical Columns in Awake
520 Mice Using Microprisms. *Neuron*, 80(4), 900–913.
521 <https://doi.org/10.1016/j.neuron.2013.07.052>
- 522 Andersen, P., Morris, R., Amaral, D., Bliss, T., & O'Keefe, J. (Eds.).
523 (2006). *The Hippocampus Book*. Oxford University Press.
524 <https://doi.org/10.1093/acprof:oso/9780195100273.001.0001>
- 525 Andersen, R. A., Snyder, L. H., Li, C.-S., & Stricanne, B. (1993).
526 Coordinate transformations in the representation of spatial
527 information. *Current Opinion in Neurobiology*, 3(2), 171–176.
528 [https://doi.org/https://doi.org/10.1016/0959-4388\(93\)90206-E](https://doi.org/https://doi.org/10.1016/0959-4388(93)90206-E)
- 529 Aronov, D., Nevers, R., & Tank, D. W. (2017). Mapping of a non-spatial
530 dimension by the hippocampal-entorhinal circuit. *Nature*,
531 543(7647), 719–722. <https://doi.org/10.1038/nature21692>
- 532 Aronov, D., & Tank, D. W. (2014). Engagement of Neural Circuits
533 Underlying 2D Spatial Navigation in a Rodent Virtual Reality
534 System. *Neuron*, 84(2).
535 <https://doi.org/10.1016/j.neuron.2014.08.042>
- 536 Attardo, A., Fitzgerald, J. E., & Schnitzer, M. J. (2015). Impermanence
537 of dendritic spines in live adult CA1 hippocampus. *Nature*,
538 523(7562), 592–596. <https://doi.org/10.1038/nature14467>
- 539 Barretto, R. P. J., Messerschmidt, B., & Schnitzer, M. J. (2009). In vivo
540 fluorescence imaging with high-resolution microlenses. *Nature
541 Methods*, 6(7), 511–512. <https://doi.org/10.1038/nmeth.1339>
- 542 Bayesian brain: Probabilistic approaches to neural coding. (2007). In
543 K. Doya, S. Ishii, A. Pouget, & R. P. N. Rao (Eds.), *Bayesian
544 brain: Probabilistic approaches to neural coding*. MIT Press.

- 545 Bellistri, E., Aguilar, J., Brotons-Mas, J. R., Foffani, G., & de la Prida, L.
546 M. (2013). Basic properties of somatosensory-evoked responses
547 in the dorsal hippocampus of the rat. *The Journal of Physiology*,
548 591(10), 2667–2686. <https://doi.org/10.1113/jphysiol.2013.251892>
- 549 Bhalla, U. S. (2014a). Chapter Fourteen - Multiscale Modeling and
550 Synaptic Plasticity. In K. T. B. T.-P. in M. B. and T. S. Blackwell
551 (Ed.), *Computational Neuroscience* (Vol. 123, pp. 351–386).
552 Academic Press. [https://doi.org/https://doi.org/10.1016/B978-0-12-397897-4.00012-7](https://doi.org/10.1016/B978-0-12-397897-4.00012-7)
- 554 Bhalla, U. S. (2014b). Molecular computation in neurons: a modeling
555 perspective. *Current Opinion in Neurobiology*, 25, 31–37.
556 <https://doi.org/https://doi.org/10.1016/j.conb.2013.11.006>
- 557 Bhalla, U. S. (2017). Synaptic input sequence discrimination on
558 behavioral timescales mediated by reaction-diffusion chemistry in
559 dendrites. *eLife*, 6, e25827. <https://doi.org/10.7554/eLife.25827>
- 560 Bhalla, U. S. (2019). Dendrites, deep learning, and sequences in the
561 hippocampus. *Hippocampus*, 29(3), 239–251.
562 <https://doi.org/https://doi.org/10.1002/hipo.22806>
- 563 Binder, M. D., Hirokawa, N., & Windhorst, U. (Eds.). (2009). *Delayed
564 Non-match-to-Sample Task BT - Encyclopedia of Neuroscience*
565 (p. 934). Springer Berlin Heidelberg. https://doi.org/10.1007/978-3-540-29678-2_1425
- 567 Brown, G. D. (1998). Nonassociative learning processes affecting
568 swimming probability in the seastar Tritonia diomedea:
569 habituation, sensitization and inhibition. *Behavioural Brain
570 Research*, 95(2), 151–165.
571 [https://doi.org/https://doi.org/10.1016/S0166-4328\(98\)00072-2](https://doi.org/https://doi.org/10.1016/S0166-4328(98)00072-2)
- 572 Buzsáki, G., & Llinás, R. (2017). Space and time in the brain. *Science
573 (New York, N.Y.)*, 358(6362), 482–485.
574 <https://doi.org/10.1126/science.aan8869>
- 575 Cai, D. J., Aharoni, D., Shuman, T., Shobe, J., Biane, J., Song, W.,
576 Wei, B., Veshkini, M., La-Vu, M., Lou, J., Flores, S. E., Kim, I.,
577 Sano, Y., Zhou, M., Baumgaertel, K., Lavi, A., Kamata, M.,
578 Tuszyński, M., Mayford, M., ... Silva, A. J. (2016). A shared neural

- 579 ensemble links distinct contextual memories encoded close in
580 time. *Nature*, 534(7605), 115–118.
581 <https://doi.org/10.1038/nature17955>
- 582 Caporale, N., & Dan, Y. (2008). Spike timing-dependent plasticity: a
583 Hebbian learning rule. *Annual Review of Neuroscience*, 31, 25–
584 46. <https://doi.org/10.1146/annurev.neuro.31.060407.125639>
- 585 Chen, T.-W., Wardill, T. J., Sun, Y., Pulver, S. R., Renninger, S. L.,
586 Baohan, A., Schreiter, E. R., Kerr, R. A., Orger, M. B., Jayaraman,
587 V., Looger, L. L., Svoboda, K., & Kim, D. S. (2013). Ultrasensitive
588 fluorescent proteins for imaging neuronal activity. *Nature*,
589 499(7458), 295–300. <https://doi.org/10.1038/nature12354>
- 590 Chun, M. M., & Johnson, M. K. (2011). Memory: enduring traces of
591 perceptual and reflective attention. *Neuron*, 72(4), 520–535.
592 <https://doi.org/10.1016/j.neuron.2011.10.026>
- 593 Conen, K. E., & Desrochers, T. M. (2022). *The Neural Basis of
594 Behavioral Sequences in Cortical and Subcortical Circuits*. Oxford
595 University Press.
596 <https://doi.org/10.1093/acrefore/9780190264086.013.421>
- 597 Davidson, T. J., Kloosterman, F., & Wilson, M. A. (2009). Hippocampal
598 replay of extended experience. *Neuron*, 63(4), 497–507.
599 <https://doi.org/10.1016/j.neuron.2009.07.027>
- 600 Denk, W., Strickler, J. H., & Webb, W. W. (1990). Two-photon laser
601 scanning fluorescence microscopy. *Science (New York, N.Y.)*,
602 248(4951), 73–76. <https://doi.org/10.1126/science.2321027>
- 603 Deshmukh, S. S., & Bhalla, U. S. (2003). Representation of odor
604 habituation and timing in the hippocampus. *The Journal of
605 Neuroscience : The Official Journal of the Society for
606 Neuroscience*, 23(5), 1903–1915.
607 <https://doi.org/10.1523/JNEUROSCI.23-05-01903.2003>
- 608 Dhawale, A. K., Poddar, R., Wolff, S. B. E., Normand, V. A.,
609 Kopelowitz, E., & Ölveczky, B. P. (2017). Automated long-term
610 recording and analysis of neural activity in behaving animals.
611 *eLife*, 6, e27702. <https://doi.org/10.7554/eLife.27702>

- 612 Dickinson, A., Nicholas, D. J., & Mackintosh, N. J. (1983). A re-
613 examination of one-trial blocking in conditioned suppression. *The*
614 *Quarterly Journal of Experimental Psychology B: Comparative and*
615 *Physiological Psychology*, 35, 67–79.
616 <https://doi.org/10.1080/14640748308400914>
- 617 Dombeck, D. A., Graziano, M. S., & Tank, D. W. (2009). Functional
618 clustering of neurons in motor cortex determined by cellular
619 resolution imaging in awake behaving mice. *The Journal of*
620 *Neuroscience : The Official Journal of the Society for*
621 *Neuroscience*, 29(44), 13751–13760.
622 <https://doi.org/10.1523/JNEUROSCI.2985-09.2009>
- 623 Dombeck, D. A., Harvey, C. D., Tian, L., Looger, L. L., & Tank, D. W.
624 (2010). Functional imaging of hippocampal place cells at cellular
625 resolution during virtual navigation. *Nature Neuroscience*, 13(11),
626 1433–1440. <https://doi.org/10.1038/nn.2648>
- 627 Dombeck, D. A., Khabbaz, A. N., Collman, F., Adelman, T. L., & Tank,
628 D. W. (2007). Imaging large-scale neural activity with cellular
629 resolution in awake, mobile mice. *Neuron*, 56(1), 43–57.
630 <https://doi.org/10.1016/j.neuron.2007.08.003>
- 631 Dombeck, D., & Tank, D. (2014). Two-photon imaging of neural activity
632 in awake mobile mice. *Cold Spring Harbor Protocols*, 2014(7),
633 726–736. <https://doi.org/10.1101/pdb.top081810>
- 634 Dudani, N., Bhalla, U. S., & Ray, S. (2013). *MOOSE, the Multiscale*
635 *Object-Oriented Simulation Environment BT - Encyclopedia of*
636 *Computational Neuroscience* (D. Jaeger & R. Jung (Eds.); pp. 1–
637 4). Springer New York. https://doi.org/10.1007/978-1-4614-7320-6_257-1
- 639 Eichenbaum, H. (2004). Hippocampus: Cognitive processes and
640 neural representations that underlie declarative memory. *Neuron*,
641 44(1), 109–120. <https://doi.org/10.1016/j.neuron.2004.08.028>
- 642 Eichenbaum, H. (2017). On the Integration of Space, Time, and
643 Memory. *Neuron*, 95(5), 1007–1018.
644 <https://doi.org/10.1016/j.neuron.2017.06.036>

- 645 Fanselow, M. S., & Dong, H.-W. (2010). Are the dorsal and ventral
646 hippocampus functionally distinct structures? *Neuron*, 65(1), 7–19.
647 <https://doi.org/10.1016/j.neuron.2009.11.031>
- 648 Fassihi, A., Akrami, A., Pulecchi, F., Schönfelder, V., & Diamond, M. E.
649 (2017). Transformation of Perception from Sensory to Motor
650 Cortex. *Current Biology : CB*, 27(11), 1585-1596.e6.
651 <https://doi.org/10.1016/j.cub.2017.05.011>
- 652 Ferbinteanu, J., & Shapiro, M. L. (2003). Prospective and retrospective
653 memory coding in the hippocampus. *Neuron*, 40(6), 1227–1239.
654 [https://doi.org/10.1016/s0896-6273\(03\)00752-9](https://doi.org/10.1016/s0896-6273(03)00752-9)
- 655 Ferbinteanu, J., Shirvalkar, P., & Shapiro, M. L. (2011). Memory
656 Modulates Journey-Dependent Coding in the Rat Hippocampus.
657 *The Journal of Neuroscience*, 31(25), 9135 LP – 9146.
658 <https://doi.org/10.1523/JNEUROSCI.1241-11.2011>
- 659 Foster, D. J. (2017). Replay Comes of Age. *Annual Review of
660 Neuroscience*, 40, 581–602. <https://doi.org/10.1146/annurev-neuro-072116-031538>
- 662 Foster, D. J., & Wilson, M. A. (2006). Reverse replay of behavioural
663 sequences in hippocampal place cells during the awake state.
664 *Nature*, 440(7084), 680–683. <https://doi.org/10.1038/nature04587>
- 665 Foster, D. J., & Wilson, M. A. (2007). Hippocampal theta sequences.
666 *Hippocampus*, 17(11), 1093–1099.
667 <https://doi.org/10.1002/hipo.20345>
- 668 Francis, M., Qian, X., Charbel, C., Ledoux, J., Parker, J. C., & Taylor,
669 M. S. (2012). Automated region of interest analysis of dynamic
670 Ca²⁺ signals in image sequences. *American Journal of
671 Physiology. Cell Physiology*, 303(3), C236-43.
672 <https://doi.org/10.1152/ajpcell.00016.2012>
- 673 Frank, L. M., Brown, E. N., & Wilson, M. (2000). Trajectory encoding in
674 the hippocampus and entorhinal cortex. *Neuron*, 27(1), 169–178.
675 [https://doi.org/10.1016/s0896-6273\(00\)00018-0](https://doi.org/10.1016/s0896-6273(00)00018-0)
- 676 Fyhn, M., Molden, S., Witter, M. P., Moser, E. I., & Moser, M.-B.
677 (2004). Spatial representation in the entorhinal cortex. *Science*

- 678 (*New York, N.Y.*), 305(5688), 1258–1264.
679 <https://doi.org/10.1126/science.1099901>
- 680 Hafting, T., Fyhn, M., Molden, S., Moser, M.-B., & Moser, E. I. (2005).
681 Microstructure of a spatial map in the entorhinal cortex. *Nature*,
682 436(7052), 801–806. <https://doi.org/10.1038/nature03721>
- 683 Han, J.-H., Kushner, S. A., Yiu, A. P., Hsiang, H.-L. L., Buch, T.,
684 Waisman, A., Bontempi, B., Neve, R. L., Frankland, P. W., &
685 Josselyn, S. A. (2009). Selective erasure of a fear memory.
686 *Science (New York, N.Y.)*, 323(5920), 1492–1496.
687 <https://doi.org/10.1126/science.1164139>
- 688 Harvey, C. D., Collman, F., Dombeck, D. A., & Tank, D. W. (2009).
689 Intracellular dynamics of hippocampal place cells during virtual
690 navigation. *Nature*, 461(7266), 941–946.
691 <https://doi.org/10.1038/nature08499>
- 692 Hebb, D. O. (1949). The organization of behavior; a
693 neuropsychological theory. In *The organization of behavior; a
694 neuropsychological theory*. Wiley.
- 695 Helmchen, F., & Denk, W. (2005). *Deep tissue two-photon microscopy*.
696 2(12), 9. <https://doi.org/10.1038/nmeth818>
- 697 Hjorth-Simonsen, A., & Jeune, B. (1972). Origin and termination of the
698 hippocampal perforant path in the rat studied by silver
699 impregnation. *The Journal of Comparative Neurology*, 144(2),
700 215–232. <https://doi.org/10.1002/cne.901440206>
- 701 Hubel, D. H., & Wiesel, T. N. (1962). Receptive fields, binocular
702 interaction and functional architecture in the cat's visual cortex.
703 *The Journal of Physiology*, 160(1), 106–154.
704 <https://doi.org/10.1113/jphysiol.1962.sp006837>
- 705 Hutchinson, J. B., & Turk-Browne, N. B. (2012). Memory-guided
706 attention: control from multiple memory systems. *Trends in
707 Cognitive Sciences*, 16(12), 576–579.
708 <https://doi.org/10.1016/j.tics.2012.10.003>
- 709 Itsikov, P. M., Vinnik, E., & Diamond, M. E. (2011). Hippocampal
710 representation of touch-guided behavior in rats: persistent and

- 711 independent traces of stimulus and reward location. *PLoS One*,
712 6(1), e16462. <https://doi.org/10.1371/journal.pone.0016462>
- 713 Jaramillo, S., & Zador, A. M. (2014). Mice and rats achieve similar
714 levels of performance in an adaptive decision-making task . In
715 *Frontiers in Systems Neuroscience* (Vol. 8).
716 <https://www.frontiersin.org/articles/10.3389/fnsys.2014.00173>
- 717 Jun, J. J., Steinmetz, N. A., Siegle, J. H., Denman, D. J., Bauza, M.,
718 Barbarits, B., Lee, A. K., Anastassiou, C. A., Andrei, A., Aydin, Ç.,
719 Barbic, M., Blanche, T. J., Bonin, V., Couto, J., Dutta, B., Gratiy,
720 S. L., Gutnisky, D. A., Häusser, M., Karsh, B., ... Harris, T. D.
721 (2017). Fully integrated silicon probes for high-density recording of
722 neural activity. *Nature*, 551(7679), 232–236.
723 <https://doi.org/10.1038/nature24636>
- 724 Kaifosh, P., Lovett-Barron, M., Turi, G. F., Reardon, T. R., & Losonczy,
725 A. (2013). Septo-hippocampal GABAergic signaling across
726 multiple modalities in awake mice. *Nature Neuroscience*, 16(9),
727 1182–1184. <https://doi.org/10.1038/nn.3482>
- 728 Kalmbach, B. E., Davis, T., Ohyama, T., Riusech, F., Nores, W. L., &
729 Mauk, M. D. (2010). Cerebellar Cortex Contributions to the
730 Expression and Timing of Conditioned Eyelid Responses. *Journal
731 of Neurophysiology*, 103(4), 2039–2049.
732 <https://doi.org/10.1152/jn.00033.2010>
- 733 Kalmbach, B. E., Ohyama, T., & Mauk, M. D. (2010). Temporal
734 Patterns of Inputs to Cerebellum Necessary and Sufficient for
735 Trace Eyelid Conditioning. *Journal of Neurophysiology*, 104(2),
736 627–640. <https://doi.org/10.1152/jn.00169.2010>
- 737 Kamondi, A. (1998). *Theta Oscillations in Somata and Dendrites of
738 Hippocampal Pyramidal Cells In Vivo: Activity-Dependent Phase-
739 Precession of Action Potentials*. 261(March), 244–261.
- 740 Kauvar, I. V., Machado, T. A., Yuen, E., Kochalka, J., Choi, M., Allen,
741 W. E., Wetzstein, G., & Deisseroth, K. (2020). Cortical
742 Observation by Synchronous Multifocal Optical Sampling Reveals
743 Widespread Population Encoding of Actions. *Neuron*, 107(2), 351–
744 367.e19. <https://doi.org/10.1016/j.neuron.2020.04.023>

- 745 Khan, A. G., Parthasarathy, K., & Bhalla, U. S. (2010). Odor
746 representations in the mammalian olfactory bulb. *Wiley*
747 *Interdisciplinary Reviews. Systems Biology and Medicine*, 2(5),
748 603–611. <https://doi.org/10.1002/wsbm.85>
- 749 Kraus, B. J., Brandon, M. P., Robinson, R. J., Connerney, M. A.,
750 Hasselmo, M. E., & Eichenbaum, H. (2015). During Running in
751 Place, Grid Cells Integrate Elapsed Time and Distance Run.
752 *Neuron*, 88(3), 578–589.
753 <https://doi.org/10.1016/j.neuron.2015.09.031>
- 754 Kraus, B., Robinson, R., White, J., Eichenbaum, H., & Hasselmo, M.
755 (2013). Hippocampal “Time Cells”: Time versus Path Integration.
756 *Neuron*, 78(6), 1090–1101.
757 <https://doi.org/10.1016/j.neuron.2013.04.015>
- 758 Kropff, E., Carmichael, J. E., Moser, M.-B., & Moser, E. I. (2015).
759 Speed cells in the medial entorhinal cortex. *Nature*, 523(7561),
760 419–424. <https://doi.org/10.1038/nature14622>
- 761 Krupa, D., & Thompson, R. (2003). Inhibiting the Expression of a
762 Classically Conditioned Behavior Prevents Its Extinction. *The*
763 *Journal of Neuroscience : The Official Journal of the Society for*
764 *Neuroscience*, 23, 10577–10584.
765 <https://doi.org/10.1523/JNEUROSCI.23-33-10577.2003>
- 766 Lovett-Barron, M., Kaifosh, P., Kheirbek, M. A., Danielson, N.,
767 Zaremba, J. D., Reardon, T. R., Turi, G. F., Hen, R., Zemelman,
768 B. V., & Losonczy, A. (2014). Dendritic inhibition in the
769 hippocampus supports fear learning. *Science (New York, N.Y.)*,
770 343(6173), 857–863. <https://doi.org/10.1126/science.1247485>
- 771 Luo, L., Callaway, E. M., & Svoboda, K. (2018). Genetic Dissection of
772 Neural Circuits: A Decade of Progress. *Neuron*, 98(2), 256–281.
773 <https://doi.org/https://doi.org/10.1016/j.neuron.2018.03.040>
- 774 MacDonald, C. J., Carrow, S., Place, R., & Eichenbaum, H. (2013).
775 Distinct hippocampal time cell sequences represent odor
776 memories in immobilized rats. *The Journal of Neuroscience : The*
777 *Official Journal of the Society for Neuroscience*, 33(36), 14607–
778 14616. <https://doi.org/10.1523/JNEUROSCI.1537-13.2013>

- 779 MacDonald, C. J., Lepage, K. Q., Eden, U. T., & Eichenbaum, H.
780 (2011). Hippocampal “time cells” bridge the gap in memory for
781 discontiguous events. *Neuron*, 71(4), 737–749.
782 <https://doi.org/10.1016/j.neuron.2011.07.012>
- 783 Manns, J. R., Clark, R. E., & Squire, L. R. (2000). Parallel acquisition
784 of awareness and trace eyeblink classical conditioning. *Learning &*
785 *Memory (Cold Spring Harbor, N.Y.)*, 7(5), 267–272.
786 <https://doi.org/10.1101/lm.33400>
- 787 Maruyama, R., Maeda, K., Moroda, H., Kato, I., Inoue, M., Miyakawa,
788 H., & Aonishi, T. (2014). Detecting cells using non-negative matrix
789 factorization on calcium imaging data. *Neural Networks : The*
790 *Official Journal of the International Neural Network Society*, 55,
791 11–19. <https://doi.org/10.1016/j.neunet.2014.03.007>
- 792 Mau, W., Sullivan, D. W., Kinsky, N. R., Hasselmo, M. E., Howard, M.
793 W., & Eichenbaum, H. (2018). The Same Hippocampal CA1
794 Population Simultaneously Codes Temporal Information over
795 Multiple Timescales. *Current Biology*, 28(10), 1499-1508.e4.
796 <https://doi.org/10.1016/j.cub.2018.03.051>
- 797 McHugh, T. J., Jones, M. W., Quinn, J. J., Balthasar, N., Coppari, R.,
798 Elmquist, J. K., Lowell, B. B., Fanselow, M. S., Wilson, M. A., &
799 Tonegawa, S. (2007). Dentate gyrus NMDA receptors mediate
800 rapid pattern separation in the hippocampal network. *Science*
801 (*New York, N.Y.*), 317(5834), 94–99.
802 <https://doi.org/10.1126/science.1140263>
- 803 McNaughton, N., & Gray, J. A. (2000). Anxiolytic action on the
804 behavioural inhibition system implies multiple types of arousal
805 contribute to anxiety. *Journal of Affective Disorders*, 61(3), 161–
806 176. [https://doi.org/10.1016/s0165-0327\(00\)00344-x](https://doi.org/10.1016/s0165-0327(00)00344-x)
- 807 Medina, J. F., Garcia, K. S., Nores, W. L., Taylor, N. M., & Mauk, M. D.
808 (2000). Timing mechanisms in the cerebellum: testing predictions
809 of a large-scale computer simulation. *The Journal of*
810 *Neuroscience : The Official Journal of the Society for*
811 *Neuroscience*, 20(14), 5516–5525.
812 <https://doi.org/10.1523/JNEUROSCI.20-14-05516.2000>

- 813 Meeks, J. P., Arnson, H. A., & Holy, T. E. (2010). Representation and
814 transformation of sensory information in the mouse accessory
815 olfactory system. *Nature Neuroscience*, 13(6), 723–730.
816 <https://doi.org/10.1038/nn.2546>
- 817 Mizrahi, A. (2004). High-Resolution In Vivo Imaging of Hippocampal
818 Dendrites and Spines. *Journal of Neuroscience*, 24(13), 3147–
819 3151. <https://doi.org/10.1523/JNEUROSCI.5218-03.2004>
- 820 Modi, M. N., Dhawale, A. K., & Bhalla, U. S. (2014). CA1 cell activity
821 sequences emerge after reorganization of network correlation
822 structure during associative learning. *eLife*, 3, e01982–e01982.
823 <https://doi.org/10.7554/eLife.01982>
- 824 Morris, R. G. M., Garrud, P., Rawlins, J. N. P., & O'Keefe, J. (1982).
825 Place navigation impaired in rats with hippocampal lesions.
826 *Nature*, 297(5868), 681–683. <https://doi.org/10.1038/297681a0>
- 827 Moser, M.-B., & Moser, E. I. (1998). Distributed encoding and retrieval
828 of spatial memory in the hippocampus. In *The Journal of
829 Neuroscience* (Vol. 18, pp. 7535–7542). Society for Neuroscience.
- 830 Moyer, J. R., Deyo, R. A., & Disterhoft, J. F. (1990). Hippocampectomy
831 disrupts trace eye-blink conditioning in rabbits. *Behavioral
832 Neuroscience*, 104(2)(Apr 1990), 243–252.
833 <https://doi.org/10.1037/0735-7044.104.2.243>
- 834 Mukamel, E. A., Nimmerjahn, A., & Schnitzer, M. J. (2009). Automated
835 analysis of cellular signals from large-scale calcium imaging data.
836 *Neuron*, 63(6), 747–760.
837 <https://doi.org/10.1016/j.neuron.2009.08.009>
- 838 Murray, T. A., & Levene, M. J. (2012). Singlet gradient index lens for
839 deep in vivo multiphoton microscopy. *Journal of Biomedical
840 Optics*, 17(2), 021106. <https://doi.org/10.1117/1.JBO.17.2.021106>
- 841 Nakashiba, T., Young, J. Z., McHugh, T. J., Buhl, D. L., & Tonegawa,
842 S. (2008). Transgenic inhibition of synaptic transmission reveals
843 role of CA3 output in hippocampal learning. *Science (New York,
844 N.Y.)*, 319(5867), 1260–1264.
845 <https://doi.org/10.1126/science.1151120>

- 846 O'Keefe, J., & Dostrovsky, J. (1971). The hippocampus as a spatial
847 map. Preliminary evidence from unit activity in the freely-moving
848 rat. *Brain Research*, 34(1), 171–175. [https://doi.org/10.1016/0006-8993\(71\)90358-1](https://doi.org/10.1016/0006-8993(71)90358-1)
- 850 O'Keefe, J., & Recce, M. L. (1993). Phase relationship between
851 hippocampal place units and the EEG theta rhythm.
852 *Hippocampus*, 3(3), 317–330.
853 <https://doi.org/10.1002/hipo.450030307>
- 854 Ohayama, T., Nores, W. L., Murphy, M., & Mauk, M. D. (2003). What
855 the cerebellum computes. *Trends in Neurosciences*, 26(4), 222–
856 227. [https://doi.org/10.1016/S0166-2236\(03\)00054-7](https://doi.org/10.1016/S0166-2236(03)00054-7)
- 857 Pachitariu, M., Stringer, C., Dipoppa, M., Schröder, S., Rossi, L. F.,
858 Dalgleish, H., Carandini, M., & Harris, K. D. (2017). Suite2p:
859 beyond 10,000 neurons with standard two-photon microscopy.
860 *BioRxiv*, 61507. <https://doi.org/10.1101/061507>
- 861 Paredes, R. M., Etzler, J. C., Watts, L. T., Zheng, W., & Lechleiter, J.
862 D. (2008). Chemical calcium indicators. *Methods (San Diego,*
863 *Calif.)*, 46(3), 143–151.
864 <https://doi.org/10.1016/j.ymeth.2008.09.025>
- 865 Pastalkova, E., Itskov, V., Amarasingham, A., & Buzsaki, G. (2008).
866 Internally Generated Cell Assembly Sequences in the Rat
867 Hippocampus. *Science*, 321(5894), 1322–1327.
868 <https://doi.org/10.1126/science.1159775>
- 869 Pavlov, I. P. (1927). Conditioned reflexes: an investigation of the
870 physiological activity of the cerebral cortex. In *Conditioned*
871 *reflexes: an investigation of the physiological activity of the*
872 *cerebral cortex*. Oxford Univ. Press.
- 873 Peron, S. P., Freeman, J., Iyer, V., Guo, C., & Svoboda, K. (2015). A
874 Cellular Resolution Map of Barrel Cortex Activity during Tactile
875 Behavior. *Neuron*, 86(3), 783–799.
876 <https://doi.org/10.1016/j.neuron.2015.03.027>
- 877 Petersen, C. C. H. (2019). Sensorimotor processing in the rodent
878 barrel cortex. *Nature Reviews. Neuroscience*, 20(9), 533–546.
879 <https://doi.org/10.1038/s41583-019-0200-y>

- 880 Pnevmatikakis, E. A., Soudry, D., Gao, Y., Machado, T. A., Merel, J.,
881 Pfau, D., Reardon, T., Mu, Y., Lacefield, C., Yang, W., Ahrens, M.,
882 Bruno, R., Jessell, T. M., Peterka, D. S., Yuste, R., & Paninski, L.
883 (2016). Simultaneous Denoising, Deconvolution, and Demixing of
884 Calcium Imaging Data. *Neuron*, 89(2), 285–299.
885 <https://doi.org/https://doi.org/10.1016/j.neuron.2015.11.037>
- 886 Poort, J., Khan, A. G., Pachitariu, M., Nemri, A., Orsolic, I., Krupic, J.,
887 Bauza, M., Sahani, M., Keller, G. B., Mrsic-Flogel, T. D., & Hofer,
888 S. B. (2015). Learning Enhances Sensory and Multiple Non-
889 sensory Representations in Primary Visual Cortex. *Neuron*, 86(6),
890 1478–1490. <https://doi.org/10.1016/j.neuron.2015.05.037>
- 891 Ranck, J. B. (1973). Studies on single neurons in dorsal hippocampal
892 formation and septum in unrestrained rats: Part I. Behavioral
893 correlates and firing repertoires. *Experimental Neurology*, 41(2),
894 462–531. [https://doi.org/https://doi.org/10.1016/0014-4886\(73\)90290-2](https://doi.org/https://doi.org/10.1016/0014-4886(73)90290-2)
- 895
- 896 Ranck, J. B. (1975). *Behavioral Correlates and Firing Repertoires of
897 Neurons in the Dorsal Hippocampal Formation and Septum of
898 Unrestrained Rats BT - The Hippocampus: Volume 2:
899 Neurophysiology and Behavior* (R. L. Isaacson & K. H. Pribram
900 (Eds.); pp. 207–244). Springer US. https://doi.org/10.1007/978-1-4684-2979-4_7
- 901
- 902 Rao, R. P. N., & Ballard, D. H. (1999). Predictive coding in the visual
903 cortex: a functional interpretation of some extra-classical
904 receptive-field effects. *Nature Neuroscience*, 2(1), 79–87.
905 <https://doi.org/10.1038/4580>
- 906
- 907 Rogerson, T., Cai, D. J., Frank, A., Sano, Y., Shobe, J., Lopez-Aranda,
908 M. F., & Silva, A. J. (2014). Synaptic tagging during memory
909 allocation. *Nature Reviews. Neuroscience*, 15(3), 157–169.
<https://doi.org/10.1038/nrn3667>
- 910
- 911 Schreurs, B. G. (1989). Classical conditioning of model systems: A
912 behavioral review. *Psychobiology*, 17(2), 145–155.
<https://doi.org/10.3758/BF03337830>
- 913
- 914 Scoville, W. B., & Milner, B. (1957). Loss of recent memory after
bilateral hippocampal lesions. In *Journal of Neurology*,

- 915 *Neurosurgery & Psychiatry* (Vol. 20, pp. 11–21). BMJ Publishing
916 Group. <https://doi.org/10.1136/jnnp.20.1.11>
- 917 Sheffield, M. E. J., & Dombek, D. A. (2014). Calcium transient
918 prevalence across the dendritic arbour predicts place field
919 properties. *Nature*, 517(7533), 200–204.
920 <https://doi.org/10.1038/nature13871>
- 921 Siegel, J. J., & Mauk, M. D. (2013). Persistent Activity in Prefrontal
922 Cortex during Trace Eyelid Conditioning: Dissociating Responses
923 That Reflect Cerebellar Output from Those That Do Not. *The*
924 *Journal of Neuroscience*, 33(38), 15272 LP – 15284.
925 <https://doi.org/10.1523/JNEUROSCI.1238-13.2013>
- 926 Siegel, J. J., Taylor, W., Gray, R., Kalmbach, B., Zemelman, B. V.,
927 Desai, N. S., Johnston, D., & Chitwood, R. A. (2015). Trace
928 Eyeblink Conditioning in Mice Is Dependent upon the Dorsal
929 Medial Prefrontal Cortex, Cerebellum, and Amygdala: Behavioral
930 Characterization and Functional Circuitry. *ENeuro*, 2(4),
931 ENEURO.0051-14.2015. <https://doi.org/10.1523/ENEURO.0051-14.2015>
- 933 Skaggs, W., McNaughton, B., Gothard, K., & Markus, E. (1996). An
934 Information-Theoretic Approach to Deciphering the Hippocampal
935 Code. *Neural Inf. Process Syst.*, 5.
- 936 Souza, B. C., Pavão, R., Belchior, H., & Tort, A. B. L. (2018). On
937 Information Metrics for Spatial Coding. *Neuroscience*, 375, 62–73.
938 <https://doi.org/10.1016/j.neuroscience.2018.01.066>
- 939 Stosiek, C., Garaschuk, O., Holthoff, K., & Konnerth, A. (2003). In vivo
940 two-photon calcium imaging of neuronal networks. *Proceedings of*
941 *the National Academy of Sciences of the United States of*
942 *America*, 100(12), 7319–7324.
943 <https://doi.org/10.1073/pnas.1232232100>
- 944 Suh, J., Rivest, A. J., Nakashiba, T., Tominaga, T., & Tonegawa, S.
945 (2011). Entorhinal cortex layer III input to the hippocampus is
946 crucial for temporal association memory. *Science (New York,*
947 *N.Y.*), 334(6061), 1415–1420.
948 <https://doi.org/10.1126/science.1210125>

- 949 Taube, J. S., Muller, R. U., & Ranck, J. B. J. (1990). Head-direction
950 cells recorded from the postsubiculum in freely moving rats. I.
951 Description and quantitative analysis. *The Journal of
952 Neuroscience : The Official Journal of the Society for
953 Neuroscience*, 10(2), 420–435.
954 <https://doi.org/10.1523/JNEUROSCI.10-02-00420.1990>
- 955 Tseng, W., Guan, R., Disterhoft, J. F., & Weiss, C. (2004). Trace
956 eyeblink conditioning is hippocampally dependent in mice.
957 *Hippocampus*, 14(1), 58–65. <https://doi.org/10.1002/hipo.10157>
- 958 Uncapher, M. R., Hutchinson, J. B., & Wagner, A. D. (2011).
959 Dissociable effects of top-down and bottom-up attention during
960 episodic encoding. *The Journal of Neuroscience : The Official
961 Journal of the Society for Neuroscience*, 31(35), 12613–12628.
962 <https://doi.org/10.1523/JNEUROSCI.0152-11.2011>
- 963 Velasco, M. G. M., & Levene, M. J. (2014). In vivo two-photon
964 microscopy of the hippocampus using glass plugs. *Biomedical
965 Optics Express*, 5(6), 1700–1708.
966 <https://doi.org/10.1364/BOE.5.001700>
- 967 Vinogradova, O. S. (2001). Hippocampus as comparator: Role of the
968 two input and two output systems of the hippocampus in selection
969 and registration of information. *Hippocampus*, 11(5), 578–598.
970 <https://doi.org/https://doi.org/10.1002/hipo.1073>
- 971 Voelcker, B., Pancholi, R., & Peron, S. (2022). Transformation of
972 primary sensory cortical representations from layer 4 to layer 2.
973 *Nature Communications*, 13(1), 5484.
974 <https://doi.org/10.1038/s41467-022-33249-1>
- 975 Wood, E. R., Dudchenko, P. A., Robitsek, R. J., & Eichenbaum, H.
976 (2000). Hippocampal Neurons Encode Information about Different
977 Types of Memory Episodes Occurring in the Same Location.
978 *Neuron*, 27(3), 623–633.
979 [https://doi.org/https://doi.org/10.1016/S0896-6273\(00\)00071-4](https://doi.org/https://doi.org/10.1016/S0896-6273(00)00071-4)
- 980 Yiu, A. P., Mercaldo, V., Yan, C., Richards, B., Rashid, A. J., Hsiang,
981 H.-L. L., Pressey, J., Mahadevan, V., Tran, M. M., Kushner, S. A.,
982 Woodin, M. A., Frankland, P. W., & Josselyn, S. A. (2014).
983 Neurons are recruited to a memory trace based on relative

- 984 neuronal excitability immediately before training. *Neuron*, 83(3),
985 722–735. <https://doi.org/10.1016/j.neuron.2014.07.017>
- 986 Zhang, S., & Manahan-Vaughan, D. (2015). Spatial olfactory learning
987 contributes to place field formation in the hippocampus. *Cerebral
988 Cortex (New York, N.Y.: 1991)*, 25(2), 423–432.
989 <https://doi.org/10.1093/cercor/bht239>
- 990 Zhou, S., Masmanidis, S. C., & Buonomano, D. V. (2020). Neural
991 Sequences as an Optimal Dynamical Regime for the Readout of
992 Time. *Neuron*, 108(4), 651-658.e5.
993 <https://doi.org/https://doi.org/10.1016/j.neuron.2020.08.020>
- 994 Zhou, Y., Won, J., Karlsson, M. G., Zhou, M., Rogerson, T., Balaji, J.,
995 Neve, R., Poirazi, P., & Silva, A. J. (2009). CREB regulates
996 excitability and the allocation of memory to subsets of neurons in
997 the amygdala. *Nature Neuroscience*, 12(11), 1438–1443.
998 <https://doi.org/10.1038/nn.2405>
- 999 Ziv, Y., Burns, L. D., Cocker, E. D., Hamel, E. O., Ghosh, K. K., Kitch,
1000 L. J., El Gamal, A., & Schnitzer, M. J. (2013). Long-term dynamics of
1001 CA1 hippocampal place codes. *Nature Neuroscience*, 16(3), 264–266.
1002 <https://doi.org/10.1038/nn.3329>
- 1003

1004 Chapter 2 – Behaviour

1005 **Towards understanding brain activity in 1006 a reproducible context**

1007 Our understanding of memory and learning depends upon the type of
1008 learning that is studied (Schreurs, 1989). Two important categories of
1009 memory and learning experiments are,
1010 1. Non-associative (Habituation and Sensitization), and
1011 2. Associative learning (Classical and Operant Conditioning).

1012 Non-associative learning paradigms provide information about how an
1013 organism responds to repeated presentations of a single stimulus
1014 (Brown, 1998). However, it was of interest to us to study how animals
1015 responded to a number of events and stimuli being associated, and
1016 how the activity of the brain relates to this. Hence, we chose to design
1017 our experiments to incorporate associative learning, which is a
1018 relatively permanent change in behaviour that results from the
1019 temporal conjunction of two or more events or stimuli.

1020 Empirically, reproducible behaviour depends on strong associations
1021 between the events or stimuli being paired, and may often require
1022 many repeated pairings or trials. Additionally, having the animal
1023 engage in the behavioural task and pay attention to the stimuli being
1024 presented, is crucial to look for important correlations between the
1025 experiment conditions (external) and brain activity (internal).

1026 Anaesthetized animals have been previously used to study brain
1027 activity and led to important discoveries, e.g. - visual representation of
1028 moving bars in the visual cortex (Hubel & Wiesel, 1962), habituation in
1029 the Hippocampus (Deshmukh & Bhalla, 2003). However, it was clear
1030 that similar experiments repeated in awake animals did not result in the
1031 same observations. Indeed, animals needed to navigate a known
1032 environment before the discovery of Place Cells (O'Keefe &
1033 Dostrovsky, 1971), Grid cells (Hafting et al., 2005), among others,
1034 could be made.

1035 The reliability of the overt behavioural responses of the experiment
1036 animals then sets the conditions and parameter list to study physiology
1037 within the confines of reproducible behavioural contexts, and was
1038 considered an important mandate for the standardization of any of the
1039 behavioural tasks described in this chapter.

1040 **Operant conditioning [Project I]**

1041 Operant conditioning is both the procedure and a type of associative
1042 learning process through which the strength of a voluntarily performed
1043 behaviour is modified by reinforcement or punishment. For example, if
1044 the animal responds to a presented stimulus by performing a lick onto
1045 a water spout, then a water reward would strengthen the behaviour
1046 while a Lithium Chloride solution would weaken it.

1047 We now describe our experiments and results with regard to operant
1048 conditioning.

1049 Required features

1050 For Project I, the goal was to study how the association of a neutral
1051 stimulus with a water reward modified the neurophysiological activity of
1052 the hippocampal CA1. For this, we required the following.

1053 1 An assortment of different stimuli and modalities (light, tone, etc.)
1054 to be presented to the animal.

1055 2 The animal must withhold any motor movement during the
1056 presentation of the stimuli, to study pure stimulus responses.

1057 3 The animal must perform a lick for a water reward after the end of
1058 the stimulus presentation.

1059 4 The animal must be able to make the association between stimuli
1060 and water reward within 7 days of training (at the time we did not have
1061 the ability to record for multiple days).

1062 The behavioural state of the animal, in terms of anxiety, motivation,
1063 attention, etc., may be variable when a naïve animal is presented with
1064 different stimuli. This may cause a large variability in the activity of
1065 cells, since the animal may not be paying attention to it. Also, if the
1066 animal were rewarded for performing the task it is expected that there
1067 would be motivation to pay attention to the stimuli presented. Finally,
1068 such a task would involve the animal associating the stimuli that it is
1069 trained to with a behavioural task and this would provide an apt context
1070 to study association related changes in stimulus responses.

1071 In this section, we discuss some important protocols that we tried and
1072 tested and a list of the various kinds of behavioural tasks we employed
1073 for head-fixed mice.

1074 For Project I, we tried several variations of operant conditioning
1075 including Stimulus Detection tasks, Delayed Non-Match to Sample
1076 (DNMS), as well as Go/No-Go tasks. Each of these tasks requires
1077 animals to perform licks to the Conditioned Stimuli and for them to be
1078 rewarded (2-3 μ L water) or punished based on the task demands and
1079 protocol design.

1080 **Water delivery and calibration**

1081 The lick port was made from a trimmed and smoothed 16 gauge
1082 syringe, connected to a water reservoir with small diameter tubing. A
1083 solenoid valve clamped onto this tubing, gated by a 12V DC signal.
1084 When this gate was opened, the volume of water could be regulated by
1085 the duration of the 12V DC signal. We calibrated the duration of gate
1086 opening to achieve ~2 μ L per pulse or spurt (Jaramillo & Zador, 2014).
1087 The weight of 100 spurts was measured and then divided by 100 to get
1088 the weight of 1 spurt. 65 ms was found to be roughly providing 2.5 μ L
1089 (this value is going to be used for behaviour). In the figure below
1090 (Figure 1), the measured volumes/weights are plotted as blue filled
1091 diamonds, error bars are presented as Standard Error and the linear
1092 trendline is shown in black.

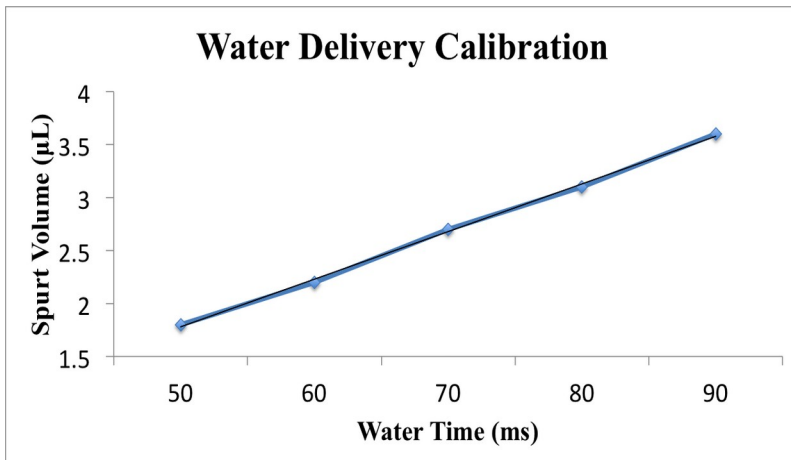


Figure 1: Water delivery calibration to reward the animal consistently with the same volume of water.

1093 Opto-islator circuit for solenoid control

1094 To be able to programmatically control the 12V DC line to the solenoid
 1095 valve, we used the following circuit (Figure 2), which accepted a 5V
 1096 digital input from the DAQ (NI USB-6001) interfacing the lab computer
 1097 to the behaviour rig.

1098 Parts list

- 1099 1. 470 ohm resistor
- 1100 2. 15 kohm resistor
- 1101 3. MCT2e
- 1102 4. ULN2003
- 1103 5. Bases (adaptors for MCT2e and ULN2003)
- 1104 6. +5V and +12V DC inputs from a Power Supply)
- 1105 7. Source of +5V DC input (DAQ, etc.)
- 1106 8. Connecting wires
- 1107 9. Load Resistance (Solenoid, etc.)

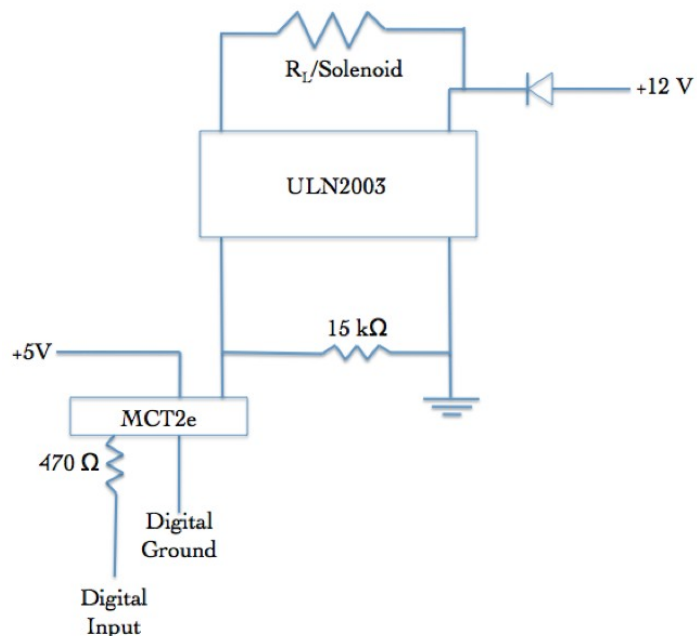


Figure 2: Optoisolator circuit to amplify +5V DC input to +12V DC output.

1108 Lick detection circuit

1109 To be able to monitor the presence or absence of licks to the port, the
 1110 conductive part (metal) of the lick port syringe was connected to a
 1111 MOSFET such that a 5V DC voltage could be read out, whenever the
 1112 animal would make contact with the port. This was designed as a
 1113 readout to Stimulus Detection by the animal. The circuit diagram is
 1114 shown below (Figure 3):

1115 Parts list

- 1116 1. +5V Power Supply
- 1117 2. 4.7 kohm resistor

- 1118 3. 22 Mohm resistor
 1119 4. IN4007 Diode
 1120 5. NPN Transistor IRF540N (MOSFET)

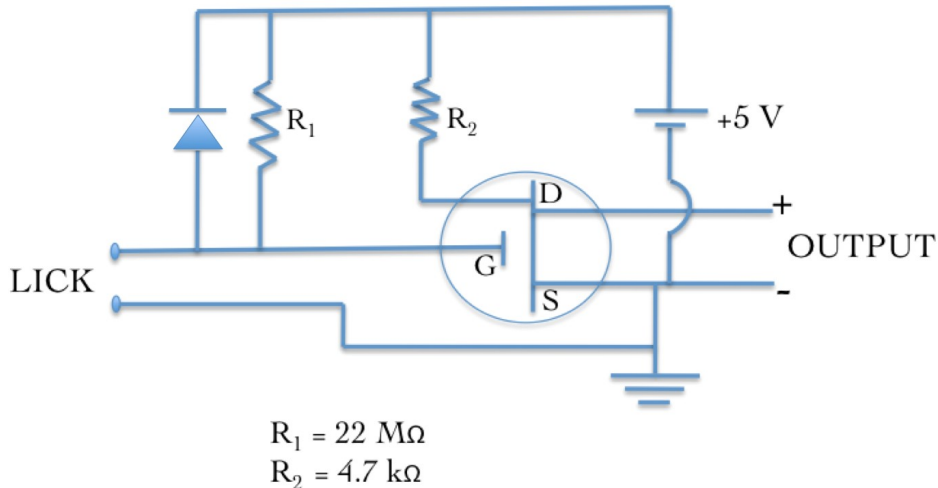


Figure 3: Lick detector circuit based on a MOSFET design. Whenever the animal performed a lick, a +5V DC Output would be read out.

1121 **Controlling task details and protocol information**

- 1123 All protocols were controlled using custom scripts written in NI LabVIEW 8. These scripts were run on a lab desktop which interfaced with the DAQ (NI USB-6001) via USB. The DAQ,
- 1126 1. Sent the 5V digital input to switch on the solenoid valve regulating water delivery, and
- 1128 2. Received the 5V digital output of the lick detection circuit whenever a lick was produced by the animal.

1130 **Head-bar implant, Animal Handling, and Water**
1131 **deprivation**

1132 All experiments were planned to be conducted on head-fixed C57Bl/6
1133 mice, with the eventual intention to perform in vivo imaging on these
1134 animals. For this, we surgically implanted metal head-bars on the skull
1135 of the animals while they were maintained on 1-2% Isoflurane, above a
1136 heating pad (35°C). Surgeries would last no longer than 30 mins per
1137 animal.

1138 After 1-7 days of recovery after surgery, we handled the animals gently
1139 for 2 days till the animals would appear comfortable with lifting and
1140 gentle collar grabbing. Next, for 3-4 days, we kept the animals head-
1141 clamped. We restricted our animals to ~1ml of water per day, keeping
1142 check that their body weight did not fall to below 80% of the weight on
1143 day 1.

1144 **PROTOCOL 1.1: Stimulus Detection Task**

1145 We first tried the simplest version of the lick task wherein an auditory
1146 tone was followed by a water reward. The animal would have to
1147 withhold licking till the end of the stimulus presentation, and then
1148 perform the lick for the reward (Figure 4).

1149 **Total number of trials:** 600/session; 1 session/day

1150 **Trial phases:**

- 1151 1. Stimulus free pre-tone (PT): 1 s
- 1152 2. Tone: 5 kHz for 1 s

- 1153 3. Critical timeout (CT): 100 ms
1154 4. Inter-trial Interval (ITI): randomized between 2 s to 5



Figure 4: Typical trial structure with the various phases. Each trial was followed by a randomized Inter-Trial Interval (ITI).

- 1155 Only licks during the critical timeout (CT) phase immediately after the
1156 Tone phase were rewarded while licks in other phases resulted in a
1157 phase restart.

1158 **PROTOCOL 1.2: Stimulus Detection Task with 1159 aversive punishment**

- 1160 **Total number of trials**: 600/session; 1 session/day

- 1161 Only licks during the critical timeout (CT) phase immediately after the
1162 Tone phase were rewarded while licks in other phases resulted in a
1163 100 air-puff to the body of the animal, before a phase restart. For
1164 Mouse 3 we started Protocol 1.2 from Session 3 while for Mouse 4 we
1165 started Protocol 1.2 from Session 2.

1166 **Results - Protocol 1.1 and 1.2**

1167 The behavioural performance for each of the experiment animals was
 1168 evaluated using custom analysis scripts written in MATLAB 2011. Here
 1169 are the results from two mice trained based on Protocols 1.1 and 1.2
 1170 (Figure 5).

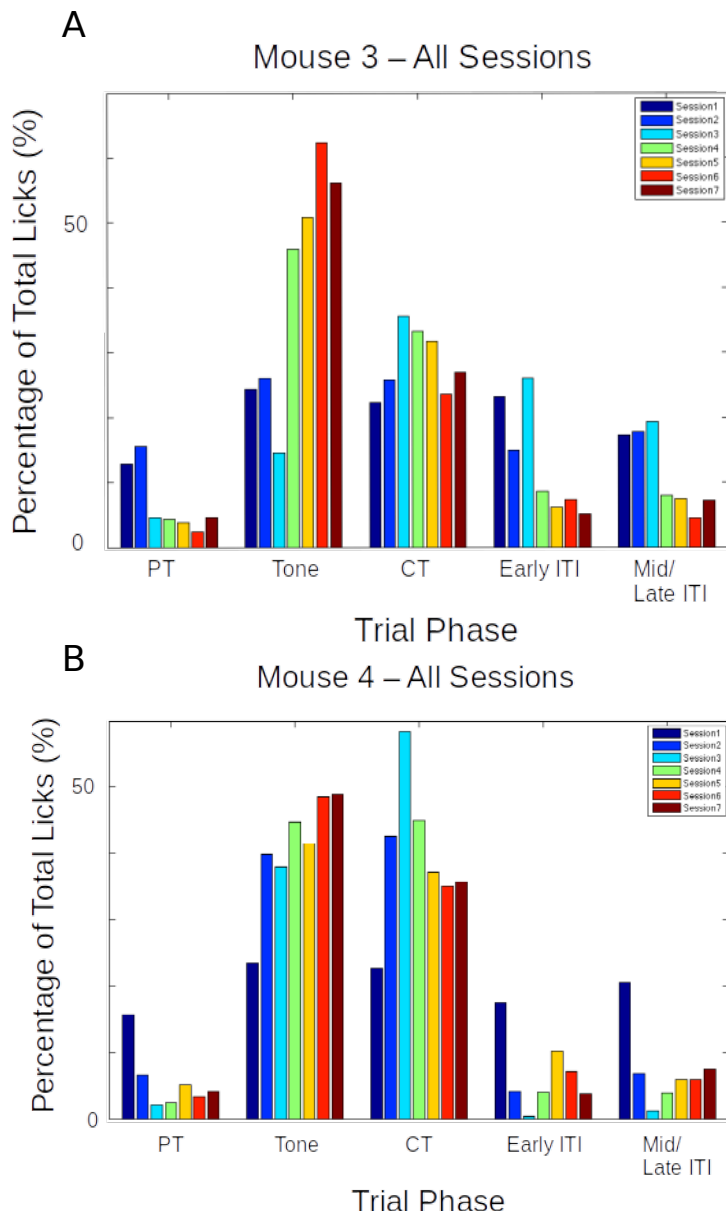


Figure 5: Performance evaluation for two example mice trained to Protocol 1.1 and 1.2. Percentage of total licks in the various trial phases (Pre-Tone, Tone, CT, and ITI), across all sessions of training (coloured bar plots) for A) Mouse 3, and B) Mouse 4

1171 In both the examples shown, animals would typically produce a great
1172 percentage of total licks even during the Tone period. This failure to
1173 withhold licks carried on for 7-14 sessions, and the task was ultimately
1174 unsuccessful.

1175 **Total animals trained:** 2

1176 **Conclusion:** Fail

1177 **Protocol 2: Stimulus Detection task with 1178 timeout box**

1179 We also tried the same Stimulus Detection protocol, without an air-puff
1180 punishment, but with incorrect licks punished by a trial abort and a
1181 stimulus-free timeout phase, which the animal could escape from if it
1182 withheld licking. We decided to train the animals in blocks, each with a
1183 specific goal that the animal had to achieve.

1184 **Trial phases:**

1185 1 Stimulus-free pre-tone (PT): 1 s

1186 2 Tone: 5 kHz for a variable duration (based on Block)

1187 3 Critical timeout (CT): 1000 ms

1188 4 Inter-trial Interval (ITI): randomized between 2 s to 5 s

1189 Figure: Typical trial structure with the various phases. Each trial was
1190 followed by a randomized Inter-Trial Interval (ITI).

1191 Only licks during the critical timeout (CT) phase immediately after the
1192 Tone phase were rewarded while licks in other phases resulted in a
1193 phase restart.

1194 **Block 1:** Unconditional Water to get the animal to associate the tone
1195 - ~20 trials
1196 - 100 or 200 ms Tone duration
1197 - Unconditional water provided at the end of the tone, irrespective of
1198 lick

1199 **Block 2:** Conditional Water to get the animal to learn that licking
1200 with/after tone is going to be rewarded
1201 - 100 or 200 ms Tone duration
1202 - 1000 ms Reward phase
1203 - Lick during/after tone (Reward phase) = reward
1204 - No lick = no reward
1205 - Lick during pre-tone = no reward/abortion of trial
1206 - Lick during ITI = no reward/abortion of trial
1207 - Animals graduate to the next Block of training only after achieving at
1208 least 70-80% success rates

1209 **Block 3:** Training the animal to learn "when" to lick
1210 - 1000 ms pre-tone, 100 or 200 ms Tone, 1000 ms Reward phase, 3-5
1211 s randomized ITI
1212 - Lick during Reward phase = reward
1213 - Any lick during the pre-tone or the tone, aborts the trial and sends the
1214 program to a Timeout phase (lasting, 2-3 s)
1215 - The timeout phase ends only when there is a 2-3 s (specified) interval
1216 of no licking

1217 - If the timeout phase ends, a new trial begins
1218 - Licks during ITI are also "punished" accordingly
1219 - Animals graduate to the next Block of training only after achieving 70-
1220 80% success rates

1221 **Block 4:** Same as Block 3, but with a gradually increasing tone
1222 duration in steps of 50/100 ms
1223 - The tone duration is gradually increased, the increase being tailored
1224 to the performance of the animal
1225 - It will be attempted to get the animals to learn to wait for 500-700 ms
1226 - Animals graduate to the next Block of the experiment only after
1227 achieving 70-80% success rates

1228 **Results - Protocol 2**

1229 The behavioural performance for each of the experiment animals was
1230 evaluated using custom analysis scripts written in MATLAB. Here are
1231 two representative examples of mice trained based on Protocol 2
1232 (Block 3).

1233 Figure: Performance evaluation for two example mice trained to
1234 Protocol 2. Percentage of total licks in the various trial phases (Pre-
1235 Tone, Tone, CT, and ITI), across all sessions of training (coloured bar
1236 plots).

1237 Again, as is clear from the examples above, that while the mice
1238 eventually produced a decent percentage of total licks in the critical
1239 timeout (CT) phase to get a water reward, they did not learn to

1240 withhold licks during the Tone phase, even after >10 sessions. The
1241 task was ultimately unsuccessful.

1242 **Total animals trained:** 4

1243 **Conclusion:** Fail

1244 **Protocol 3: Delayed Non-Match to Sample (DNMS)**

1246 Delayed Non-Match to Sample (DNMS) is a task that is ideally suited
1247 to study working memory and recognition (Binder et al., 2009), but we
1248 decided to try it. This task involves trial-by-trial presentation of two
1249 stimuli separated by a stimulus-free delay interval. For any given trial,
1250 If the two pseudorandomly chosen pairs of stimuli were identical, then
1251 licks would not be rewarded. However, if the pair of stimuli were
1252 different, then licks would be rewarded with 2 μ L water.

1253 We tried to incorporate more tones, in the hope that this may improve
1254 the chances of the animals focusing on the task specifics, instead of
1255 producing licks to just any particular stimulus.

1256 **Tones used:** 6000 Hz, 8500 Hz, 10000 Hz, and 11500 Hz

1257 **Trial phases:**

- 1258 1. Pre-Tone duration (ms): 1000 ms
- 1259 2. CS 1 duration (ms): 350 ms
- 1260 3. Delay Interval duration (ms): 250 ms
- 1261 4. CS 2 duration (ms): 350 ms (unless a correct lick is
1262 elicited)

1263 5. ITI duration (s): randomized from 1 s to 3 s

1264 **Punishment:** Timeout Box (minimum of 3s of no licks to escape)

1265 **Reward:** 2 µL of water

1266 **Results - Protocol 3**

1267 >70-80% of the trials had to be aborted because the animals would not
1268 withhold licking after the 1st of the pair of tones was presented. This
1269 did not change even after 7 days (sessions) of training.

1270 **Total animals trained:** 6

1271 **Conclusion:** Fail

1272 **Protocol 4: Go/No-Go Task**

1273 In an attempt to simplify the behavioural task, we decided to
1274 reconfigure the DNMS task to a simpler Go/No-Go task. Here, we
1275 would again present the animal with two stimuli, but with the only
1276 condition being that the animal would have to lick after the second
1277 stimulus, and not before. This simplifies the behaviour to a certain
1278 extent, because the animals need only use the first stimulus as a cue
1279 for the second. Failure to perform this task could more easily then be
1280 attributed to a lack of attention in that trial. Only the data from the trials
1281 where the animal succeeds to do the task would be considered for
1282 analysis. Training related changes in actual stimulus representations
1283 would be carefully dissected out. Furthermore, such a task would

1284 control for the behavioural state of the animal and help provide
1285 important datasets.

1286 In terms of imaging, we hoped to use the no-go stimulus to record a
1287 clean stimulus response without the possible contamination of
1288 movement (licking behaviour), and the go stimulus to verify attention
1289 (Figure 6).

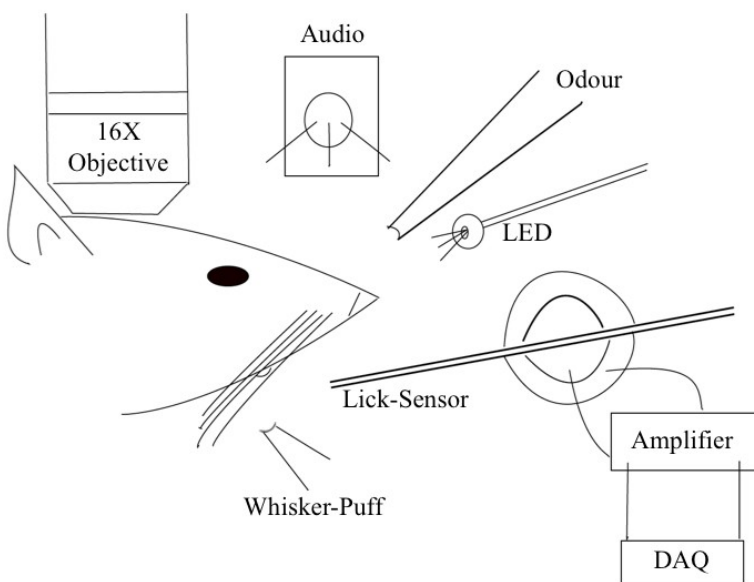


Figure 6: Schematic representation of the experimental setup for a detection task where the animal must perform a lick upon correctly detecting the presence of the conditioned stimulus (CS; from a range of modalities).

1290 Trials were designed to go through the following phases and have the
1291 animal graduate to subsequent phases, only after correctly performing
1292 the behaviour:
1293 1. Pre-tone: Stimulus-free period; no lick
1294 2. No-go tone: 7kHz tone period; no lick
1295 3. Go tone: 10kHz tone period; lick for reward

1296 If the animal would perform an incorrect lick, the particular phase
1297 currently occurring was restarted. Only licks to the Go tone were
1298 rewarded (Figure 7).

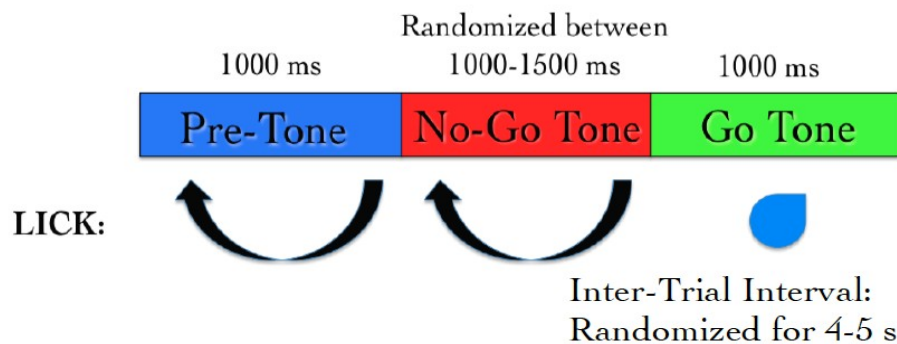


Figure 7: Typical trial structure with the various phases and lick dependent relationships.

1299 Results - Protocol 4

1300 The behavioural performance improves only after several sessions of
1301 training (~3-4 sessions). This is primarily due to an increase in the
1302 percentage of trials with a correct Go tone lick, as shown (Figure 8).

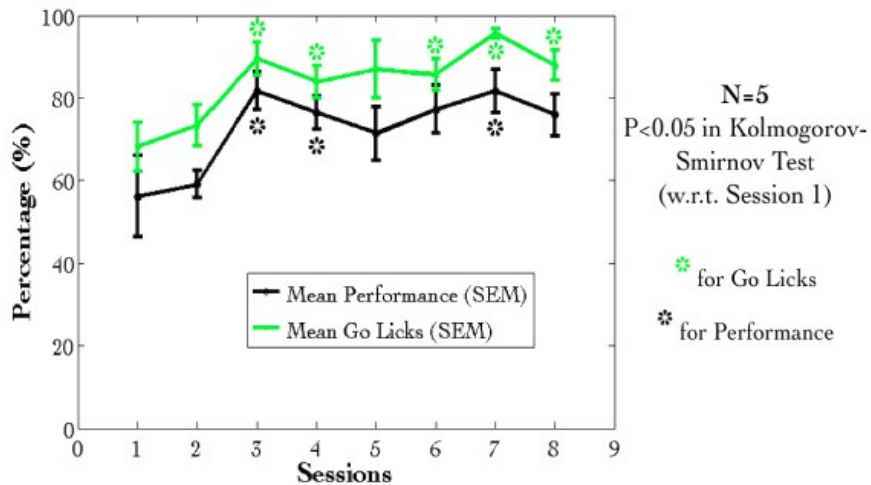


Figure 8: Mean Performance (%) and Mean Go Tone Lick Percentage (%) with Session for the Go/No-Go Task, plotted in black and green, respectively.

1303 However, a plot of the lick histogram for the various trial phases
 1304 revealed that despite reaching the maximum success rate, the animals
 1305 continued to lick during the no-go tone phase (incorrect lick) for a long
 1306 duration of time (Figure 9). There was no difference in the amounts of
 1307 time spent in the pre-tone or no-go tone phases. This suggested that
 1308 the animals did not discriminate between the Go and no-go tones.
 1309 Accordingly, the current protocol was not being learnt as expected.

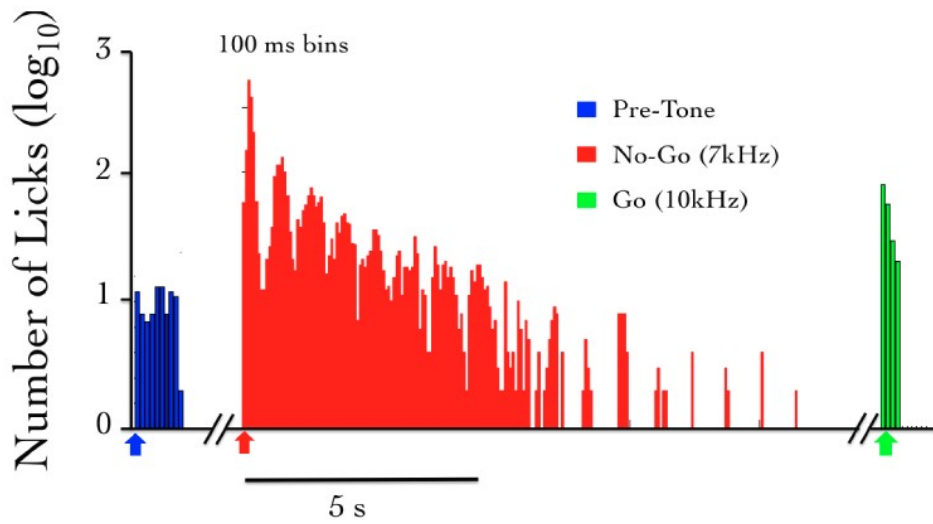


Figure 9: The number of licks in the pre-tone (blue), no-go tone (red), and go tone (green) phases, in a representative animal, in a session with maximum Performance (%).

1310 We were not able to get discriminatory detection. Animals would resort
 1311 to performing licks continuously and agnostically to the go and no-go
 1312 stimulus. In a study published many years later, it was determined that
 1313 any discriminatory task such as the one described above, would
 1314 require even up to 4 weeks of training, since the animal was not
 1315 punished with anything more than a delay or phase restart.

1316 **Total animals trained:** 5

1317 **Conclusion:** Fail

1318 Eventually, we had to abandon these experiments, to switch to an
 1319 aversive conditioning task, viz., Trace Eye-Blink Conditioning (TEC).
 1320 With the change in the main behavioural task we also changed the
 1321 project goals. The TEC task was standardized with the intention to
 1322 work on Project II which is to study how animals make complex
 1323 associations between different types of stimuli and how they adapt to
 1324 changes to the inter-stimulus interval (ISI).

1325 Trace Eye-Blink Conditioning [Project II]

1326 Eye-blink Conditioning is a class of Classical Conditioning and requires
1327 the presentation of a neutral stimulus (Conditioned Stimulus, CS) along
1328 with an eye-blink eliciting, mildly aversive stimulus (Unconditioned
1329 Stimulus, US). Depending on whether the CS presentation overlaps
1330 with the US presentation or if the two stimuli are separated by a
1331 stimulus free interval in between (Trace interval), the concomitant
1332 procedure is called Delay Conditioning or Trace Conditioning,
1333 respectively (Figure 10). In either case, precise timing of the CS and
1334 US is mandated.



Figure 10: Schematic representation to showcase the two main subtypes of Classical Conditioning (Eye-Blink Conditioning, for our experiments) based on the relative timing and presentation of the CS and US.

1335 The CS is usually an auditory tone or a visual stimulus (e.g.- LED
1336 Flash), while the US is typically a mild air-puff to the cornea, or a
1337 gentle electric shock to the eye-lid. Naive animals (rabbits, rodents,

1338 monkeys, etc.) produce a robust, reflexive eye-blink to the US
1339 (Unconditioned Response, UR) and ignore the CS, in early trials.
1340 However, with repeated pairing of CS and US, the animals are able to
1341 associate the two, and use the CS as a cue to predict the US,
1342 producing a partial, preemptive eye-blink just before the expected time
1343 of the US (Conditioned Response, CR). The CR develops in amplitude
1344 over multiple pairings or training sessions. In well trained animals, the
1345 CR begins at a time point closer and closer to the CS onset, and
1346 usually merges with the UR. The animals produce this CR in an
1347 attempt to avoid the US.

1348 Traditionally, Trace Eye-Blink Conditioning has been an important
1349 hippocampus-dependent behavioural task, and has been adapted to a
1350 variety of different species, spanning rabbits, rats, and mice.

1351 Damage or inhibition of the hippocampus has been shown to limit task
1352 acquisition without affecting other non-hippocampus dependent tasks
1353 such as Delay Conditioning. In an experiment, Ibotenic Acid was used
1354 in a session dependent fashion, to observe both limitations in first
1355 acquiring the Trace Conditioning task, as well as detriments to
1356 behavioural recall, even after animals learn the task to a high degree of
1357 proficiency, suggesting the pivotal role that the hippocampus plays in
1358 temporal tasks of this nature (Tseng et al., 2004).

1359 A single session of Trace Eye-Blink Conditioning, with strong stimuli
1360 (CS and US), has been previously employed (Modi et al., 2014), but
1361 with only upto 50% of the animals learning the task. Typically animals
1362 require around 3-7 sessions (~200-600 trials) to robustly learn the task.
1363 Accordingly, we designed and standardized a multi-session version of

1364 TEC, to allow more animals to learn and acquire the task, based on
1365 previously published work (Siegel et al., 2015).

1366 **Tracking eye-blink responses**

1367 The most foolproof way to track eye-blink responses (especially with
1368 head-fixed animals) chronically (for multiple sessions across days), is
1369 to use a video camera. We used a Point Grey Chameleon3 1.3 MP
1370 Monochrome USB3.0 camera) for this purpose. It is cost effective and
1371 with proper scaling of the resolution and field of view, can achieve
1372 recording rates of >200 frames per second. An important criteria for
1373 getting faster frame rates is to have better illumination, so that the
1374 camera may be set to lower exposure settings. We used a set of 5-10
1375 Red colour LEDs as the light source, and these are run using a 12V
1376 DC line, with current limited resistors in series. Additionally, we used
1377 an IR-blocking filter to avoid capturing the 2-Photon excitation light
1378 (910-920 nm) when conduction behaviour and imaging experiments
1379 simultaneously. Finally, to focus the light from the eye of the animal
1380 onto the camera sensor, we used a Tamron M118FM16 lens (1/1.8,
1381 16mm F/1.4).

1382 **Treadmill and tracking running speed**

1383 Allowing the head-fixed animals to run on a treadmill was an important
1384 behaviour rig consideration, as this allows the animals to be more
1385 comfortable and less stressed. We used a 6 inch cylindrical massage
1386 roller with a stainless steel axle running along the length. This axle had

1387 ball bearings on the two ends, to allow for free rotation against clamps.
1388 Additionally, we used linear actuators to be able to adjust the height of
1389 the treadmill relative to the head-fixing clamps.

1390 On one side of the treadmill, we used a printed pattern of black
1391 squares (side length: 1cm) along the circumference. This allowed an
1392 IR LED - Photodetector pair to catch the edges of the black printed
1393 squares. The number of edges detected per unit time, then gave us the
1394 run speed of the animals being trained. We followed previously
1395 published routines and protocols (Siegel et al., 2015) for setting up the
1396 treadmill and run speed tracking (Figure 11).

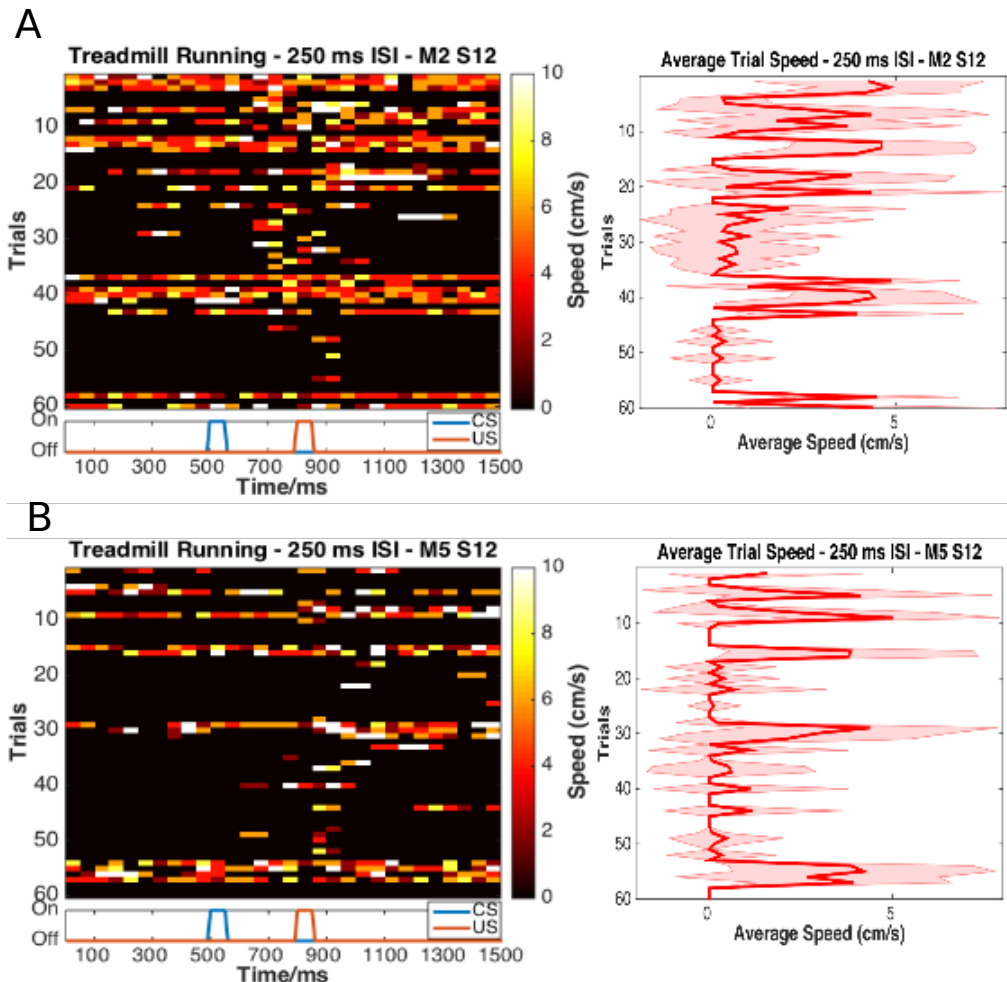


Figure 11: Trial by trial (left), and trial-averaged running speed (right) for two example animals, A: M2 Session 12; B: M5 Session 12.

1397 Behaviour rig and protocol control - Software

1398 For our initial experiments we used the open-source behaviour
 1399 controlling software suite Bonsai (Windows version). Later on, we were
 1400 able to implement our own custom codes that allowed integration of
 1401 the video camera, Arduino for stimulus delivery and treadmill tracking,
 1402 and the software side of the protocols. Dilawar S. Rajput was

1403 instrumental in setting up the camera pipeline and integrating it into the
1404 Arduino code. The Camera server was implemented in C++ with
1405 Spinnaker API (Point Grey) and this fetched frames from the camera.
1406 The camera client was written in python, and this read the frames to
1407 produce a copy to monitor the video feed live, as well as write the
1408 video frames to disk as .tif files.

1409 With this setup, the maximum memory usage was ~1.3 GB RAM, and
1410 the code (available at <https://github.com/BhallaLab/PointGreyCamera>)
1411 had the following dependencies:

- 1412 • libopencv-dev, python-opencv
- 1413 • cmake, g++, gnu-make
- 1414 • libtiff-dev, python-tifffile, python-numpy
- 1415 • python-gnuplotlib, gnuplot-x11

1416

1417 An important requirement for our behaviour experiment design was to
1418 be able to train the animals systematically under reproducible
1419 conditions, with the aim to have stable behavioural training and animal
1420 performance. We used a blue LED as the Conditioned Stimulus (CS,
1421 50 ms flash) with an air-puff to the eye serving as the Unconditioned
1422 Stimulus (US, 50 ms pulse). We used an Arduino to orchestrate
1423 stimulus delivery and protocol design (Figure 12). All experiments were
1424 performed on head-fixed C57Bl6 mice, since we planned to use a
1425 stationary, custom-built two-microscope to image hippocampal CA1
1426 activity during task acquisition and recall.

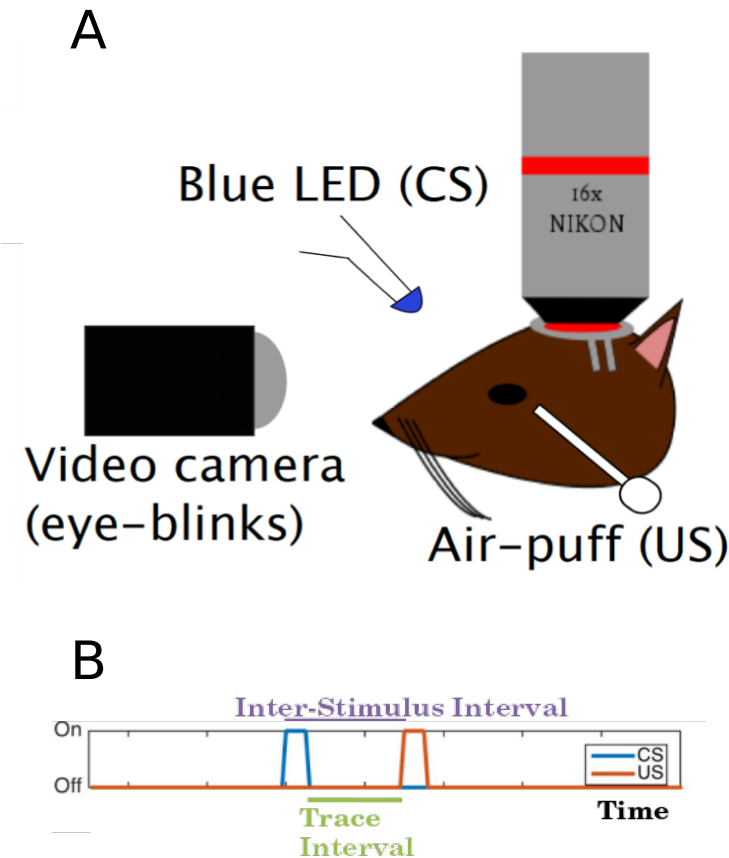


Figure 12: Schematic representation of A: the behaviour rig with 2-Photon imaging, to train head-fixed mice on a Trace Eye-Blink Conditioning (TEC) task, and B: relative time intervals between the CS and US.

1427 Analysis - TEC

1428 Once the .tif movies of the eye of the animal being trained were saved,
 1429 they were analyzed by a custom script written in MATLAB, wherein for
 1430 every frame we (Figure 13),
 1431 1. Adjust contrast (optional)
 1432 2. Apply a median filter (optional)
 1433 3. Crop out the pixels defining the eye and surrounding
 1434 (identical number of pixels for all trials and animals)

- 1435 4. Binarize the image of the eye to get black pixels defining the
 1436 visible (opened) portion of the eye
 1437 5. Count the relative proportion of open vs closed eye pixels in
 1438 the cropped image, and
 1439 6. Assign each frame with a Fraction of Eye Closure (FEC)
 1440 score.

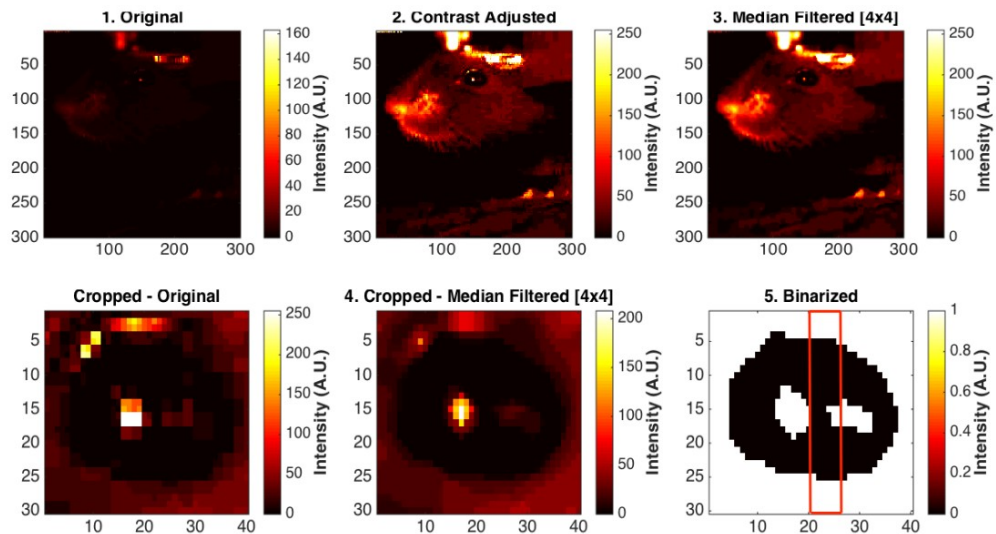


Figure 13: Steps from behaviour video frame to Fraction of Eye-Closed (FEC) analysis

- 1441 The FEC score then allowed us to analyse each trial's worth of frames
 1442 for eye-blinks. There are many features of the eye-blink that could be
 1443 used to gauge the overall performance of the animal in terms of both
 1444 the Conditioned Response (CR) as well as the Unconditioned
 1445 Response (UR), but for our experiments, we chose to use Eye-Blink
 1446 Amplitude (Siegel et al., 2015). Additionally, we studied whether the
 1447 animals could produce CRs in the absence of the US, by
 1448 pseudorandomly selecting 10% trials to skip the US (Probe Trials).

1449 Results - TEC

1450 1. Animals showcase task acquisition by performing Conditioned
1451 Responses (CRs), observed as pre-emptive blinks timed to
1452 avoid the aversive US. The kinetics of the CR (timing,
1453 amplitude, etc.) are dependent on the amount of training, but
1454 are identical across paired and probe trials (Figure 14).

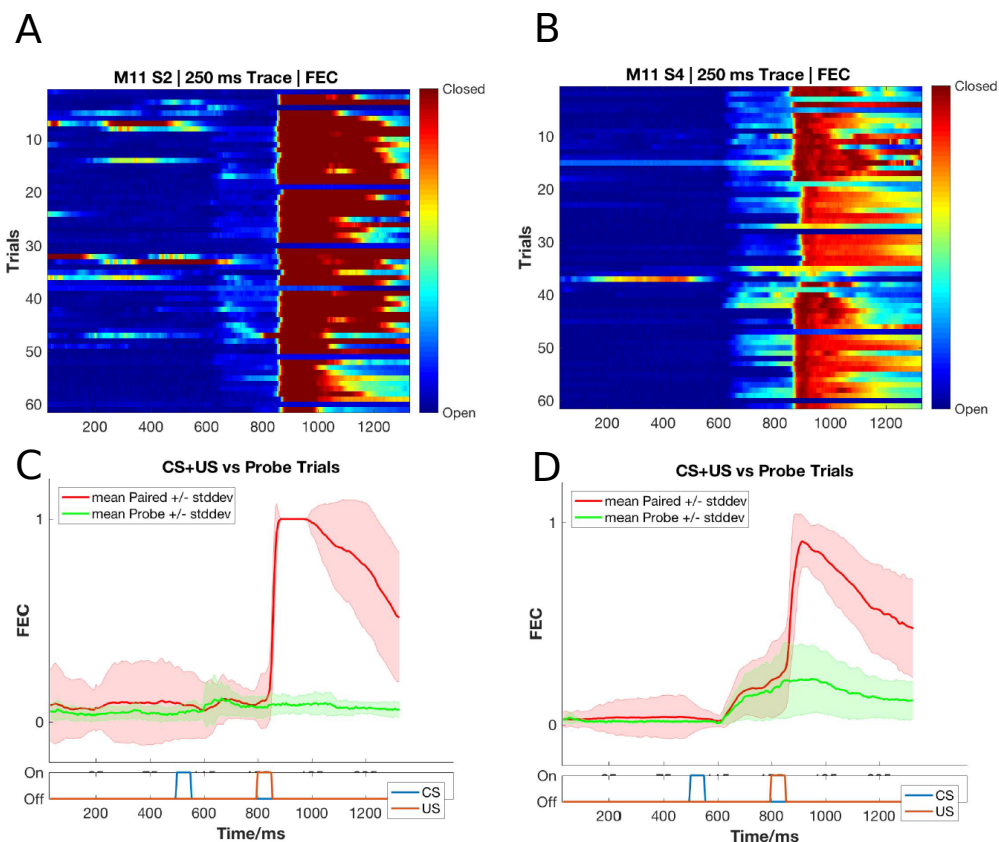


Figure 14: Conditioned Responses (CRs) are small amplitude eye-blanks triggered by the CS, and develop with multiple training sessions, while Unconditioned Responses are large eye-blanks to the US, typically consistent across sessions. (A,B) Trial-by-trial FEC traces for A) M11 Session 2, and B) Session 4. (C,D) Trial-averaged FEC traces for C) Session 2 and D) Session 4, with paired (red) and probe (green) trials.

1455 2. Most animals can pick up the task within 4-7 sessions (1
1456 session/day, 60 trials/session), even if on water deprivation.
1457 Animals can also be subsequently trained to different inter-
1458 stimulus intervals. Using the Conditioned Response (CR)
1459 amplitude, each trial can be binarized to whether a CR was
1460 elicited (Hit Trial) or not (Miss Trial), by thresholding at mean
1461 trial FEC + 2*Std. Dev.. Performance for the session is then
1462 estimated as the ratio of Hit Trials to Total Trials (Figure 15).

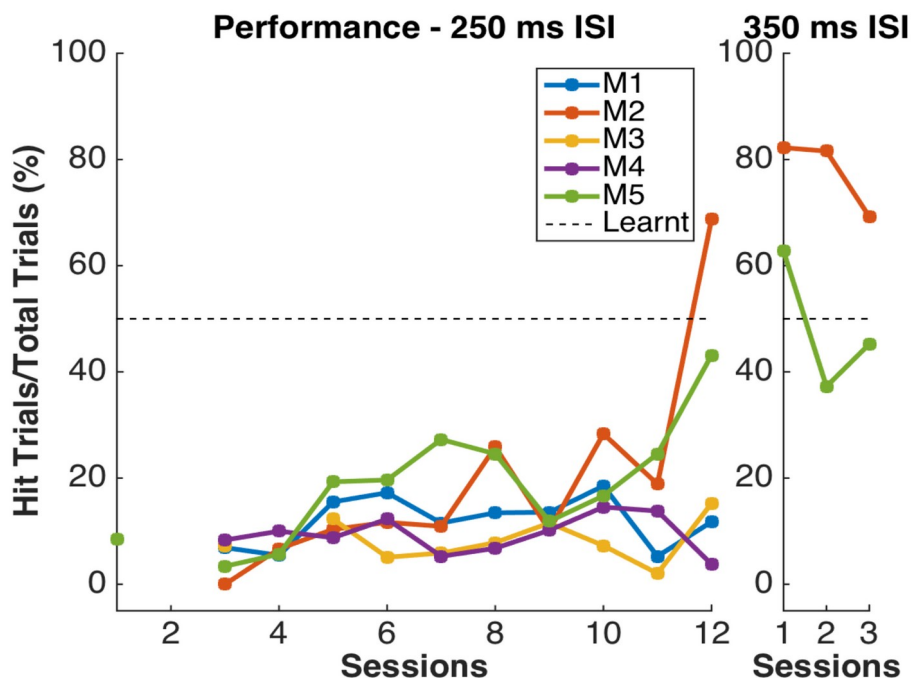


Figure 15: Performance in terms of the percentage of Hit Trials to total trials across sessions, including an ISI switch from 250 ms to 350 ms.

1463 3. Animals that learn multiple ISIs, especially when the second ISI
 1464 is $\geq 2x$ the first ISI, showcase complex eye-blanks without
 1465 extinction of the previously learnt CRs. Once an animal
 1466 showcases the ability to produce Conditioned Responses (CRs)
 1467 to one inter-stimulus interval (ISI), this interval can be
 1468 elongated. In the example shown below we first trained the
 1469 animal to a 250 ms ISI, and then switched to a 500 ms ISI
 1470 (Figure 16).

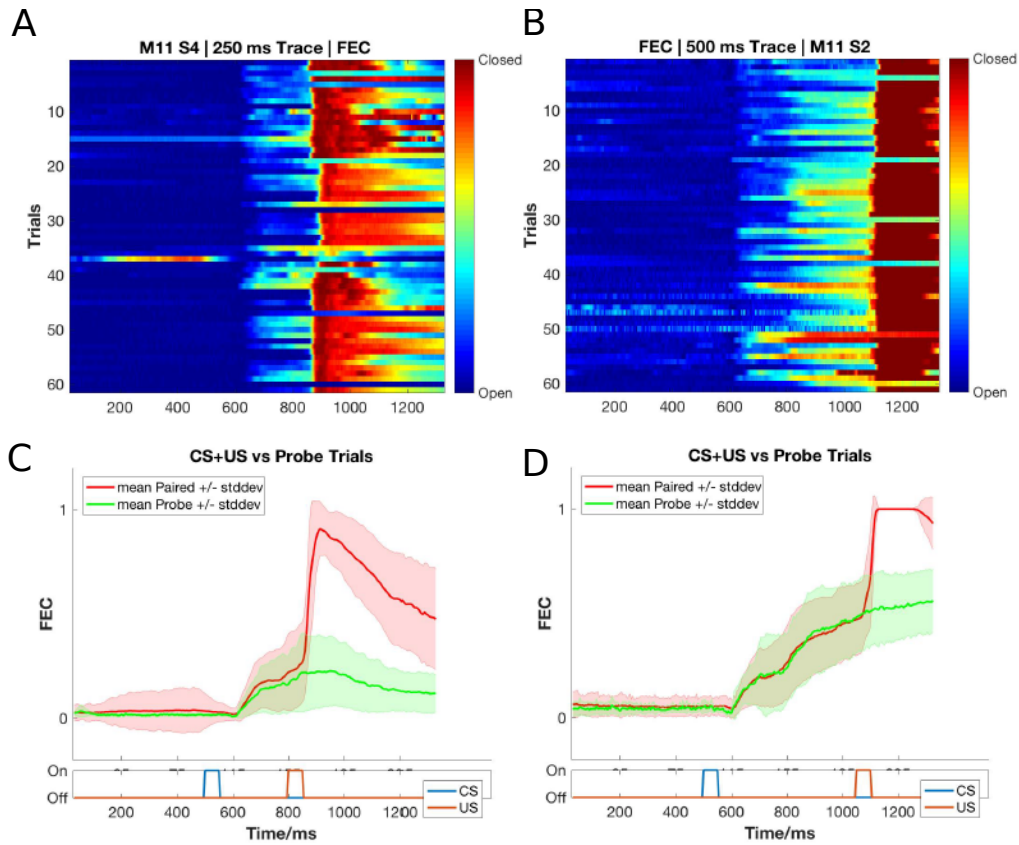


Figure 16: Conditioned Responses (CRs) are preserved for previously learnt ISIs, and switching the ISI to longer intervals results in Complex (multi-CR) eye-blink responses. (A,B) Trial-by-trial FEC scores for A) 250 ms ISI (left) and B) 500 ms ISI. (C,D) Trial-averaged FEC traces for C) 250 ms ISI (left) and D) 500 ms ISI (right), with paired (red) and probe (green) trials.

- 1471 4. The onset of the Conditioned Response (CR) is not affected by
 1472 the ISI switch, irrespective of how strongly the animals learn the
 1473 task. CRs during paired and probe trials were near identical,
 1474 showcasing that the animal (Figure 17, Figure 18).

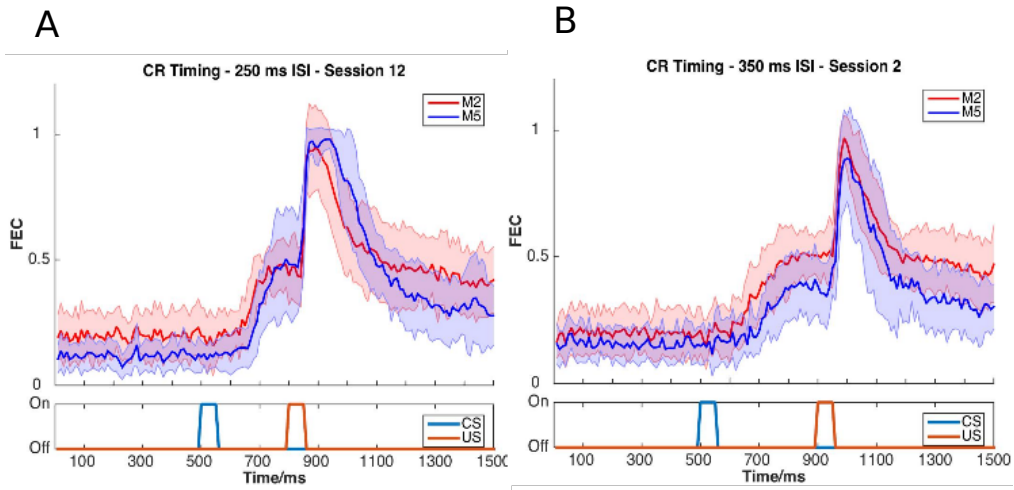


Figure 17: Conditioned Response (CR) onset timing is maintained across ISI switches. Representative examples from a short ISI switch from A) 250 ms to B) 350 ms (right).

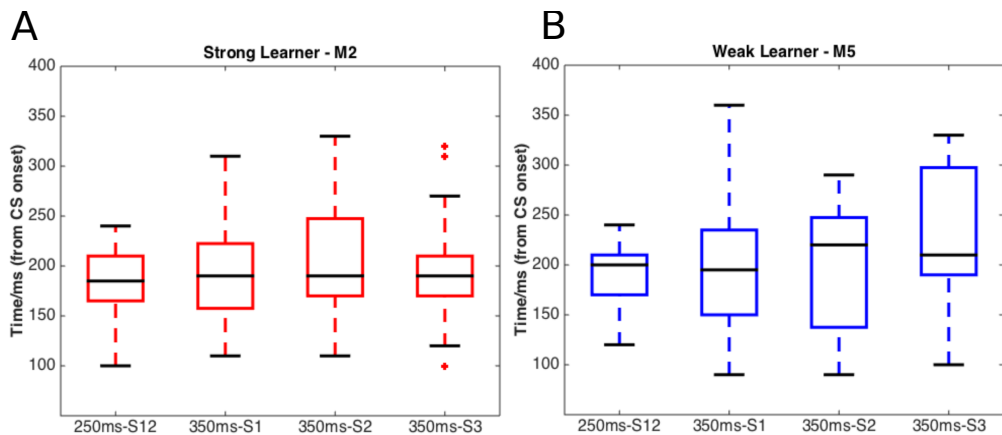


Figure 18: Bar plots for Conditioned Response (CR) onset across multiple sessions of training after ISI switch from 250 ms to 350 ms, irrespective of how strongly the animals learnt the task. A) red, strong learner, and B) blue, weak learner.

1475 5. Animals can also be trained to very long ISIs from Session 1,
 1476 with acquisition taking <10-14 days. Here we tried to train
 1477 animals to either a 550 ms ISI or a 750 ms ISI. Note, however,
 1478 that unless multiple ISIs are taught to the same animal, the CR
 1479 eye-blink is singular (Figure 19).

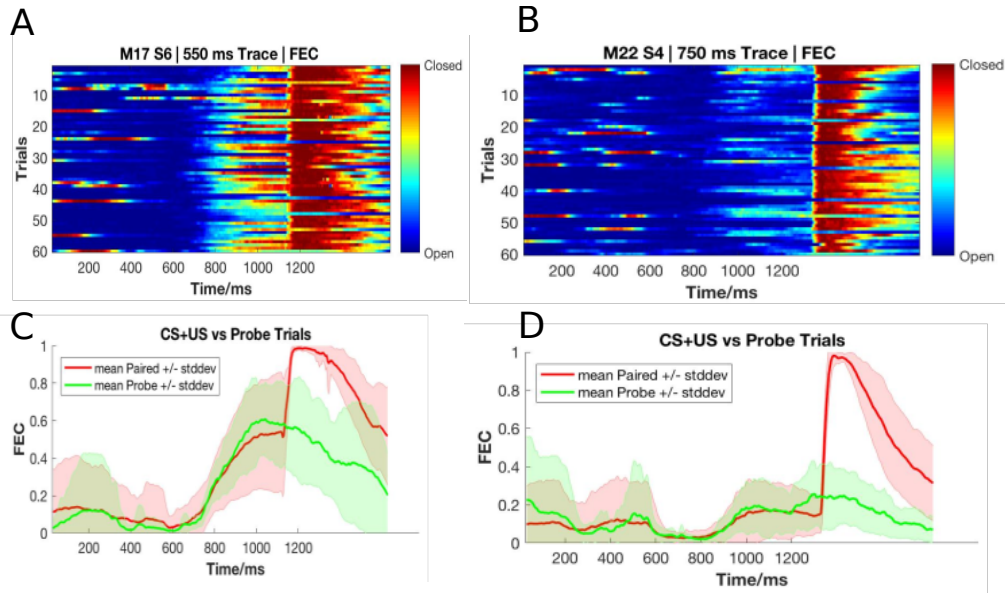


Figure 19: Representative example of mice trained to 550 ms ISI (Session 6) and 750 ms ISI (Session 4). (A,B), Trial-by-trial FEC responses for A) 550ms ISI, and B) 750ms ISI. (C,D) Trial-averaged FEC responses for C) 550 ms ISI, and D) 750 ms ISI, with paired (red) and probe trials (green).

1480 **Total animals trained:** <check lab notes>

1481 **Conclusion:** Success

1482

Chapter 3 - Imaging

1483 The mammalian hippocampus is considered important in the formation
1484 of new memories about experienced events (episodic or
1485 autobiographical memory), general declarative memory (memories that
1486 can be explicitly verbalized), spatial memory and navigation, and
1487 associations between stimuli that are distinct in time, among other
1488 functions. To achieve this, the Hippocampus must integrate information
1489 from different areas of the cortex.

1490 Much of the cortical information that enters the Hippocampus (at the
1491 Dentate Gyrus), comes through the Entorhinal Cortex, along the
1492 Perforant Path (Hjorth-Simonsen & Jeune, 1972). The Dentate Gyrus
1493 cell network then relays this information to the CA3 cell network
1494 through Mossy Fibers, which in turn relays the information to CA1
1495 cells, through the Schaffer Collateral Fibers. This is popularly known as
1496 the Trisynaptic Circuit and there is scope and evidence for computation
1497 and information processing at every step (MacDonald et al., 2011;
1498 McHugh et al., 2007; Modi et al., 2014; Nakashiba et al., 2008; Suh et
1499 al., 2011). Finally, the CA1 cells have their outputs to other brain
1500 regions. It is important to note, however, that regions like the CA1 are
1501 known to have access to information directly from other brain regions,
1502 as well (P. Andersen et al., 2006).

1503 Literature in the field suggests that naïve animals may have some
1504 sensory gating of “Neutral” stimuli at the level of the CA1 (Abe et al.,
1505 2014; Bellistri et al., 2013; Kamondi, 1998). The source of this
1506 inhibition (at least the step before the local interneurons) seems to be

1507 the Medial Septum, through Fimbria-Fornix (Abe et al., 2014). Also,
1508 behavioural relevance allows the CA1 to elicit depolarizations (D. A.
1509 Dombeck et al., 2010; Harvey et al., 2009; Itskov et al., 2011;
1510 MacDonald et al., 2011, 2013; Modi et al., 2014; Pastalkova et al.,
1511 2008).

1512 The Hippocampus consists of ventral and dorsal portions both of which
1513 are of similar composition but are parts of different neural circuits
1514 (Moser & Moser, 1998). It has been reviewed that it is the dorsal
1515 hippocampus that performs primarily cognitive functions and in
1516 memory function, while the ventral hippocampus modulates emotional
1517 and affective processes (Fanselow & Dong, 2010).

1518 **Physiology in the hippocampus**

1519 The Hippocampus is located deep in the medial temporal lobe of
1520 mammals and is defined by several sub-structures, including the
1521 Dentate Gyrus (one site for information input to the hippocampus) and
1522 the Hippocampus Proper constituted by the CA1, CA2, CA3 and CA4
1523 cellular levels.

1524 Using extracellular tungsten microelectrodes in naïve unanesthetized
1525 rabbits serially exposed to multimodal stimuli (Vinogradova, 2001), it
1526 was reported that in the CA1,
1527 1. A major fraction the reactive neurons have unimodal responses
1528 (41-44%)
1529 2. Multimodal neurons are modality-unspecific but have
1530 differentiated responses to stimuli of different modalities and even to
1531 various stimuli within a single modality

1532 3. Many neurons respond by Phasic (evoked responses last for the
1533 duration and as long as the stimulus) and Specific (stimulus-specific
1534 pattern) responses

1535 4. Neurons with inhibitory responses are encountered less
1536 frequently than those with various types of excitatory

1537 5. Habituation (non-responsiveness to repeatedly presented stimuli) is
1538 present though not among all the responsive cells (71-75%) and is
1539 often gradual

1540 Imaging based activity studies have the advantage of being able to
1541 capture many more cells (>100 from the same animal) during
1542 experiments (D. A. Dombeck et al., 2010; Peron et al., 2015) as
1543 compared to typical electrophysiological measurements. Also, imaging
1544 provides an unambiguous method to identify cells that are not active
1545 during a period of interest. Finally, imaging techniques have gained
1546 momentum in the study of the hippocampal CA1 various spatial scales,
1547 from cellular resolution somatic studies (D. A. Dombeck et al., 2010;
1548 Modi et al., 2014), to dendritic (Mizrahi, 2004; Sheffield & Dombeck,
1549 2014), as well as axonic boutons terminating on the CA1 interneuron
1550 populations (Kaifosh et al., 2013; Lovett-Barron et al., 2014), *in vivo*.

1551 Firstly, it must clearly be determined if the CA1 cells in naive animals,
1552 indeed do not show depolarization responses to neutral stimuli in
1553 larger samples of CA1 cells, *in vivo*. Next, it becomes pivotal to
1554 understand the network and cellular mechanisms that underlie
1555 behavioral learning induced changes in CA1 responses.

1556 Depending on the intended duration of the imaging experiments, viz., a
1557 few hours (single session) or a few days and weeks (multiple
1558 sessions), we were able to standardize both an Acute as well as a

1559 Chronic *in vivo* hippocampal preparation. We now discuss the *in vivo*
1560 Hippocampal preparation, physiology recordings, and a brief summary
1561 of the results. An important perspective for our experiments was to
1562 study how sensory stimulus responses of Hippocampal CA1 develop
1563 with associative learning.

1564 **Methodology - Acute and chronic imaging**

1565 **[Projects I & II]**

1566 The overall experiment deals with optically measuring the activity of
1567 the dorsal CA1 Hippocampal neurons when different stimulus
1568 modalities are presented to a male C57BL/6 mouse. The thesis covers
1569 experiments conducted acutely (lasting <10 hours) using OGB-1 as a
1570 calcium sensor), as well as chronically (~7-21 days) using a genetically
1571 encoded calcium indicator, GCaMP6f).

1572 The hippocampus cannot be imaged directly, through the cortex since
1573 the layer of cortex is too thick (of the order of millimeters) to allow
1574 proper excitation of the sample. The excitation light is expected to be
1575 scattered completely, well before the imaging depth of the CA1 layer.
1576 These layers of cortex have to accordingly be carefully suctioned out to
1577 allow the microscope objective to have optical access to the exposed
1578 tissue (Figure 20).

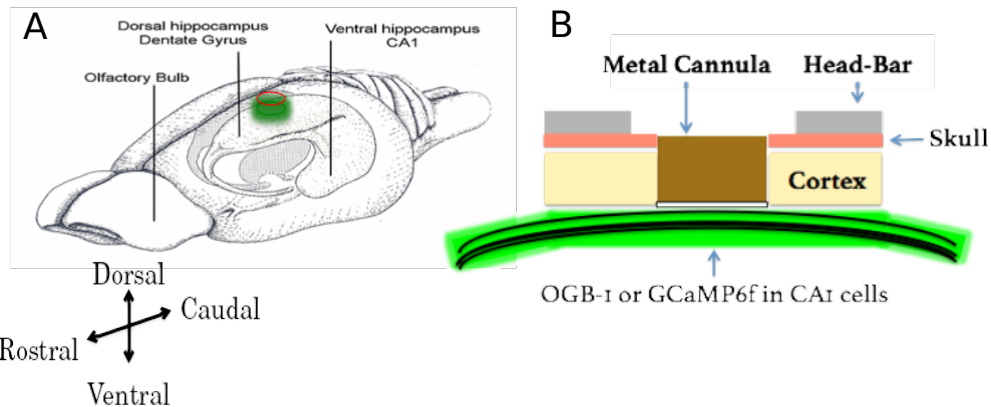


Figure 20: (A) A schematic of the rodent brain, showcasing the two hippocampi, one in each hemisphere. The hippocampi lie ~1 mm (mice) below the cortical surface. (B) The hippocampal preparation allows optical access to the deep lying hippocampal CA1 cells, relative to the skull/cortex. The CA1 cell bodies arrange in a laminar fashion, as a tight cell body layer that can be visualized by fluorescence (using either OGB-1 or GCaMP).

1579 We first put the animal under anesthesia using a vapor chamber
 1580 saturated with 3% isoflurane. Next, the animal is cheek-clamped and
 1581 anesthesia is maintained using 1-2% isoflurane, provided directly to
 1582 the nozzle of the animal, keeping track of ~1 Hz breathing rate and a
 1583 body temperature of 35-37 °C (with heating pad). The animal is given a
 1584 haircut and an ~5 cm circular incision is made on the scalp, revealing
 1585 the skull below. We then affix headbars and skull screws with the help
 1586 of dental cement, to be able to clamp the animal post surgery on the 2-
 1587 Photon Microscope.

1588 The left, dorsal hippocampus is targeted with a 3-5 mm circular
 1589 craniotomy aimed at 1.5 mm left and 2.0 mm behind bregma, carefully
 1590 tearing and peeling out the Dura, to reveal the cortex.

1591 We perform a Hippocampal Preparation, to aspirate out the cortex
1592 (part of the somatosensory cortex) under repeated washes of Cortex
1593 Buffer (see table 1 for recipe), and expose a part of the dorsal
1594 hippocampal surface.
1595 Depending on the requirement for the preparation, viz., acute or
1596 chronic imaging, we used different sensors.

1597 **Preparation of Cortex Buffer**

1598 To prepare 1000 ml of cortex buffer, weigh out the required amount of
1599 the salts, NaCL, KCl, Glucose and HEPES (see table 1 for recipe) and
1600 make up the volume of the solution with Milli Q Water till about slightly
1601 less than 1000 ml. Measure the pH using a calibrated pH meter. The
1602 expected pH is slightly acidic (around 5), so use 1M NaOH (aq) to set
1603 the pH to 7.35.
1604 Then, fill up the volume to 1000 ml and verify the pH (should not have
1605 changed). Filter the contents through a 0.22 um membrane using a
1606 vacuum filtration, and store at 6 °C.

Table 1: Recipe for ready-to-use cortex buffer. The buffer is typically prepared and stored in aliquots to be used each week. The correct pH range of the buffer was often a crucial factor ensuring the success of the hippocampal preparation.

Ingredient	Concentration (mM)	Amount (g or ml)
NaCl (s)	125	7.31 g
KCl (s)	5	0.373 g

Glucose (s)	10	1.8 g
HEPES (s)	10	2.38 g
CaCl2 (aq)	2	1.6 ml of 1.25 M stock solution
MgCl2 (aq)	2	1.5 ml of 1.3 M stock solution0

1607 **Oregon Green Bapta-1 Injections for
1608 acute imaging**

1609 For acute/single-day experiments, we injected OGB-1 using pulled,
 1610 dye loaded micropipettes at a depth of 100-150 µm (Figure 20) from
 1611 the topmost layer of exposed tissue, till a slow but detectable pulse of
 1612 dye (visualized as a red/pink solution; see table 2 for recipe) may be
 1613 visible just below the tissue surface. This allows the dye to be soaked
 1614 up by the basal dendrites of the CA1 and takes 30-60 mins for
 1615 incorporation into the cytoplasm. We typically allow the animal 1-2
 1616 hours of respite before the subsequent imaging session. High pressure
 1617 ejection of the dye into the tissue may damage the neuropil, while very
 1618 low pressures or clogs in the pipette affect the spread of the dye
 1619 across the tissue. We aimed to image ~100 x 100 µm² of the tissue in
 1620 any particular ROI, and achieved this with 5 minute injections with
 1621 each micropipette aiming to load the dye at 2-3, well separated
 1622 positions spread across the entire exposed dorsal surface. We
 1623 estimate that the dye volume was <1000 nl/injection. After the injection

1624 cycle with any micropipette, we leave the tissue undisturbed for at least
1625 5-10 mins before pulling the micropipette out of the tissue.

1626 <Table 2 here>

1627 Once all the injections are complete, the exposure is sealed using 5%
1628 low gelling agarose, just before it sets, making sure the temperature is
1629 cool enough to avoid heat-related tissue damage. Place a drop of the
1630 5% agarose solution on the back of the hand to test the temperature.

1631 OGB-1 is eventually cleared from the cytoplasm but allows for a limited
1632 window for imaging studies (Stosiek et al., 2003). Reopening the
1633 agarose seal and re-injections were never attempted to prevent
1634 unnecessary damage to the underlying tissue. Additionally, the
1635 agarose plug itself was found to be unstable beyond 1-3 days. This
1636 resulted in the imaging possibility being limited to the same day as the
1637 surgery (acute imaging).

1638 **GCAMP and chronic imaging**

1639 For chronic/multi-day experiments, we standardized a stereotaxic viral
1640 injection step, where we inject the gene for GCaMP5 or GCaMP6f into
1641 the dorsal hippocampus at -1.5 mm lateral, 2 mm posterior, and 1.3
1642 mm dorsal from bregma on the skull surface (Figure 21).

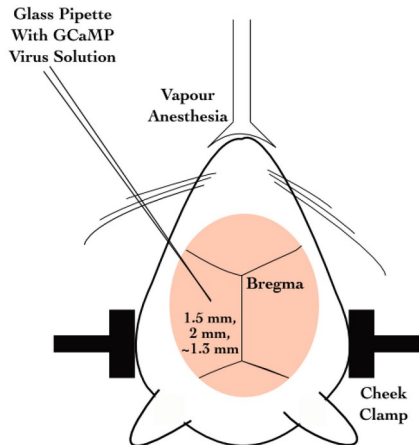


Figure 21: Schematic representation for stereotaxic viral injection.

1643 Later on, we switched to directly using GCaMP6f transgenic mice
1644 (background: C56BL/6) which express GCaMP6f in the Hippocampus
1645 (Chen et al., 2013), and thus circumvented the dye loading or viral
1646 injection steps, aiding in the potential success of the preparations, by
1647 way of tissue health and recording quality.

1648 **Results - Imaging**

1649 **2-Photon calcium imaging of hippocampal CA1, 1650 *in vivo***

1651 Next, we subject the CA1 cells to Imaging. The CA1 cell body layer is
1652 ~200 µm deep in through the hippocampal surface. At these depths,
1653 scattering of excitation as well as emission light is significant. However,
1654 we are able to image at these depths with Two-Photon Imaging
1655 LASER Scanning Imaging (810 nm for OGB-1 and 910 nm for

1656 GCaMP5/GCaMP6f), where a high intensity pulsed LASER allows for
1657 Two-Photons to near instantaneously excite fluorophores in a thin z-
1658 slice plane which is the focal plane of the Objective. There is
1659 scattering, but this since only the focal plane is excited any and all
1660 emitted photons that we capture are part of the signal. We use a 16x
1661 water immersion, 0.8 NA, 3 mm working distance Objective, to get a
1662 large field of view.

1663 **Acute Imaging of OGB-1 loaded hippocampal
1664 CA1**

1665 OGB-1 spreads throughout the cytoplasm and neuropil, and infiltrates
1666 the cell nucleus, giving the cells the appearance of solid circles (cells).
1667 The cell body (soma) ranges from 10-15 μm depending on the
1668 orientation of the imaging layer in 3D tissue space (Figure 22A).

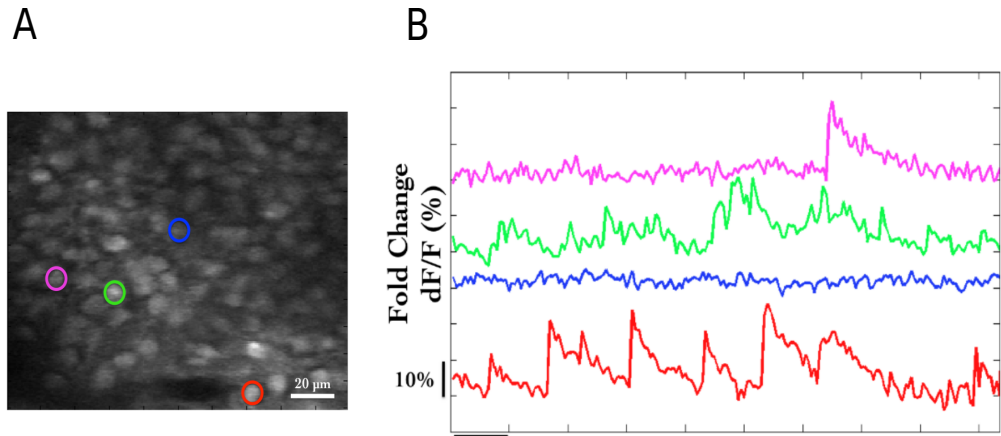


Figure 22: (A) Representative Two-Photon Calcium Image of a plane of Hippocampal CA1 cells, bolus loaded with Oregon Green Bapta-1 (OGB-1), at an instant in time. Example cells marked out post-hoc as pink, green, blue and red. Scale bar 20 μ m. (B) Representative dF/F (%) traces for the calcium activity recorded in a single 10s video for example cells pink, green, blue, and red. Scale bar (1 sec; 10% dF/F).

1669 Each cell in the recorded region of interest (ROI), is identified, marked
 1670 out (in pixel identity), based on local activity of correlated pixels in the
 1671 time series movies. The average intensity of the pixels corresponding
 1672 to each cell for each frame in each recording video, is saved as the
 1673 raw calcium fluorescence trace. Next, these raw calcium traces are
 1674 baseline normalized to equate the baselines for each cell at 0, and
 1675 describe the dynamic range of the intensity values as 0 to 1, or 1 to
 1676 100%. Here are the corresponding time series of baseline normalized
 1677 dF/F for the representative example cells (the same blue, green, and
 1678 red cells as above) are shown (Figure 22B).

1679 **Chronic imaging of GCaMP expressing**
 1680 **hippocampal CA1**

1681 For chronic imaging, tissue health was of paramount concern since it
1682 could easily degrade in time (Figure 23). With practice and
1683 standardization, we were able to get the preparations to survive for 2-4
1684 weeks at very good signal-to-noise. Preparations that resulted in very
1685 poor signal-to-noise were often recorded but have been filtered out of
1686 the data showcased in this thesis. While preparations can sometimes
1687 last even months, typically it is crucial to consider if the ROI for
1688 recording could provide >20 cells, to continue the experiment.
1689 GCaMP is typically designed to be cytosolic and does not typically
1690 cross into the cell nucleus. GCaMP labeled cell bodies appear as
1691 doughnuts in the imaging slice (Figure 23, Figure 24).

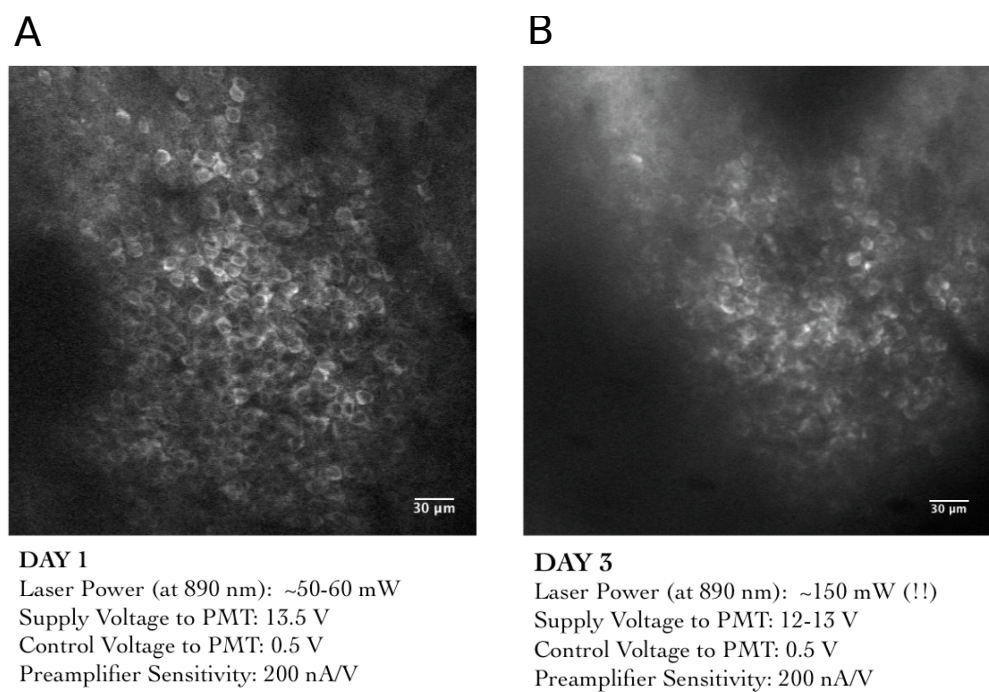


Figure 23: Tissue Degradation over time. Representative Two-Photon Calcium images of a snapshot in time of the Hippocampal CA1 cell body layer on A) Day 1 after the surgery and B) Day 3, after the surgery.

1692 Recordings with very good signal-to-noise, where the same chronically
1693 labeled CA1 cells could be anatomically identified on subsequent days
1694 even >2-3 weeks post surgery (Figure 24) were eventually acquired,
1695 and are featured in the data presented in Chapter 4.

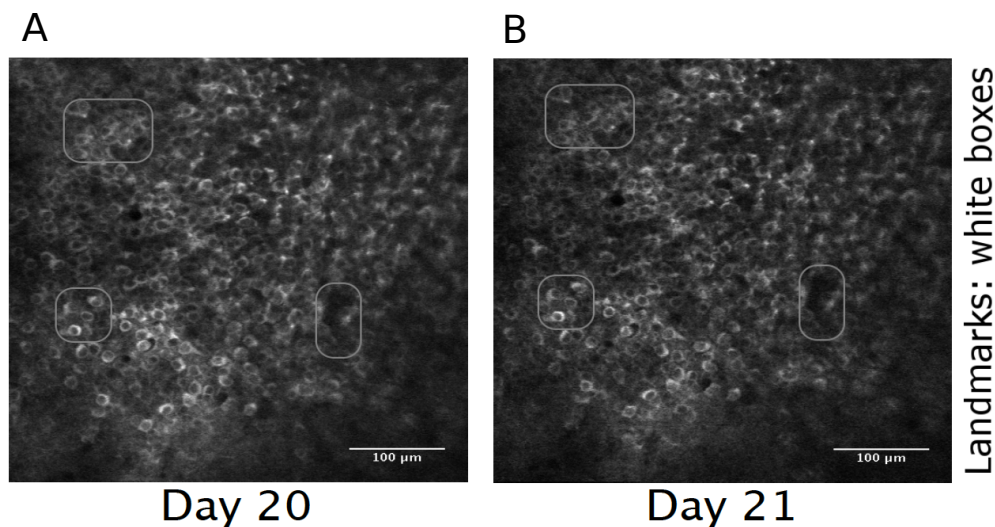


Figure 24: Chronic calcium imaging of the same Hippocampal CA1 cells over weeks. Representative 2-Photon images from A) Day 20, and B) Day 21, after surgery. Landmarks have been marked and were used to confirm frame registration and identify cells.

1696 The magnification and resolution of the field of view are important
1697 parameters to consider when balancing magnification for the resolution
1698 and the maximization of the number of cells being simultaneously
1699 recorded from (Figure 25).

1700 While recording at high frame rates for live imaging, we capture a
1701 relatively large number of cells (~100) in time-series imaging frames, at
1702 frame rates of around 10-15 fps. Subsequently, we subject the animal
1703 to various stimuli across trials and save these images for analysis.

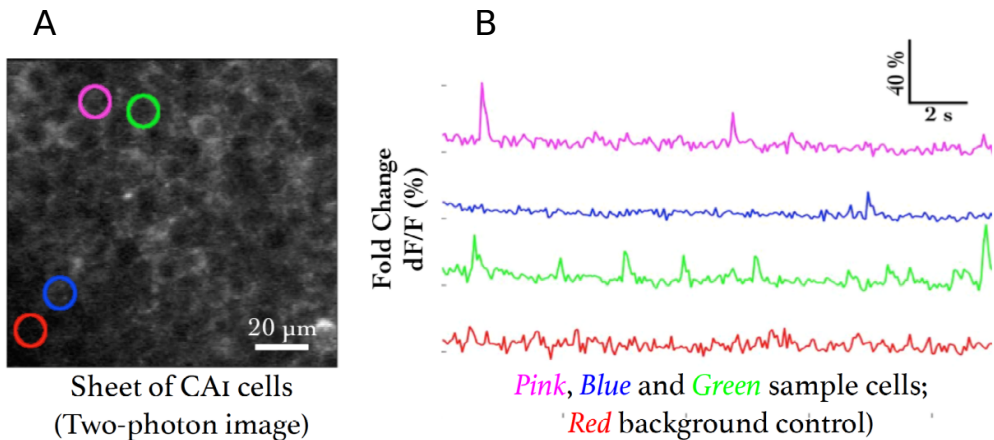


Figure 25: (A) Representative Two-Photon Calcium Image of a plane of Hippocampal CA1 cells expressing GCaMP6f at an instant in time. Example cells marked out post-hoc in pink, blue, and green, with no-cell background in red. Scale bar 20 μm . (B) Representative $dF/F\ (\%)$ traces for the calcium activity recorded in a single 10s video for example cells in pink, blue, and green, with no-cell background in red. Scale bar (2 sec; 10% dF/F).

1704 **Spontaneous activity during non-stimulus 1705 periods**

1706 We recorded the calcium activity from a large number of Hippocampal
1707 Cells while presenting various neutral and conditioning stimuli,
1708 including fairly large periods of time before and after stimulus
1709 presentation. Activity of cells, typically observed *in vivo*, in these
1710 periods is termed spontaneous activity. Cells may showcase variable
1711 rate (number of calcium events per sec) and timing. Given proper
1712 signal isolation for identified cells in an ROI, each source or “cell” may
1713 be considered independent.

1714 **Spatial organization of activity correlated cells**
1715 **during spontaneous activity**

1716 We studied the Pearson's Correlation Coefficient for the activity traces
1717 across all cell pairs. Cell pairs showcased a range of correlation
1718 coefficients (Figure 26) and we were able to cluster cells based on
1719 activity using Meta-K Means (Modi et al., 2014; unpublished data from
1720 Ashesh Dhawale's Thesis).

1721 These results matched the same published previously in the lab (Modi
1722 et al., 2014).

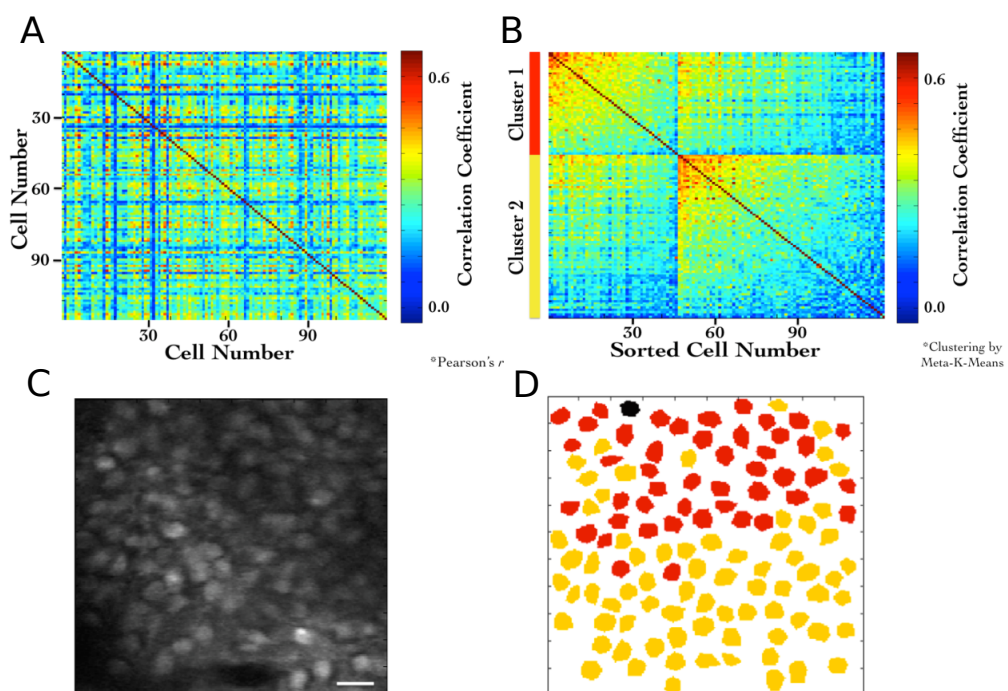


Figure 26: (A) Correlation Coefficients for cell pairs from an example two-photon recording. (B) Meta-K Means clustering with cell pairs using the heuristic that within group pairs would be more similar than between group pairs. In this example, the cells were clustered into two groups (red and yellow). (C) Two-Photon image of the field of view of cells. (D) Spatial organization of correlated cell-pair groups (Modi et al., 2014).

1723 **Stimulus evoked responses**

1724 We also recorded calcium activity from the same cells during
1725 presentation of various neutral stimuli to the animals. Here are the
1726 results of the auditory (tone) and somatosensory (whisker) stimulus
1727 experiments.

1728 A neutral auditory tone at 5000 Hz (for 1 sec) was presented to the
1729 animals N= 6 animals; 25 trials). We observed no clear signs of cell
1730 activity modulation by neutral tones. Below, we show an example
1731 animal with trial-averaged calcium traces as dF/F (%), across all
1732 recorded cells with a 1 sec tone presentation (Figure 27A). We also
1733 presented animals to whisker stimulation by playing a 1s long air-puff
1734 (5 LPM) to the ipsilateral (left) whisker (N = 5 animals; 25 trials). In this
1735 case, we observed whisker-stimulation based cell activity modulation.
1736 Below, we show the trial-averaged calcium traces as dF/F (%) of the
1737 same example animal as above, presented with a 1 sec whisker-puff
1738 (Figure 27B).

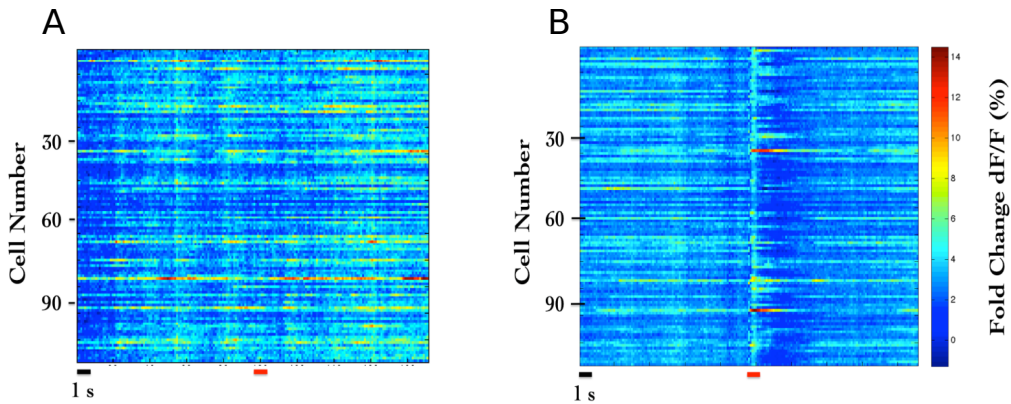


Figure 27: (A) Trial-averaged (25 trials) calcium activity from ~100 CA1 cells in trials where a 5000 Hz tone was presented (red bar). (B) Trial-averaged (18 trials) calcium activity from the same cells in trials where a 5 LPM air-puff to the ipsilateral whiskers was presented (red bar).

1739 More short-range localized clustering of groups of cell-pairs with
 1740 correlated activity were observed post whisker-stimulation.

1741 **Chronic imaging now possible for weeks with**
 1742 **the same mouse**

1743 The need for multi-day tracking was mandated for recordings through
 1744 behavioural training, since the animals typically only learn Trace Eye-
 1745 Blink Conditioning (TEC; Chapter 2) over the course of 3-7 days
 1746 (Siegel et al., 2015). A different experiment design would have been to
 1747 train animals and then perform the hippocampal preparation to record
 1748 CA1 neural activity while the animal(s) exhibit learnt Conditioned
 1749 Responses (CRs). However, we argued against this experimental
 1750 design, on account of the following.

1751 1. The actual cellular and network mechanisms that allow for the
1752 animal to learn the behavioural task would be very difficult to study
1753 given that the learning period would have passed.
1754 2. The success rate of the hippocampal preparation is typically very
1755 low, while TEC is typically learnt by >50% animals (Modi et al., 2014;
1756 Siegel et al., 2015). We had argued for exposing the hippocampus for
1757 imaging before behavioural training since any successful preparations
1758 could then be subjected to the relatively more consistent behavioural
1759 training.
1760 3. Having the preparation performed before training minimizes the
1761 number of times the animal would be subjected to surgery (to just the
1762 once), improving chances of animal health through the experiment.

1763 Next, we discuss some preliminary results from the chronic imaging
1764 datasets. A non-overlapping set of results that feature in “Chapter 4 -
1765 Analysis” of this thesis, have been skipped here for brevity.

1766 **[Legacy] Analysis to identify time cells**

1767 The analysis algorithm pertaining only to the results presented here in
1768 “Chapter 3 - Imaging”, was adapted from William Mau’s Temporal
1769 Information method ((Mau et al., 2018); Chapter 4 - “Analysis”). This
1770 analysis algorithm was not developed to the extent of the Python/C++
1771 implementation featured in “Chapter 4 - Analysis” and is expected to
1772 be subject to some degree of Type I (false positives) and Type II (false
1773 negative) errors.

1774 1. Filter to select for cells that had activity in >25% of trials
1775 (irrespective of tuning)

1776 2. Develop Event Time Histograms, using Area Under the Curve
 1777 for a binsize of 3 frames, centering the “0 ms” to the onset of the
 1778 Conditioned Stimulus for visualization.
 1779 3. Estimate Temporal Information (TI), using
 1780 $TI = 1/\lambda * \sum_j \lambda_j \log_2 (\lambda_j / \lambda) P_j$
 1781 where,
 1782 λ : Average Transient rate for each cell
 1783 λ_j : Average transient rate for each cell in bin “j”
 1784 P_j : Probability that the mouse was in time bin “j”
 1785 For every trial, random shuffle the frame points to develop a random
 1786 activity model (1000 times) and ensure that $\lambda > \lambda_{rand}$ in more than
 1787 99% of the models. If yes, then the cell has time locking with temporal
 1788 information (TI; in bits) as a measurement for time information. Filtering
 1789 for cells active in >25% trials with a $\lambda > \lambda_{rand}$ in >99% shuffles, along
 1790 with the estimation of TI, provide us a handle on reliability.

1791 **Time Cells**
 1792 During the experience of temporally organized events or stimuli, in this
 1793 case post training to Trace Eye-Blink Conditioning, a rough contingent
 1794 of ~20% of the total cells recorded, were observed to showcase time-
 1795 locked calcium activity mapping the Blue LED or Conditioned Stimulus
 1796 (CS) to the air-puff or Unconditioned Stimulus (US). These cells were
 1797 classified as time cells. Here are some example time cells (Figure 28).

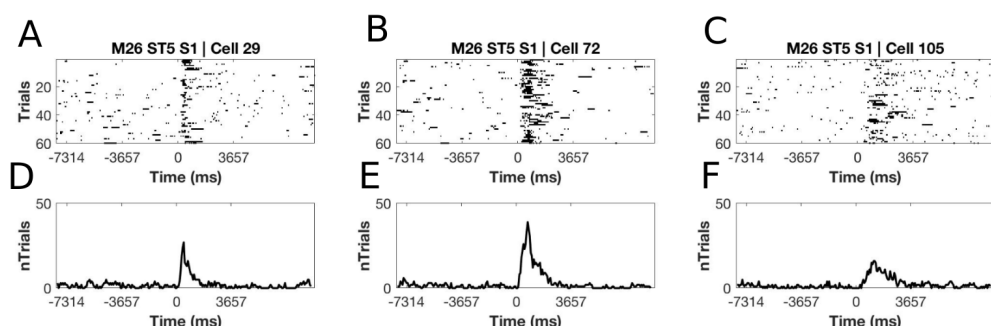


Figure 28: Example Time Cells visualized as event raster plots (A, B, C), along with the trial-summed activity profiles (D, E, F) suggesting ~50% hit trials, for cells 29 and 72 from Session 1 (session type 5) with mouse M26, and slightly lower reliability (~25% hit trials) from cell 105.

1798 **Other Cells**

1799 On the other hand, most cells did not clear our analysis algorithm
1800 checkpoints and were classified as other cells. Here are some example
1801 Other Cells (Figure 29) from the same session with mouse M26
1802 (Session 1; session type 5).

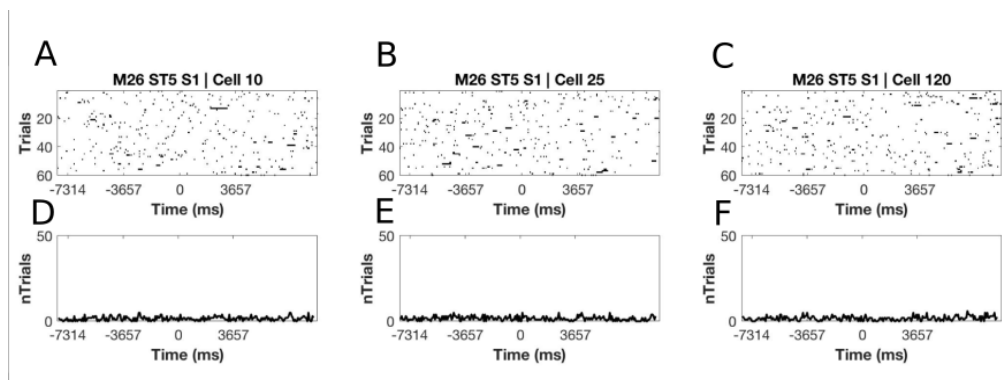


Figure 29: Example Other Cells visualized as event raster plots (A, B, C), along with the trial-summed activity profiles (D, E, F) for cells 10, 25, and 120 from Session 1 (session type 5) with mouse M26

1803 Considering only the classified time cells, we sorted cells based on the
1804 time of the peak of the trial-average activity and a spatiotemporal
1805 sequence was visualized (Figure 30; also see “Chapter 4 - Analysis
1806 Figure 7H”).

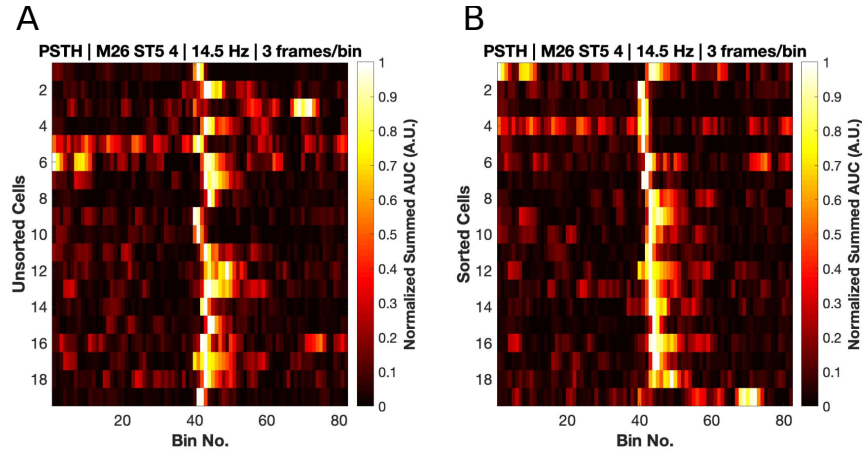


Figure 30: Event Time Histograms or tuning curves for Identified Time-Locked Cells with trial-summed peaks in session 4 of training (session type 5) with mouse M26. (A) Unsorted list of Time cells. (B) Peak-sorted list of the same cells. Here, 1 bin = 3 frames = ~ 210 ms (sampling rate 14.5 Hz without binning; ~ 5 Hz with binning). As per the (legacy) session type 5 protocol, the CS (50 ms Blue LED flash) was presented in frame bin 39 a conservative stimulus-free trace interval during frame bins 40 and 41, and the US (50 ms airpuff to ipsilateral eye) presented in frame bin 42.

1807 We did not observe any obvious trend in the temporal information of
 1808 time cells with peak times. For the same cells as in Figure , we now
 1809 look at the actual Temporal Information estimates (Figure 31).

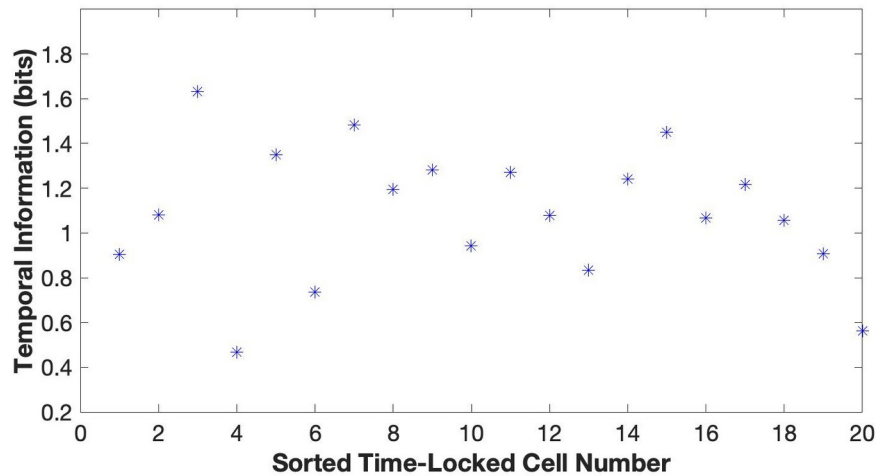


Figure 31: Temporal Information (bits) vs Sorted time cell number from the analytically identified Time Cells in Session 4 (session type 5) with mouse M26. No clear trend was observed.

1810 **Tuning, re-tuning, and de-tuning of time cells across sessions**

1812 A crucial advantage of the chronic preparation was that many
 1813 anatomically aligned and classified cells (as cell ROIs), could be
 1814 recorded from over several days and sessions, to look for possible
 1815 changes in calcium activity profiles across sessions in the same set of
 1816 cells.

1817 We noticed some evidence for an expansion of the set of identified
 1818 time cells with sessions, up to a reliable pool of ~20% time cells.
 1819 Altogether, from the pool of chronically aligned cells (across sessions),
 1820 there was an increase from 7.7% to 23.1% of time cells. Considering
 1821 the full cohort cells (irrespective of tracking across multiple training
 1822 sessions) the increase was from 7.2% to 21.1% time cells. Here are

1823 the classified time cells between two independent recording sessions,
 1824 early in training (Figure 32).

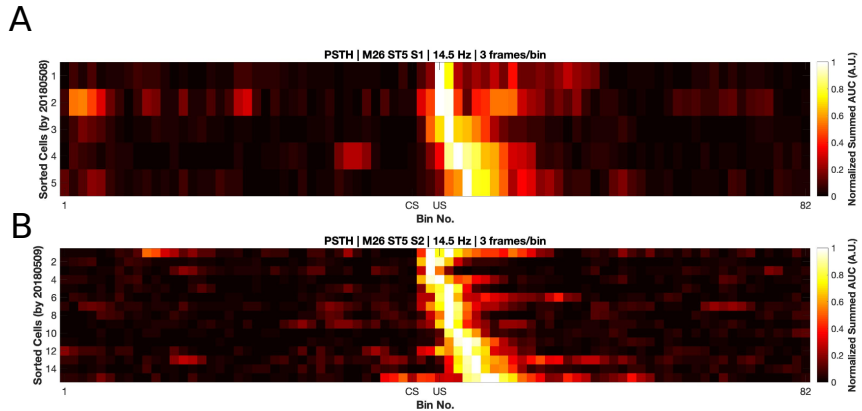


Figure 32: More time cells observed to attain tuning as training sessions. Event Time Histograms of the identified set of time cells between A) Sessions 1 and (B) Session 2, with mouse M26 (session type 5).

1825 The same may also be visualized as trial-averaged calcium activity
 1826 profiles for all recorded cells across independent recording sessions
 1827 (Figure 33).

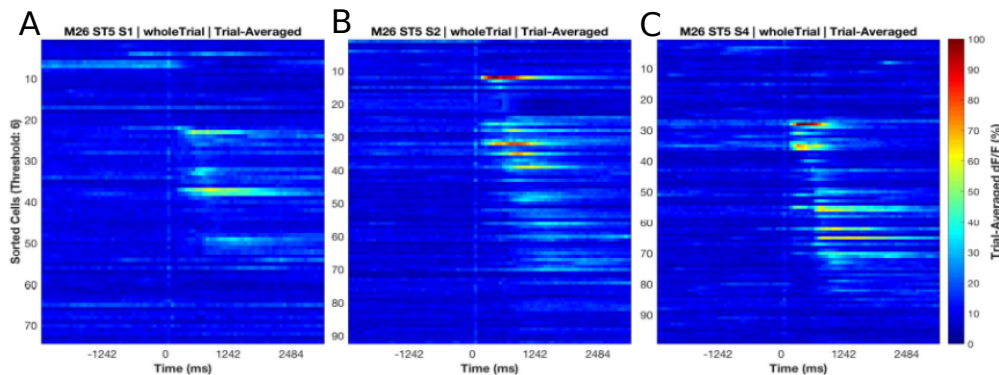


Figure 33: Sorted Time Cells form Sequences that develop with learning. Trial-Averaged calcium activity traces for all recorded cells across A) Session 1, B) Session 2, and C) Session 4, with mouse M26 (session type 5). Time 0 ms was aligned to the CS. The CS + Trace + US interval lasted from 0-600 ms, here.

1828 Chronically tracked Time Cells that showed reliable tuning across
1829 sessions were then compared to look for any shifts in the peak tuning
1830 bin.

1831 We observed examples of cells that maintained their tuning across
1832 pairs of sessions (Figure 34).

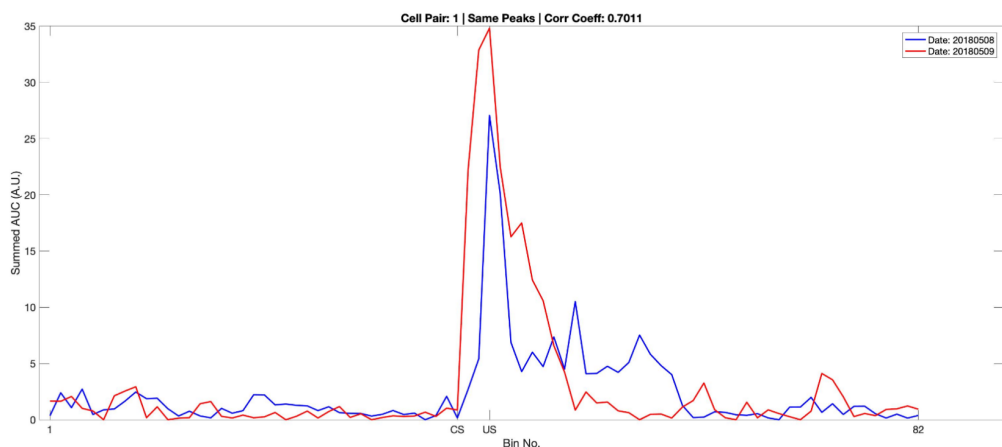


Figure 34: Same/similar tuning across session 1 and session 2 for this example time cell. Blue Event Time Histograms represent the tuning curve for the cell for session 1 (date: 20180508) and Red represent the same but for session 2 (date: 20180509). Pearson's correlation coefficient between the two session pairs was 0.7011.

1833 Here are examples for earlier Event Time Histogram (tuning curve)
1834 peaks across sessions (Figure 35) for Mouse M26, session type 5,
1835 session 1 vs 2.

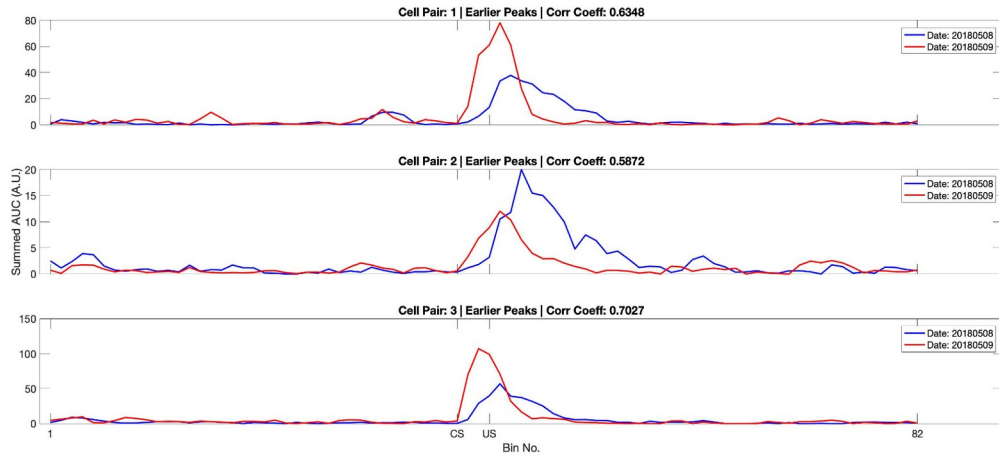


Figure 35: Three example chronically tracked cell pairs with tuning peaks arriving earlier with training sessions (rows). Blue Event Time Histograms represent the tuning curve for any cell for session 1 (date: 20180508) and Red represent the same but for session 2 (date: 20180509). Pearson's correlation coefficient between the session pairs was 0.6.348, 0.5872 and 0.7027 for A) cell pair 1, B) cell pair 2, and C) cell pair3, respectively.

1836 Here is an example of a cell showcasing de-tuning across sessions
 1837 (Figure 36).

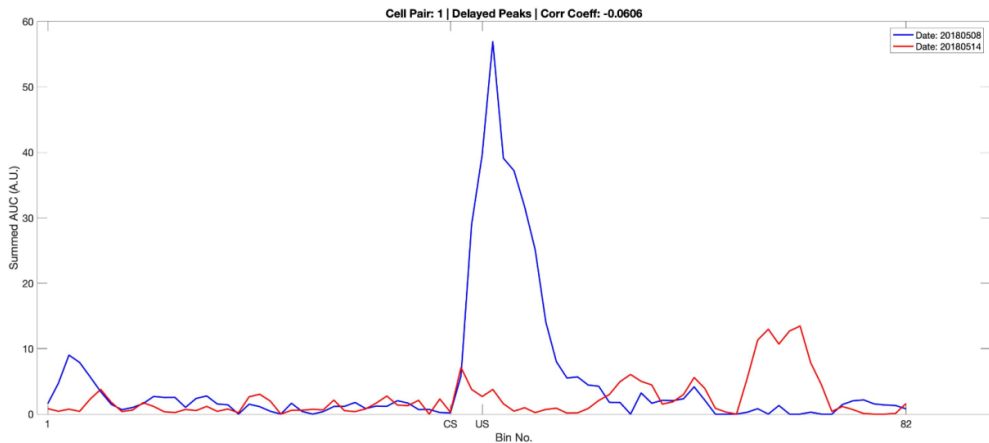


Figure 36: Example chronically tracked cell pair with de-tuning between session 1 and 4. Blue Event Time Histograms represent the tuning curve for the example cell for session 1 (date: 20180508) and Red represent the same but for session 4 (date: 20180514). Pearson's correlation coefficient between the two curves was -0.0606.

1838 A full summary of the correlation based peak timing analysis for
 1839 chronically identified time cells with mouse M26 are shown (Figure 37).
 1840 Across all same cell pairs, there was positive correlation (>0.2) in 71%
 1841 of Time Cells. Also a comparison of the tuning curve peaks between
 1842 the same time cell pairs revealed that a majority of the re-tuned peaks
 1843 occurred earlier in time, going across sessions (71%), with an equal
 1844 proportion of cells without much re-tuning (14%) or de-tuning to later
 1845 time points (14%).

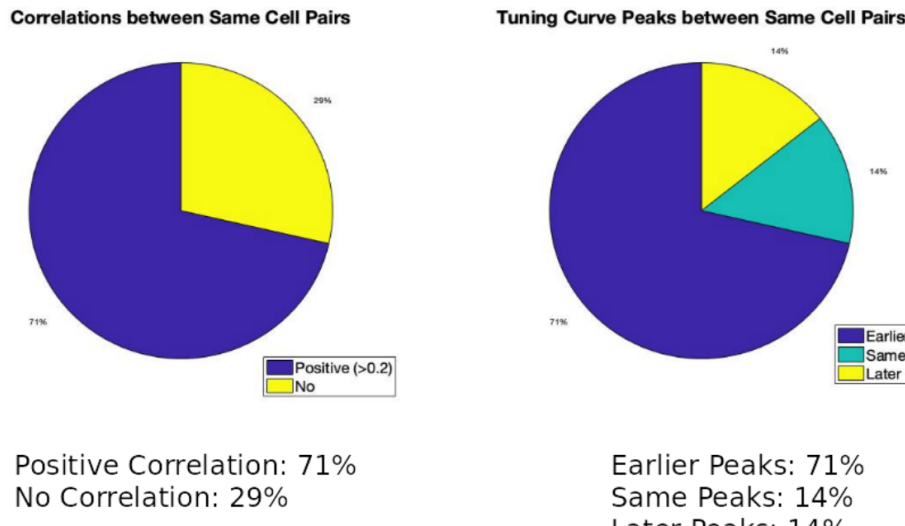


Figure 37: Comparing time cells across sessions for all cells.

1846 An essential summary of the key preliminary results observed using
 1847 real physiology data:
 1848 1. Time cell tuning curve peaks typically began only after the
 1849 presentation of the CS.
 1850 2. The width of the tuning curve peaks for Time Cells increased with
 1851 tuning to later frame bins. This was consistent with the recordings
 1852 presented in literature under physiological conditions (B. J. Kraus et
 1853 al., 2015; MacDonald et al., 2011, 2013; Mau et al., 2018; Modi et al.,
 1854 2014; Pastalkova et al., 2008).
 1855 3. Pairwise time cell tuning curves for different Time Cells may have
 1856 some overlap in timing, but peaks were observed in all frame bins
 1857 between the CS and the US. This particular observation is confounded
 1858 by the short number of Trace period frames recorded and the
 1859 requirement to consider 3 recording frames to every bin (Mau et al.,
 1860 2018), decreasing the effective sampling rate even further (14.5 Hz
 1861 without binning, to ~5 Hz with binning). Further experiments may be
 1862 necessary to interpret. However the observation is still consistent with

1863 previous literature (B. J. Kraus et al., 2015; MacDonald et al., 2011,
1864 2013; Mau et al., 2018; Modi et al., 2014; Pastalkova et al., 2008).

1865 4. A surprisingly large number of Time cells could be identified with
1866 tuning peaks for frame bins occurring after the termination of the US.

1867 5. Considering all chronically tracked cells, the classified and sorted
1868 Time Cells formed sequences that were dynamic across learning
1869 sessions. Many Time Cells developed tuning curves with sessions
1870 while some Time Cells lost their tuning.

1871 6. For the majority of Time cells, re-tuning occurred with initial tuning
1872 to the timing of the US in earlier sessions, followed by a shift to earlier
1873 time points for the tuning peak, as training progressed through
1874 sessions.

1875 Future directions to be explored in the lab include studying the
1876 reliability of a larger pool of chronically tracked cells with switches in
1877 the inter-stimulus interval (ISI) between the CS and the US as well as
1878 with a larger palette of different stimuli testing out a battery of
1879 Conditioned Stimuli (CS1, CS2, etc.) and Unconditioned Stimuli (US1,
1880 US2, etc.). The goal is to understand how well the internal neural
1881 spatiotemporal CA1 sequence maps to the external behavioural
1882 protocol parameters, *in vivo*.

1883 – Bibliography

1884 Chapter 5 – Discussion

1885 Ramón y Cajal, one of the pioneers of neuroscience around 1900,
1886 utilized Camillo Golgi's staining method to conclusively describe
1887 neurons in the brain as independent functional units connected to each
1888 other in intricate small-world networks with many billions of nodes.
1889 These neurons have since been described not just anatomically, but
1890 also on the basis of genetics, development, and neurophysiology.

1891 In the sub-discipline of Learning and Memory, a very popular neuron
1892 type by way of such studies is the pyramidal neuron, an example of
1893 which is the hippocampal CA1 pyramidal neuron. This thesis describes
1894 a toolkit of techniques ranging in a wide, multi-disciplinary scope,
1895 assembled with standardized hardware and software routines studying
1896 animal behaviour, network neurophysiology, and statistical analyses.
1897 The aim of the toolkit was to provide the experimental ability to study
1898 the hippocampal CA1 neuron network, under strictly controlled
1899 behavioural contexts designed to train experimental mice on temporal
1900 or episodic memory tasks. Specifically, these tasks such as Trace Eye-
1901 Blink Conditioning (TEC) have previously been described to elicit
1902 hippocampal CA1 sequences (B. J. Kraus et al., 2015; MacDonald et
1903 al., 2011, 2013; Mau et al., 2018; Modi et al., 2014; Pastalkova et al.,
1904 2008). This spatiotemporal network activity sequence is dynamic and
1905 built from individual hippocampal CA1 pyramidal neurons showcasing
1906 time tuned activity through spiking. These cells are called time cells
1907 (Eichenbaum 2017).

1908 **Engrams associated with Learning and**

1909 **Memory**

1910 The term "engram" (coined by Richard Semon) refers to the physical
1911 substrate of memory in the organism, used for storing and recalling
1912 memories. Donald Hebb's theory of Hebbian Plasticity (Hebb,
1913 1949) postulated that memory formation was correlated to modulations
1914 in synaptic strength and connectivity. The theory critically emphasized
1915 that the pair of neurons connected through the synapse undergoing
1916 plasticity to strengthen efficacy, required the spiking activity of both
1917 neurons. In subsequent decades, research into the idea led to the
1918 theory of spike-timing-dependent plasticity (Caporale & Dan, 2008), a
1919 mechanism of synaptic plasticity based on the relative timing of activity
1920 of the neurons. It is still a matter of debate whether the biophysical
1921 manifestation of the engram is the synapse, the activity of the neurons,
1922 biophysical and chemical processes, but it is likely that the engram is
1923 distributed across several computational scales in the brain.

1924 Eric Kandel's experiments with the Aplysia sensory neurons studied gill
1925 withdrawal - an aversive but stable, adaptive behaviour. The reliability
1926 of this learned response allowed the experiments to include crucial
1927 electrophysiological and neurochemical circuit dissections that
1928 ultimately lead to the discovery of the entire neural circuit orchestrating
1929 the task, even to the level of cellular signaling. This led to decades of
1930 research focused on the plasticity of synapses across nervous systems
1931 in the animal kingdom.

1932 Research exploring causal relationships between the physical or
1933 functional integrity of various brain regions and overt behaviour has
1934 been crucial to mapping many brain regions to specific functions and

1935 motor responses. Technological advancements in molecular
1936 neuroscience led to the development of a number of fluorescent
1937 sensors, conditional tagging, activators and inhibitors that allowed
1938 cellular resolution tracing of the engram (Luo et al., 2018).

1939 Experiments by Sheena Josselyn, Alcino Silva, and colleagues led to
1940 the discovery that the intrinsic excitability of a pyramidal neuron in any
1941 network positively biased the probability of recruitment to the engram
1942 (Han et al., 2009; Rogerson et al., 2014; Yiu et al., 2014; Y. Zhou et
1943 al., 2009), viz., the tagged set of cells were active when memory was
1944 learnt and recalled. The engram seemed to be described in terms of
1945 the cellular sub-population involved but the experiment could only
1946 identify the same over a relatively longer window of time (~mins.). This
1947 could lead to only a static list of cells which may even have included
1948 False Positives (Type I error). Importantly, any dynamics in the
1949 spatiotemporal patterns of activity of the pyramidal neurons were not
1950 amenable to study at shorter timescales (~ms.). On the other hand,
1951 physiological recordings could describe these dynamics at short
1952 timescales, but were rarely translated to chronic measurements of the
1953 activity of the same cells across days and sessions, given technical
1954 limitations at the time.

1955 **Engrams are likely dynamic**

1956 Place cells and their role in spatial navigation have been described in
1957 great detail through decades of research ever since they were first
1958 described by John O'Keefe (O'Keefe & Dostrovsky, 1971). We did not
1959 explicitly study Place Cells in this thesis but some key discoveries in
1960 literature require mention, with the goal to build a case for a theory of
1961 CA1 ensemble sequences (Modi et al., 2014). Briefly, place cells are

1962 pyramidal neurons that showcased a higher than baseline probability
1963 of firing action potentials whenever animals navigating spatial
1964 environments visited specific locations, often in a sequence of place
1965 cells mapped to the real spatial trajectory of the animal (Ferbinteanu &
1966 Shapiro, 2003; Foster, 2017; Frank et al., 2000; Wood et al., 2000).

1967 As the animal enters these landmark locations in any spatial context,
1968 these place cells showcase Phase Precession, firing earlier in phase to
1969 cycles of Theta a network rhythm clocked at ~4-10 Hz, as the animal's
1970 position changes relative to the landmark. These navigation mapped
1971 place cell sequences are called Theta Sequences (Foster & Wilson,
1972 2007), typically mapped to a few active neurons at a time.

1973 In very specific contexts, these place cells express activity sequences
1974 synchronized to Sharp Wave Ripples, a different network activity
1975 phenomenon clocked at ~10-30 Hz, often not tied to the animal's
1976 location, called Replay Sequences (Foster & Wilson, 2006). These
1977 sequences have been described to play out typically in temporal order
1978 to models of place cell sequences describing known trajectories in
1979 space.

1980 There is variability in the firing of place cells in any spatial context, and
1981 studies have mapped specific sequences to very specific trajectory
1982 goals (going towards or away from locations) with modulation by both
1983 egocentric and allocentric orientations cues (Davidson et al., 2009;
1984 Ferbinteanu et al., 2011; Ferbinteanu & Shapiro, 2003; Frank et al.,
1985 2000; Wood et al., 2000) and movement speed based estimates of
1986 distance (Kropff et al., 2015).

1987 Place cell and time cell sequences have many similarities and
1988 differences in descriptive neurophysiology, but may emerge from the
1989 same memory organization principles (Buzsáki & Llinás, 2017). It is
1990 argued that there is significance to the exact phrasing of the CA1
1991 sequence in any given context. Furthermore, a very interesting feature
1992 observed is Time-stamping, viz., time dependent overlap of ensemble
1993 responses to different contexts and behavioural parameters (Cai et al.,
1994 2016; Mau et al., 2018).

1995 Trace Eye-Blink Conditioning is a behavioural context which has been
1996 shown to feature CA1 time cell activity sequences. Transient increases
1997 in CA1 excitability post acquisition of the task were described up to 4-5
1998 days (Moyer et al., 1990) and could be important to the forging of the
1999 task specific spatiotemporal sequences during learning. Moreover,
2000 Trace Eye-Blink Conditioning in mice has been previously observed to
2001 elicit CA1 activity sequences even in a single session of training (Modi
2002 et al., 2014).

2003 Internally driven as opposed to externally driven network models of
2004 activity sequences have been proposed as the mechanism driving
2005 hippocampal CA1 sequences (Buzsáki & Llinás, 2017; Eichenbaum,
2006 2017). The CA1 neurons participating in any sequence may represent
2007 physiologically mappable attractors in temporally specific contexts. The
2008 standardized protocols described in the thesis are expected to aid in
2009 future experiments studying hippocampal CA1 sequences.

2010 **The study of hippocampal CA1 sequences**

2011 We standardized a multi-day Trace Eye-Blink Conditioning ("Chapter 2
2012 - Behaviour") training system for mice based on previous literature
2013 (Modi et al., 2014; Siegel et al., 2015) and could demonstrate several
2014 types of behavioural adaptations that experimental animals could learn
2015 under a variety of experiment conditions and modulations. Notably,
2016 1. The animals typically learnt the tasks quickly, within 1-2 weeks of
2017 training.
2018 2. Modulating the inter-stimulus interval (ISI) between the CS and
2019 US results affected the expression of the conditioned response (CR).
2020 3. A wide palette of stimuli may now be incorporated into existing
2021 protocols as either of the presented stimuli

2022 Simultaneous large-scale recordings have been fundamental to the
2023 discovery of long spatiotemporal activity patterns with several
2024 participant CA1 neurons (Davidson et al., 2009; Foster, 2017).
2025 Electrical recordings provide many orders of magnitude better temporal
2026 resolution, not to mention being a direct readout of action potentials.
2027 However at the time of the design of the thesis, imaging based
2028 approaches could yield more recorded neurons per experiment animal.
2029 We standardized 2-photon fluorescence based chronic imaging of
2030 hippocampal CA1 neurons to allow calcium imaging based recording of
2031 the spatiotemporal sequences across multiple days ("Chapter 3 -
2032 Imaging"). This gave us the ability to
2033 1. Record neurophysiology over a large population of neurons
2034 (~100), in conjunction with temporally relevant behavioural contexts
2035 and modulations, albeit at ~100 ms temporal resolution.
2036 2. Chronically track cells across various behaviour sessions without
2037 ambiguity.
2038 3. Allow for scalability in the per animal yield of recording neurons
2039 with the use of faster and modern 2-photon microscope hardware

2040 utilizing Resonant Scanning instead of Galvo Scanning, as well as
2041 multi-channel imaging.

2042 **Engrams are likely distributed**

2043 An important consideration is that while different brain regions have
2044 been studied and identified with various functions, each brain region is
2045 typically involved in a variety of functions and almost the whole brain in
2046 entirety, is involved in any real life task. Imaging multiple brain regions
2047 at near cellular resolution has been reported using Cortical
2048 Observation by Synchronous Multifocal Optical Sampling or COSMOS
2049 (Kauvar et al., 2020). However, we had limited our physiology
2050 experiments strictly to the dorsal Hippocampal CA1, in the left
2051 hemisphere. Multi-region imaging would require a second excitation-
2052 emission path, a technical and experimental paradigm which was not
2053 considered within the scope of this thesis.

2054 Similarly, important engram motifs at subcellular spatial scales were
2055 beyond the scope of the experiments in this thesis. Multiscale models
2056 of network function (Bhalla, 2014a, 2014b; Dudani et al., 2013) would
2057 be required to complement any physiology, as a possible way to
2058 address the issue of engram motifs at variable spatial scales.

2059 For our chronic 2-photon calcium imaging recordings, we had sampled
2060 from ~100-150 hippocampal CA1 neurons per mouse, using Galvo
2061 Scanning in our custom-built 2-Photon microscope (Modi et al.,
2062 2014) at a frame rate of ~14.5 Hz. We had to limit our scope of inquiry
2063 to randomly sampled populations of CA1 pyramidal neurons from the
2064 same CA1 microcircuit.

2065 Future directions include the use of Resonant Scanning to achieve
2066 higher frame rates at better lateral resolution sampling up to ~100x
2067 more neurons.

2068 **Mapping sequences to abstract variables**

2069 The Hippocampus may use non-visuospatial resources (specifically
2070 shown using Olfaction), to generate spatial representations, when
2071 vision is compromised (Zhang & Manahan-Vaughan, 2015).

2072 In a sound manipulation task (SMT) rats changed the frequency of
2073 auditory tones in their environment, by self-initiated joystick control,
2074 ramping logarithmic sweeps of frequency space. The rate of change in
2075 frequency could be manipulated either by the animal or
2076 pseudorandomly by the experimenter. This study describes neural
2077 activity recorded from the medial entorhinal cortex (MEC) as well as
2078 the hippocampal CA1 with sub-populations that were found tuned to
2079 specific frequency “landmarks” during the auditory sequence (Aronov
2080 et al., 2017). The CA1 were, thus, argued to be capable of tuning to
2081 abstract variables and were designed to map out sequences of
2082 events/stimuli in their own spatiotemporal patterns of activity.

2083 The ubiquity of neural sequences in a wide variety of systems has
2084 been discussed previously (Bhalla, 2019; Conen & Desrochers, 2022;
2085 S. Zhou et al., 2020)(Bhalla, 2017; Conen & Desrochers, 2022)(Bhalla,
2086 2019), and over a century of research has discovered remarkable
2087 physiological features that may be used to identify neurons that
2088 participate in these sequences. However, research is still required to
2089 carefully dissect out the contribution that each participant neuron has
2090 to behaviour, an important goal in neuroscience (Ranck, 1973, 1975).

2091 The use of user-configurable, categorically labeled synthetic calcium
2092 activity profiles allowed us to probe and compare a range of different
2093 time cell detection algorithms, identifying strategies to best classify
2094 time cells. We were able to identify Temporal Information as a strong
2095 contender for the choice of algorithm for such classification (“Chapter 4
2096 - Analysis”; (Ananthamurthy & Bhalla, 2023). The algorithms
2097 developed along the way were tested within the time scales of ~100
2098 ms, that correspond to Replay Sequences or other behaviour
2099 timescale sequences. We expect the analysis routines to be useful in a
2100 variety of different experiments that could potentially help describe the
2101 neural code in more detail.

2102 **Does the brain create or predict?**

2103 Predictive coding has been considered as a way for the brain to
2104 ultimately use external sensory information to minimize prediction
2105 errors during tasks (“Bayesian Brain Probabilistic Approaches to
2106 Neural Coding.,” 2007; Rao & Ballard, 1999). One of the core ideas of
2107 Bayesian approaches to neurophysiology and behaviour is that the
2108 brain could be modelled as a prediction machine that is constantly
2109 modelling the change of variables. These variables may be external or
2110 internal yet salient concepts to any experimental animal, arguably
2111 expressed in neurophysiology as the dynamics of engrams. The ability
2112 of the mammalian hippocampus to bind both information streams to
2113 create new, more elaborate engrams, is likely crucial to the learning of
2114 new concepts behaviourally (Eichenbaum, 2017).

2115 Attentional states have been shown to have a bidirectional relationship
2116 with the expression of memory and learning (Chun & Johnson, 2011;

2117 Hutchinson & Turk-Browne, 2012; Uncapher et al., 2011). Specifically,
2118 Trace Eye-Blink Conditioning (TEC) performance has been suggested
2119 to be positively correlated with attention (Manns et al., 2000). The
2120 question of the effect of attentional states on the dynamics of the
2121 associated engram motivated an important milestone for the Thesis,
2122 viz., to combine stable, adaptable behaviour studies with large-scale
2123 neurophysiology.

2124 We were able to train head-fixed mice to TEC and confirm adaptable
2125 conditioned responses to task variables. We were also able to
2126 simultaneous record from ~100 hippocampal CA1 cell bodies as the
2127 animals acquired top behavioural performance. We observed in our
2128 preliminary results that many identified time cells showcased the ability
2129 to tune to different time points across sessions or days, as has been
2130 previously reported (Mau et al., 2018).

2131 Several more high quality recordings and behaviour modulations would
2132 be required to conclusively describe time cells physiology and engram
2133 dynamics, at least at the level of a sub-population of hippocampal CA1.
2134 However, progress has been made to suggest the best time cell
2135 detection algorithm(s) based on their sensitivity to different recording
2136 parameters (Ananthamurthy & Bhalla, 2023). We hope that the Thesis
2137 is of aid to future research on the neural mechanisms of Learning and
2138 Memory by the nervous system.

2139 **Code Availability**

2140 All our code for Synthetic Data generation and time cell Analysis is
2141 available at <https://www.github.com/bhallalab/TimeCellAnalysis>.

2142 All our code for conducting Trace Eye-Blink Conditioning (TEC)

2143 behaviour is available at

2144 <https://www.github.com/ananthamurthy/eyeBlinkBehaviour>.

2145 Analysis scripts for evaluating TEC performance are available at

2146 <https://github.com/ananthamurthy/MATLAB/tree/master/TECAnalysis>.

2147 – Bibliography

2148

All Bibliography

- 2149
2150 Abe, R., Sakaguchi, T., Matsumoto, N., Matsuki, N., &
2151 Ikegaya, Y. (2014). Sound-induced hyperpolarization of
2152 hippocampal neurons. *Neuroreport*, 25(13), 1013-1017.
2153 <https://doi.org/10.1097/WNR.0000000000000206>
- 2154 Ananthamurthy, K. G., & Bhalla, U. S. (2023). Synthetic Data
2155 Resource and Benchmarks for Time Cell Analysis and
2156 Detection Algorithms. *ENeuro*, ENEURO.0007-22.2023.
2157 <https://doi.org/10.1523/ENEURO.0007-22.2023>
- 2158 Andermann, M. L., Gilfoy, N. B., Goldey, G. J., Sachdev, R. N.
2159 S., Wölfel, M., McCormick, D. A., Reid, R. C., & Levene,
2160 M. J. (2013). Chronic Cellular Imaging of Entire Cortical
2161 Columns in Awake Mice Using Microprisms. *Neuron*,
2162 80(4), 900-913.
2163 <https://doi.org/10.1016/j.neuron.2013.07.052>
- 2164 Andersen, P., Morris, R., Amaral, D., Bliss, T., & O'Keefe, J.
2165 (Eds.). (2006). *The Hippocampus Book*. Oxford University
2166 Press.
2167 <https://doi.org/10.1093/acprof:oso/9780195100273.001.001>
- 2168
2169 Andersen, R. A., Snyder, L. H., Li, C.-S., & Stricanne, B.
2170 (1993). Coordinate transformations in the representation
2171 of spatial information. *Current Opinion in Neurobiology*,
2172 3(2), 171-176.
2173 [https://doi.org/https://doi.org/10.1016/0959-4388\(93\)90206-E](https://doi.org/https://doi.org/10.1016/0959-4388(93)90206-E)
- 2174
2175 Aronov, D., Nevers, R., & Tank, D. W. (2017). Mapping of a
2176 non-spatial dimension by the hippocampal-entorhinal
2177 circuit. *Nature*, 543(7647), 719-722.
2178 <https://doi.org/10.1038/nature21692>

- 2179 Aronov, D., & Tank, D. W. (2014). Engagement of Neural
2180 Circuits Underlying 2D Spatial Navigation in a Rodent
2181 Virtual Reality System. *Neuron*, 84(2).
2182 <https://doi.org/10.1016/j.neuron.2014.08.042>
- 2183 Attardo, A., Fitzgerald, J. E., & Schnitzer, M. J. (2015).
2184 Impermanence of dendritic spines in live adult CA1
2185 hippocampus. *Nature*, 523(7562), 592–596.
2186 <https://doi.org/10.1038/nature14467>
- 2187 Barreto, R. P. J., Messerschmidt, B., & Schnitzer, M. J.
2188 (2009). In vivo fluorescence imaging with high-resolution
2189 microlenses. *Nature Methods*, 6(7), 511–512.
2190 <https://doi.org/10.1038/nmeth.1339>
- 2191 Bayesian brain: Probabilistic approaches to neural coding.
2192 (2007). In K. Doya, S. Ishii, A. Pouget, & R. P. N. Rao
2193 (Eds.), *Bayesian brain: Probabilistic approaches to neural*
2194 *coding*. MIT Press.
- 2195 Bellistri, E., Aguilar, J., Brotons-Mas, J. R., Foffani, G., & de la
2196 Prida, L. M. (2013). Basic properties of somatosensory-
2197 evoked responses in the dorsal hippocampus of the rat.
2198 *The Journal of Physiology*, 591(10), 2667–2686.
2199 <https://doi.org/10.1113/jphysiol.2013.251892>
- 2200 Bhalla, U. S. (2014a). Chapter Fourteen - Multiscale
2201 Modeling and Synaptic Plasticity. In K. T. B. T.-P. in M. B.
2202 and T. S. Blackwell (Ed.), *Computational Neuroscience*
2203 (Vol. 123, pp. 351–386). Academic Press.
2204 <https://doi.org/https://doi.org/10.1016/B978-0-12-397897-4.00012-7>
- 2206 Bhalla, U. S. (2014b). Molecular computation in neurons: a
2207 modeling perspective. *Current Opinion in Neurobiology*,
2208 25, 31–37.
2209 <https://doi.org/https://doi.org/10.1016/j.conb.2013.11.006>
- 2210 Bhalla, U. S. (2017). Synaptic input sequence discrimination
2211 on behavioral timescales mediated by reaction-diffusion

- 2212 chemistry in dendrites. *ELife*, 6, e25827.
2213 <https://doi.org/10.7554/eLife.25827>
- 2214 Bhalla, U. S. (2019). Dendrites, deep learning, and sequences
2215 in the hippocampus. *Hippocampus*, 29(3), 239-251.
2216 <https://doi.org/https://doi.org/10.1002/hipo.22806>
- 2217 Binder, M. D., Hirokawa, N., & Windhorst, U. (Eds.). (2009).
2218 *Delayed Non-match-to-Sample Task BT - Encyclopedia of*
2219 *Neuroscience* (p. 934). Springer Berlin Heidelberg.
2220 https://doi.org/10.1007/978-3-540-29678-2_1425
- 2221 Brown, G. D. (1998). Nonassociative learning processes
2222 affecting swimming probability in the seashell Tritonia
2223 diomedea: habituation, sensitization and inhibition.
2224 *Behavioural Brain Research*, 95(2), 151-165.
2225 [https://doi.org/https://doi.org/10.1016/S0166-4328\(98\)00072-2](https://doi.org/https://doi.org/10.1016/S0166-4328(98)00072-2)
- 2227 Buzsáki, G., & Llinás, R. (2017). Space and time in the brain.
2228 *Science (New York, N.Y.)*, 358(6362), 482-485.
2229 <https://doi.org/10.1126/science.aan8869>
- 2230 Cai, D. J., Aharoni, D., Shuman, T., Shobe, J., Biane, J., Song,
2231 W., Wei, B., Veshkini, M., La-Vu, M., Lou, J., Flores, S. E.,
2232 Kim, I., Sano, Y., Zhou, M., Baumgaertel, K., Lavi, A.,
2233 Kamata, M., Tuszyński, M., Mayford, M., ... Silva, A. J.
2234 (2016). A shared neural ensemble links distinct
2235 contextual memories encoded close in time. *Nature*,
2236 534(7605), 115-118. <https://doi.org/10.1038/nature17955>
- 2237 Caporale, N., & Dan, Y. (2008). Spike timing-dependent
2238 plasticity: a Hebbian learning rule. *Annual Review of*
2239 *Neuroscience*, 31, 25-46.
2240 <https://doi.org/10.1146/annurev.neuro.31.060407.125639>
- 2241 Chen, T.-W., Wardill, T. J., Sun, Y., Pulver, S. R., Renninger,
2242 S. L., Baohan, A., Schreiter, E. R., Kerr, R. A., Orger, M.
2243 B., Jayaraman, V., Looger, L. L., Svoboda, K., & Kim, D.
2244 S. (2013). Ultrasensitive fluorescent proteins for imaging

- 2245 neuronal activity. *Nature*, 499(7458), 295–300.
2246 <https://doi.org/10.1038/nature12354>
- 2247 Chun, M. M., & Johnson, M. K. (2011). Memory: enduring
2248 traces of perceptual and reflective attention. *Neuron*,
2249 72(4), 520–535.
2250 <https://doi.org/10.1016/j.neuron.2011.10.026>
- 2251 Conen, K. E., & Desrochers, T. M. (2022). *The Neural Basis*
2252 *of Behavioral Sequences in Cortical and Subcortical*
2253 *Circuits*. Oxford University Press.
2254 <https://doi.org/10.1093/acrefore/9780190264086.013.421>
- 2255 Davidson, T. J., Kloosterman, F., & Wilson, M. A. (2009).
2256 Hippocampal replay of extended experience. *Neuron*,
2257 63(4), 497–507.
2258 <https://doi.org/10.1016/j.neuron.2009.07.027>
- 2259 Denk, W., Strickler, J. H., & Webb, W. W. (1990). Two-photon
2260 laser scanning fluorescence microscopy. *Science (New*
2261 *York, N.Y.)*, 248(4951), 73–76.
2262 <https://doi.org/10.1126/science.2321027>
- 2263 Deshmukh, S. S., & Bhalla, U. S. (2003). Representation of
2264 odor habituation and timing in the hippocampus. *The*
2265 *Journal of Neuroscience : The Official Journal of the*
2266 *Society for Neuroscience*, 23(5), 1903–1915.
2267 <https://doi.org/10.1523/JNEUROSCI.23-05-01903.2003>
- 2268 Dhawale, A. K., Poddar, R., Wolff, S. B. E., Normand, V. A.,
2269 Kopelowitz, E., & Ölveczky, B. P. (2017). Automated long-
2270 term recording and analysis of neural activity in behaving
2271 animals. *eLife*, 6, e27702.
2272 <https://doi.org/10.7554/eLife.27702>
- 2273 Dickinson, A., Nicholas, D. J., & Mackintosh, N. J. (1983). A
2274 re-examination of one-trial blocking in conditioned
2275 suppression. *The Quarterly Journal of Experimental*
2276 *Psychology B: Comparative and Physiological Psychology*,
2277 35, 67–79. <https://doi.org/10.1080/14640748308400914>

- 2278 Dombeck, D. A., Graziano, M. S., & Tank, D. W. (2009).
2279 Functional clustering of neurons in motor cortex
2280 determined by cellular resolution imaging in awake
2281 behaving mice. *The Journal of Neuroscience : The Official*
2282 *Journal of the Society for Neuroscience*, 29(44), 13751-
2283 13760. <https://doi.org/10.1523/JNEUROSCI.2985-09.2009>
- 2284 Dombeck, D. A., Harvey, C. D., Tian, L., Looger, L. L., &
2285 Tank, D. W. (2010). Functional imaging of hippocampal
2286 place cells at cellular resolution during virtual
2287 navigation. *Nature Neuroscience*, 13(11), 1433-1440.
2288 <https://doi.org/10.1038/nn.2648>
- 2289 Dombeck, D. A., Khabbaz, A. N., Collman, F., Adelman, T. L.,
2290 & Tank, D. W. (2007). Imaging large-scale neural activity
2291 with cellular resolution in awake, mobile mice. *Neuron*,
2292 56(1), 43-57.
2293 <https://doi.org/10.1016/j.neuron.2007.08.003>
- 2294 Dombeck, D., & Tank, D. (2014). Two-photon imaging of
2295 neural activity in awake mobile mice. *Cold Spring Harbor*
2296 *Protocols*, 2014(7), 726-736.
2297 <https://doi.org/10.1101/pdb.top081810>
- 2298 Dudani, N., Bhalla, U. S., & Ray, S. (2013). *MOOSE, the*
2299 *Multiscale Object-Oriented Simulation Environment BT -*
2300 *Encyclopedia of Computational Neuroscience* (D. Jaeger
2301 & R. Jung (Eds.); pp. 1-4). Springer New York.
2302 https://doi.org/10.1007/978-1-4614-7320-6_257-1
- 2303 Eichenbaum, H. (2004). Hippocampus: Cognitive processes
2304 and neural representations that underlie declarative
2305 memory. *Neuron*, 44(1), 109-120.
2306 <https://doi.org/10.1016/j.neuron.2004.08.028>
- 2307 Eichenbaum, H. (2017). On the Integration of Space, Time,
2308 and Memory. *Neuron*, 95(5), 1007-1018.
2309 <https://doi.org/10.1016/j.neuron.2017.06.036>
- 2310 Fanselow, M. S., & Dong, H.-W. (2010). Are the dorsal and
2311 ventral hippocampus functionally distinct structures?

- 2312 *Neuron*, 65(1), 7-19.
2313 <https://doi.org/10.1016/j.neuron.2009.11.031>
- 2314 Fassihi, A., Akrami, A., Pulecchi, F., Schönfelder, V., &
2315 Diamond, M. E. (2017). Transformation of Perception
2316 from Sensory to Motor Cortex. *Current Biology: CB*,
2317 27(11), 1585-1596.e6.
2318 <https://doi.org/10.1016/j.cub.2017.05.011>
- 2319 Ferbinteanu, J., & Shapiro, M. L. (2003). Prospective and
2320 retrospective memory coding in the hippocampus.
2321 *Neuron*, 40(6), 1227-1239. [https://doi.org/10.1016/s0896-6273\(03\)00752-9](https://doi.org/10.1016/s0896-6273(03)00752-9)
- 2323 Ferbinteanu, J., Shirvalkar, P., & Shapiro, M. L. (2011).
2324 Memory Modulates Journey-Dependent Coding in the Rat
2325 Hippocampus. *The Journal of Neuroscience*, 31(25), 9135
2326 LP – 9146. <https://doi.org/10.1523/JNEUROSCI.1241-11.2011>
- 2328 Foster, D. J. (2017). Replay Comes of Age. *Annual Review of
2329 Neuroscience*, 40, 581-602.
2330 <https://doi.org/10.1146/annurev-neuro-072116-031538>
- 2331 Foster, D. J., & Wilson, M. A. (2006). Reverse replay of
2332 behavioural sequences in hippocampal place cells during
2333 the awake state. *Nature*, 440(7084), 680-683.
2334 <https://doi.org/10.1038/nature04587>
- 2335 Foster, D. J., & Wilson, M. A. (2007). Hippocampal theta
2336 sequences. *Hippocampus*, 17(11), 1093-1099.
2337 <https://doi.org/10.1002/hipo.20345>
- 2338 Francis, M., Qian, X., Charbel, C., Ledoux, J., Parker, J. C., &
2339 Taylor, M. S. (2012). Automated region of interest
2340 analysis of dynamic Ca²⁺ signals in image sequences.
2341 *American Journal of Physiology. Cell Physiology*, 303(3),
2342 C236-43. <https://doi.org/10.1152/ajpcell.00016.2012>
- 2343 Frank, L. M., Brown, E. N., & Wilson, M. (2000). Trajectory
2344 encoding in the hippocampus and entorhinal cortex.

- 2345 *Neuron*, 27(1), 169–178. [https://doi.org/10.1016/s0896-6273\(00\)00018-0](https://doi.org/10.1016/s0896-6273(00)00018-0)
- 2347 Fyhn, M., Molden, S., Witter, M. P., Moser, E. I., & Moser, M.-B. (2004). Spatial representation in the entorhinal cortex. *Science (New York, N.Y.)*, 305(5688), 1258–1264. <https://doi.org/10.1126/science.1099901>
- 2351 Hafting, T., Fyhn, M., Molden, S., Moser, M.-B., & Moser, E. I. (2005). Microstructure of a spatial map in the entorhinal cortex. *Nature*, 436(7052), 801–806. <https://doi.org/10.1038/nature03721>
- 2355 Han, J.-H., Kushner, S. A., Yiu, A. P., Hsiang, H.-L. L., Buch, T., Waisman, A., Bontempi, B., Neve, R. L., Frankland, P. W., & Josselyn, S. A. (2009). Selective erasure of a fear memory. *Science (New York, N.Y.)*, 323(5920), 1492–1496. <https://doi.org/10.1126/science.1164139>
- 2360 Harvey, C. D., Collman, F., Dombeck, D. A., & Tank, D. W. (2009). Intracellular dynamics of hippocampal place cells during virtual navigation. *Nature*, 461(7266), 941–946. <https://doi.org/10.1038/nature08499>
- 2364 Hebb, D. O. (1949). The organization of behavior; a neuropsychological theory. In *The organization of behavior; a neuropsychological theory*. Wiley.
- 2367 Helmchen, F., & Denk, W. (2005). *Deep tissue two-photon microscopy*. 2(12), 9. <https://doi.org/10.1038/nmeth818>
- 2369 Hjorth-Simonsen, A., & Jeune, B. (1972). Origin and termination of the hippocampal perforant path in the rat studied by silver impregnation. *The Journal of Comparative Neurology*, 144(2), 215–232. <https://doi.org/10.1002/cne.901440206>
- 2374 Hubel, D. H., & Wiesel, T. N. (1962). Receptive fields, binocular interaction and functional architecture in the cat's visual cortex. *The Journal of Physiology*, 160(1), 106–154. <https://doi.org/10.1113/jphysiol.1962.sp006837>

- 2378 Hutchinson, J. B., & Turk-Browne, N. B. (2012). Memory-
2379 guided attention: control from multiple memory systems.
2380 *Trends in Cognitive Sciences*, 16(12), 576-579.
2381 <https://doi.org/10.1016/j.tics.2012.10.003>
- 2382 Itskov, P. M., Vinnik, E., & Diamond, M. E. (2011).
2383 Hippocampal representation of touch-guided behavior in
2384 rats: persistent and independent traces of stimulus and
2385 reward location. *PLoS One*, 6(1), e16462.
2386 <https://doi.org/10.1371/journal.pone.0016462>
- 2387 Jaramillo, S., & Zador, A. M. (2014). Mice and rats achieve
2388 similar levels of performance in an adaptive decision-
2389 making task . In *Frontiers in Systems Neuroscience*
2390 (Vol. 8).
2391 <https://www.frontiersin.org/articles/10.3389/fnsys.2014.00173>
- 2393 Jun, J. J., Steinmetz, N. A., Siegle, J. H., Denman, D. J., Bauza,
2394 M., Barbarits, B., Lee, A. K., Anastassiou, C. A., Andrei,
2395 A., Aydin, Ç., Barbic, M., Blanche, T. J., Bonin, V., Couto,
2396 J., Dutta, B., Gratiy, S. L., Gutnisky, D. A., Häusser, M.,
2397 Karsh, B., ... Harris, T. D. (2017). Fully integrated silicon
2398 probes for high-density recording of neural activity.
2399 *Nature*, 551(7679), 232-236.
2400 <https://doi.org/10.1038/nature24636>
- 2401 Kaifosh, P., Lovett-Barron, M., Turi, G. F., Reardon, T. R., &
2402 Losonczy, A. (2013). Septo-hippocampal GABAergic
2403 signaling across multiple modalities in awake mice.
2404 *Nature Neuroscience*, 16(9), 1182-1184.
2405 <https://doi.org/10.1038/nn.3482>
- 2406 Kalmbach, B. E., Davis, T., Ohyama, T., Riusech, F., Nores,
2407 W. L., & Mauk, M. D. (2010). Cerebellar Cortex
2408 Contributions to the Expression and Timing of
2409 Conditioned Eyelid Responses. *Journal of
2410 Neurophysiology*, 103(4), 2039-2049.
2411 <https://doi.org/10.1152/jn.00033.2010>

- 2412 Kalmbach, B. E., Ohyama, T., & Mauk, M. D. (2010).
2413 Temporal Patterns of Inputs to Cerebellum Necessary
2414 and Sufficient for Trace Eyelid Conditioning. *Journal of*
2415 *Neurophysiology*, 104(2), 627-640.
2416 <https://doi.org/10.1152/jn.00169.2010>
- 2417 Kamondi, A. (1998). *Theta Oscillations in Somata and*
2418 *Dendrites of Hippocampal Pyramidal Cells In Vivo:*
2419 *Activity-Dependent Phase-Precession of Action Potentials.*
2420 261(March), 244-261.
- 2421 Kauvar, I. V., Machado, T. A., Yuen, E., Kochalka, J., Choi, M.,
2422 Allen, W. E., Wetzstein, G., & Deisseroth, K. (2020).
2423 Cortical Observation by Synchronous Multifocal Optical
2424 Sampling Reveals Widespread Population Encoding of
2425 Actions. *Neuron*, 107(2), 351-367.e19.
2426 <https://doi.org/10.1016/j.neuron.2020.04.023>
- 2427 Khan, A. G., Parthasarathy, K., & Bhalla, U. S. (2010). Odor
2428 representations in the mammalian olfactory bulb. *Wiley*
2429 *Interdisciplinary Reviews. Systems Biology and Medicine*,
2430 2(5), 603-611. <https://doi.org/10.1002/wsbm.85>
- 2431 Kraus, B. J., Brandon, M. P., Robinson, R. J., Connerney, M.
2432 A., Hasselmo, M. E., & Eichenbaum, H. (2015). During
2433 Running in Place, Grid Cells Integrate Elapsed Time and
2434 Distance Run. *Neuron*, 88(3), 578-589.
2435 <https://doi.org/10.1016/j.neuron.2015.09.031>
- 2436 Kraus, B., Robinson, R., White, J., Eichenbaum, H., &
2437 Hasselmo, M. (2013). Hippocampal "Time Cells": Time
2438 versus Path Integration. *Neuron*, 78(6), 1090-1101.
2439 <https://doi.org/10.1016/j.neuron.2013.04.015>
- 2440 Kropff, E., Carmichael, J. E., Moser, M.-B., & Moser, E. I.
2441 (2015). Speed cells in the medial entorhinal cortex.
2442 *Nature*, 523(7561), 419-424.
2443 <https://doi.org/10.1038/nature14622>
- 2444 Krupa, D., & Thompson, R. (2003). Inhibiting the Expression
2445 of a Classically Conditioned Behavior Prevents Its

- 2446 Extinction. *The Journal of Neuroscience : The Official*
2447 *Journal of the Society for Neuroscience*, 23, 10577-
2448 10584. <https://doi.org/10.1523/JNEUROSCI.23-33-10577.2003>
- 2450 Lovett-Barron, M., Kaifosh, P., Kheirbek, M. A., Danielson,
2451 N., Zaremba, J. D., Reardon, T. R., Turi, G. F., Hen, R.,
2452 Zemelman, B. V., & Losonczy, A. (2014). Dendritic
2453 inhibition in the hippocampus supports fear learning.
2454 *Science (New York, N.Y.)*, 343(6173), 857-863.
2455 <https://doi.org/10.1126/science.1247485>
- 2456 Luo, L., Callaway, E. M., & Svoboda, K. (2018). Genetic
2457 Dissection of Neural Circuits: A Decade of Progress.
2458 *Neuron*, 98(2), 256-281.
2459 <https://doi.org/https://doi.org/10.1016/j.neuron.2018.03.040>
- 2461 MacDonald, C. J., Carrow, S., Place, R., & Eichenbaum, H.
2462 (2013). Distinct hippocampal time cell sequences
2463 represent odor memories in immobilized rats. *The*
2464 *Journal of Neuroscience : The Official Journal of the*
2465 *Society for Neuroscience*, 33(36), 14607-14616.
2466 <https://doi.org/10.1523/JNEUROSCI.1537-13.2013>
- 2467 MacDonald, C. J., Lepage, K. Q., Eden, U. T., & Eichenbaum,
2468 H. (2011). Hippocampal “time cells” bridge the gap in
2469 memory for discontiguous events. *Neuron*, 71(4), 737-
2470 749. <https://doi.org/10.1016/j.neuron.2011.07.012>
- 2471 Manns, J. R., Clark, R. E., & Squire, L. R. (2000). Parallel
2472 acquisition of awareness and trace eyeblink classical
2473 conditioning. *Learning & Memory (Cold Spring Harbor,*
2474 *N.Y.)*, 7(5), 267-272. <https://doi.org/10.1101/lm.33400>
- 2475 Maruyama, R., Maeda, K., Moroda, H., Kato, I., Inoue, M.,
2476 Miyakawa, H., & Aonishi, T. (2014). Detecting cells using
2477 non-negative matrix factorization on calcium imaging
2478 data. *Neural Networks : The Official Journal of the*
2479 *International Neural Network Society*, 55, 11-19.
2480 <https://doi.org/10.1016/j.neunet.2014.03.007>

- 2481 Mau, W., Sullivan, D. W., Kinsky, N. R., Hasselmo, M. E.,
2482 Howard, M. W., & Eichenbaum, H. (2018). The Same
2483 Hippocampal CA1 Population Simultaneously Codes
2484 Temporal Information over Multiple Timescales. *Current*
2485 *Biology*, 28(10), 1499-1508.e4.
2486 <https://doi.org/10.1016/j.cub.2018.03.051>
- 2487 McHugh, T. J., Jones, M. W., Quinn, J. J., Balthasar, N.,
2488 Coppari, R., Elmquist, J. K., Lowell, B. B., Fanselow, M.
2489 S., Wilson, M. A., & Tonegawa, S. (2007). Dentate gyrus
2490 NMDA receptors mediate rapid pattern separation in the
2491 hippocampal network. *Science (New York, N.Y.)*,
2492 317(5834), 94-99.
2493 <https://doi.org/10.1126/science.1140263>
- 2494 McNaughton, N., & Gray, J. A. (2000). Anxiolytic action on
2495 the behavioural inhibition system implies multiple types
2496 of arousal contribute to anxiety. *Journal of Affective*
2497 *Disorders*, 61(3), 161-176. [https://doi.org/10.1016/s0165-0327\(00\)00344-x](https://doi.org/10.1016/s0165-0327(00)00344-x)
- 2499 Medina, J. F., Garcia, K. S., Nores, W. L., Taylor, N. M., &
2500 Mauk, M. D. (2000). Timing mechanisms in the
2501 cerebellum: testing predictions of a large-scale computer
2502 simulation. *The Journal of Neuroscience : The Official*
2503 *Journal of the Society for Neuroscience*, 20(14), 5516-
2504 5525. <https://doi.org/10.1523/JNEUROSCI.20-14-05516.2000>
- 2506 Meeks, J. P., Arnson, H. A., & Holy, T. E. (2010).
2507 Representation and transformation of sensory
2508 information in the mouse accessory olfactory system.
2509 *Nature Neuroscience*, 13(6), 723-730.
2510 <https://doi.org/10.1038/nn.2546>
- 2511 Mizrahi, A. (2004). High-Resolution In Vivo Imaging of
2512 Hippocampal Dendrites and Spines. *Journal of*
2513 *Neuroscience*, 24(13), 3147-3151.
2514 <https://doi.org/10.1523/JNEUROSCI.5218-03.2004>

- 2515 Modi, M. N., Dhawale, A. K., & Bhalla, U. S. (2014). CA1 cell
2516 activity sequences emerge after reorganization of
2517 network correlation structure during associative
2518 learning. *eLife*, 3, e01982-e01982.
2519 <https://doi.org/10.7554/eLife.01982>
- 2520 Morris, R. G. M., Garrud, P., Rawlins, J. N. P., & O'Keefe, J.
2521 (1982). Place navigation impaired in rats with
2522 hippocampal lesions. *Nature*, 297(5868), 681–683.
2523 <https://doi.org/10.1038/297681a0>
- 2524 Moser, M.-B., & Moser, E. I. (1998). Distributed encoding
2525 and retrieval of spatial memory in the hippocampus. In
2526 *The Journal of Neuroscience* (Vol. 18, pp. 7535–7542).
2527 Society for Neuroscience.
- 2528 Moyer, J. R., Deyo, R. A., & Disterhoft, J. F. (1990).
2529 Hippocamectomy disrupts trace eye-blink conditioning
2530 in rabbits. *Behavioral Neuroscience*, 104(2)(Apr 1990),
2531 243–252. <https://doi.org/10.1037/0735-7044.104.2.243>
- 2532 Mukamel, E. A., Nimmerjahn, A., & Schnitzer, M. J. (2009).
2533 Automated analysis of cellular signals from large-scale
2534 calcium imaging data. *Neuron*, 63(6), 747–760.
2535 <https://doi.org/10.1016/j.neuron.2009.08.009>
- 2536 Murray, T. A., & Levene, M. J. (2012). Singlet gradient index
2537 lens for deep in vivo multiphoton microscopy. *Journal of
2538 Biomedical Optics*, 17(2), 021106.
2539 <https://doi.org/10.1117/1.JBO.17.2.021106>
- 2540 Nakashiba, T., Young, J. Z., McHugh, T. J., Buhl, D. L., &
2541 Tonegawa, S. (2008). Transgenic inhibition of synaptic
2542 transmission reveals role of CA3 output in hippocampal
2543 learning. *Science (New York, N.Y.)*, 319(5867), 1260–
2544 1264. <https://doi.org/10.1126/science.1151120>
- 2545 O'Keefe, J., & Dostrovsky, J. (1971). The hippocampus as a
2546 spatial map. Preliminary evidence from unit activity in
2547 the freely-moving rat. *Brain Research*, 34(1), 171–175.
2548 [https://doi.org/10.1016/0006-8993\(71\)90358-1](https://doi.org/10.1016/0006-8993(71)90358-1)

- 2549 O'Keefe, J., & Recce, M. L. (1993). Phase relationship
2550 between hippocampal place units and the EEG theta
2551 rhythm. *Hippocampus*, 3(3), 317-330.
2552 <https://doi.org/10.1002/hipo.450030307>
- 2553 Ohya, T., Nores, W. L., Murphy, M., & Mauk, M. D. (2003).
2554 What the cerebellum computes. *Trends in Neurosciences*,
2555 26(4), 222-227. [https://doi.org/10.1016/S0166-2236\(03\)00054-7](https://doi.org/10.1016/S0166-2236(03)00054-7)
- 2557 Pachitariu, M., Stringer, C., Dipoppa, M., Schröder, S., Rossi,
2558 L. F., Dalgleish, H., Carandini, M., & Harris, K. D. (2017).
2559 Suite2p: beyond 10,000 neurons with standard two-
2560 photon microscopy. *BioRxiv*, 61507.
2561 <https://doi.org/10.1101/061507>
- 2562 Paredes, R. M., Etzler, J. C., Watts, L. T., Zheng, W., &
2563 Lechleiter, J. D. (2008). Chemical calcium indicators.
2564 *Methods (San Diego, Calif.)*, 46(3), 143-151.
2565 <https://doi.org/10.1016/j.ymeth.2008.09.025>
- 2566 Pastalkova, E., Itskov, V., Amarasingham, A., & Buzsaki, G.
2567 (2008). Internally Generated Cell Assembly Sequences in
2568 the Rat Hippocampus. *Science*, 321(5894), 1322-1327.
2569 <https://doi.org/10.1126/science.1159775>
- 2570 Pavlov, I. P. (1927). Conditioned reflexes: an investigation of
2571 the physiological activity of the cerebral cortex. In
2572 *Conditioned reflexes: an investigation of the physiological*
2573 *activity of the cerebral cortex*. Oxford Univ. Press.
- 2574 Peron, S. P., Freeman, J., Iyer, V., Guo, C., & Svoboda, K.
2575 (2015). A Cellular Resolution Map of Barrel Cortex
2576 Activity during Tactile Behavior. *Neuron*, 86(3), 783-799.
2577 <https://doi.org/10.1016/j.neuron.2015.03.027>
- 2578 Petersen, C. C. H. (2019). Sensorimotor processing in the
2579 rodent barrel cortex. *Nature Reviews. Neuroscience*,
2580 20(9), 533-546. <https://doi.org/10.1038/s41583-019-0200-y>

- 2582 Pnevmatikakis, E. A., Soudry, D., Gao, Y., Machado, T. A.,
2583 Merel, J., Pfau, D., Reardon, T., Mu, Y., Lacefield, C.,
2584 Yang, W., Ahrens, M., Bruno, R., Jessell, T. M., Peterka,
2585 D. S., Yuste, R., & Paninski, L. (2016). Simultaneous
2586 Denoising, Deconvolution, and Demixing of Calcium
2587 Imaging Data. *Neuron*, 89(2), 285–299.
2588 <https://doi.org/https://doi.org/10.1016/j.neuron.2015.11.037>
- 2590 Poort, J., Khan, A. G., Pachitariu, M., Nemri, A., Orsolic, I.,
2591 Krupic, J., Bauza, M., Sahani, M., Keller, G. B., Mrsic-
2592 Flogel, T. D., & Hofer, S. B. (2015). Learning Enhances
2593 Sensory and Multiple Non-sensory Representations in
2594 Primary Visual Cortex. *Neuron*, 86(6), 1478–1490.
2595 <https://doi.org/10.1016/j.neuron.2015.05.037>
- 2596 Ranck, J. B. (1973). Studies on single neurons in dorsal
2597 hippocampal formation and septum in unrestrained rats:
2598 Part I. Behavioral correlates and firing repertoires.
2599 *Experimental Neurology*, 41(2), 462–531.
2600 [https://doi.org/https://doi.org/10.1016/0014-4886\(73\)90290-2](https://doi.org/https://doi.org/10.1016/0014-4886(73)90290-2)
- 2602 Ranck, J. B. (1975). *Behavioral Correlates and Firing
2603 Repertoires of Neurons in the Dorsal Hippocampal
2604 Formation and Septum of Unrestrained Rats BT - The
2605 Hippocampus: Volume 2: Neurophysiology and Behavior*
2606 (R. L. Isaacson & K. H. Pribram (Eds.); pp. 207–244).
2607 Springer US. https://doi.org/10.1007/978-1-4684-2979-4_7
- 2609 Rao, R. P. N., & Ballard, D. H. (1999). Predictive coding in
2610 the visual cortex: a functional interpretation of some
2611 extra-classical receptive-field effects. *Nature
2612 Neuroscience*, 2(1), 79–87. <https://doi.org/10.1038/4580>
- 2613 Rogerson, T., Cai, D. J., Frank, A., Sano, Y., Shobe, J., Lopez-
2614 Aranda, M. F., & Silva, A. J. (2014). Synaptic tagging
2615 during memory allocation. *Nature Reviews*.

- 2616 *Neuroscience*, 15(3), 157-169.
2617 <https://doi.org/10.1038/nrn3667>
- 2618 Schreurs, B. G. (1989). Classical conditioning of model
2619 systems: A behavioral review. *Psychobiology*, 17(2), 145-
2620 155. <https://doi.org/10.3758/BF03337830>
- 2621 Scoville, W. B., & Milner, B. (1957). Loss of recent memory
2622 after bilateral hippocampal lesions. In *Journal of*
2623 *Neurology, Neurosurgery & Psychiatry* (Vol. 20, pp. 11-
2624 21). BMJ Publishing Group.
2625 <https://doi.org/10.1136/jnnp.20.1.11>
- 2626 Sheffield, M. E. J., & Dombeck, D. A. (2014). Calcium
2627 transient prevalence across the dendritic arbour predicts
2628 place field properties. *Nature*, 517(7533), 200-204.
2629 <https://doi.org/10.1038/nature13871>
- 2630 Siegel, J. J., & Mauk, M. D. (2013). Persistent Activity in
2631 Prefrontal Cortex during Trace Eyelid Conditioning:
2632 Dissociating Responses That Reflect Cerebellar Output
2633 from Those That Do Not. *The Journal of Neuroscience*,
2634 33(38), 15272 LP - 15284.
2635 <https://doi.org/10.1523/JNEUROSCI.1238-13.2013>
- 2636 Siegel, J. J., Taylor, W., Gray, R., Kalmbach, B., Zemelman, B.
2637 V., Desai, N. S., Johnston, D., & Chitwood, R. A. (2015).
2638 Trace Eyeblink Conditioning in Mice Is Dependent upon
2639 the Dorsal Medial Prefrontal Cortex, Cerebellum, and
2640 Amygdala: Behavioral Characterization and Functional
2641 Circuitry. *ENeuro*, 2(4), ENEURO.0051-14.2015.
2642 <https://doi.org/10.1523/ENEURO.0051-14.2015>
- 2643 Skaggs, W., McNaughton, B., Gothard, K., & Markus, E.
2644 (1996). An Information-Theoretic Approach to
2645 Deciphering the Hippocampal Code. *Neural Inf. Process*
2646 *Syst.*, 5.
- 2647 Souza, B. C., Pavão, R., Belchior, H., & Tort, A. B. L. (2018).
2648 On Information Metrics for Spatial Coding.

- 2649 *Neuroscience*, 375, 62-73.
2650 <https://doi.org/10.1016/j.neuroscience.2018.01.066>
- 2651 Stosiek, C., Garaschuk, O., Holthoff, K., & Konnerth, A.
2652 (2003). In vivo two-photon calcium imaging of neuronal
2653 networks. *Proceedings of the National Academy of
2654 Sciences of the United States of America*, 100(12), 7319-
2655 7324. <https://doi.org/10.1073/pnas.1232232100>
- 2656 Suh, J., Rivest, A. J., Nakashiba, T., Tominaga, T., &
2657 Tonegawa, S. (2011). Entorhinal cortex layer III input to
2658 the hippocampus is crucial for temporal association
2659 memory. *Science (New York, N.Y.)*, 334(6061), 1415-
2660 1420. <https://doi.org/10.1126/science.1210125>
- 2661 Taube, J. S., Muller, R. U., & Ranck, J. B. J. (1990). Head-
2662 direction cells recorded from the postsubiculum in freely
2663 moving rats. I. Description and quantitative analysis. *The
2664 Journal of Neuroscience : The Official Journal of the
2665 Society for Neuroscience*, 10(2), 420-435.
2666 <https://doi.org/10.1523/JNEUROSCI.10-02-00420.1990>
- 2667 Tseng, W., Guan, R., Disterhoft, J. F., & Weiss, C. (2004).
2668 Trace eyeblink conditioning is hippocampally dependent
2669 in mice. *Hippocampus*, 14(1), 58-65.
2670 <https://doi.org/10.1002/hipo.10157>
- 2671 Uncapher, M. R., Hutchinson, J. B., & Wagner, A. D. (2011).
2672 Dissociable effects of top-down and bottom-up attention
2673 during episodic encoding. *The Journal of Neuroscience :
2674 The Official Journal of the Society for Neuroscience*,
2675 31(35), 12613-12628.
2676 <https://doi.org/10.1523/JNEUROSCI.0152-11.2011>
- 2677 Velasco, M. G. M., & Levene, M. J. (2014). In vivo two-photon
2678 microscopy of the hippocampus using glass plugs.
2679 *Biomedical Optics Express*, 5(6), 1700-1708.
2680 <https://doi.org/10.1364/BOE.5.001700>
- 2681 Vinogradova, O. S. (2001). Hippocampus as comparator: Role
2682 of the two input and two output systems of the

- 2683 hippocampus in selection and registration of information.
2684 *Hippocampus*, 11(5), 578–598.
2685 <https://doi.org/https://doi.org/10.1002/hipo.1073>
- 2686 Voelcker, B., Pancholi, R., & Peron, S. (2022). Transformation
2687 of primary sensory cortical representations from layer 4
2688 to layer 2. *Nature Communications*, 13(1), 5484.
2689 <https://doi.org/10.1038/s41467-022-33249-1>
- 2690 Wood, E. R., Dudchenko, P. A., Robitsek, R. J., &
2691 Eichenbaum, H. (2000). Hippocampal Neurons Encode
2692 Information about Different Types of Memory Episodes
2693 Occurring in the Same Location. *Neuron*, 27(3), 623–633.
2694 <https://doi.org/https://doi.org/10.1016/S0896->
2695 6273(00)00071-4
- 2696 Yiu, A. P., Mercaldo, V., Yan, C., Richards, B., Rashid, A. J.,
2697 Hsiang, H.-L. L., Pressey, J., Mahadevan, V., Tran, M. M.,
2698 Kushner, S. A., Woodin, M. A., Frankland, P. W., &
2699 Josselyn, S. A. (2014). Neurons are recruited to a memory
2700 trace based on relative neuronal excitability immediately
2701 before training. *Neuron*, 83(3), 722–735.
2702 <https://doi.org/10.1016/j.neuron.2014.07.017>
- 2703 Zhang, S., & Manahan-Vaughan, D. (2015). Spatial olfactory
2704 learning contributes to place field formation in the
2705 hippocampus. *Cerebral Cortex (New York, N.Y. : 1991)*,
2706 25(2), 423–432. <https://doi.org/10.1093/cercor/bht239>
- 2707 Zhou, S., Masmanidis, S. C., & Buonomano, D. V. (2020).
2708 Neural Sequences as an Optimal Dynamical Regime for
2709 the Readout of Time. *Neuron*, 108(4), 651–658.e5.
2710 <https://doi.org/https://doi.org/10.1016/j.neuron.2020.08.0>
2711 20
- 2712 Zhou, Y., Won, J., Karlsson, M. G., Zhou, M., Rogerson, T.,
2713 Balaji, J., Neve, R., Poirazi, P., & Silva, A. J. (2009). CREB
2714 regulates excitability and the allocation of memory to
2715 subsets of neurons in the amygdala. *Nature Neuroscience*, 12(11), 1438–1443.
2716 <https://doi.org/10.1038/nn.2405>

2718 Ziv, Y., Burns, L. D., Cocker, E. D., Hamel, E. O., Ghosh, K.
2719 K., Kitch, L. J., El Gamal, A., & Schnitzer, M. J. (2013). Long-
2720 term dynamics of CA1 hippocampal place codes. *Nature
2721 Neuroscience*, 16(3), 264-266.
2722 <https://doi.org/10.1038/nn.3329>
2723